

Monterrey Institute of Technology and Higher Education

Campus Monterrey

School of Engineering and Sciences



“Micro machinability of net shapes of Selective Laser Melting of Ti-6Al-4V for minimum material removal using ball end mill”

A thesis presented by

Pavel Celis Retana

Submitted to the

School of Engineering and Sciences

In partial fulfillment of the requirement for the degree of

Master of Science

In Manufacturing Systems

Monterrey Nuevo Leon, May 15th, 2018

Monterrey Institute of Technology and Higher Education

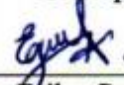
Campus Monterrey

School of Engineering and Sciences

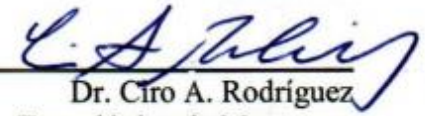
The committee members, hereby, certify that have read the thesis presented by Pavel Celis Retana and that it is fully adequate in scope and quality as a partial requirement for the degree of Master of Science in Manufacturing Systems



Dr. Elisa Virginia Vázquez Lepe
Tecnológico de Monterrey
School of Engineering and Sciences
Principal Advisor



Dr. Erika García López
Tecnológico de Monterrey
School of Engineering and Sciences
Co-advisor



Dr. Ciro A. Rodríguez
Tecnológico de Monterrey
School of Engineering and Sciences
Committee Member



Dr. Jesús A. Sandoval Robles
Tecnológico de Monterrey
School of Engineering and Sciences
Committee Member



Dr. Ruben Morales Menendez

Associate Dean of Graduate Studies

School of Engineering and Sciences

Monterrey Nuevo León, May 15th, 2018

Declaration of Authorship

I, Pavel Celis Retana, declare that this thesis titled, “Micro machinability of net shapes of Selective Laser Melting of Ti-6Al-4V for minimum material removal using ball end mill” and the work presented in it are my own. I confirm that:

- This work was done wholly or mainly while in candidature for a research degree at this University.
- Where any part of this thesis has previously been submitted for a degree or any other qualification at this University or any other institution, this has been clearly stated.
- Where I have consulted the published work of others, this is always clearly attributed.
- Where I have quoted from the work of others, the source is always given. With the exception of such quotations, this thesis is entirely my own work.
- I have acknowledged all main sources of help.
- Where the thesis is based on work done by myself jointly with others, I have made clear exactly what was done by others and what I have contributed myself.



Pavel Celis Retana

Monterrey Nuevo León, May 20th, 2018

@2018 by Pavel Celis Retana

All rights reserved

Dedication

I dedicate this thesis to my parents and my family, who always believed in this project and gave me their support, patience and encouragement to complete my goals.

Acknowledgements

I would like to thank to all the people who trusted in me and supported me through all my courses, capacitation's and work during my master's degree. Thanks to the assistants, friends and co-workers who were part of this experience in the long nights of work and joy.

I want to thank Dr. Elisa Vazquez who is my advisor for my thesis development, also Dr. Erika Garcia who supported me during the investigation and experimental trials of this project, for providing me the tools and knowledge to overcome the problems presented and guiding me step by step to accomplish this goal of my life.

Thanks to the Tecnologico de Monterrey and Conacyt, who gave me the opportunity to continue developing my skills, for providing me the installations and the knowledge of the professors involved during this 2 years and the economic support for living.

“Micro machinability of net shapes of Selective Laser Melting of Ti-6Al-4V for minimum material removal using ball end mill”

By

Pavel Celis Retana

Miniaturization of medical devices is playing an important role in the manufacture industry. New drug delivery systems are being studied and developed, therefore materials to produce these devices must be investigated extensively. The objective of this work is to experimentally investigate and compare the machinability of Ti-6Al-4V titanium alloy produced via Selective laser melting (SLM) against the conventional machining method. 18 patches of 09 needles each were fabricated and machined with different cutting feeds (120,150 and 180mm/min) with aid of a minimum quantity lubrication (MQL) system. Machinability was examined in terms of cutting forces, tool wear, surface roughness and geometrical dimensions. Each cutting feed was tested by fabricating 3 patches from solid blocks of titanium with square tools of .8mm. Finish pass was performed with a .2mm micro ball end mill with a constant spiral toolpath. Comparison was performed by fabricating four patches with SLM with an excess material of 150 μ m and machined with the same previous parameters. 3D images obtained by optical microscope reveal that the main force applied in the finishing of needles is the Z axis and cutting forces were higher when machining SLM patches. Tool calibration is the main factor to obtain high precision in geometrical dimensions due to the variation in length because of thermal expansion. Surface roughness for all tests were below 1 μ m with best results when cutting feed is set at 120mm/min, reduction in edge radius for ball end mills affected negatively the surface roughness. An economic comparison was performed and showed that the SLM process has clear advantage over subtractive manufacture.

Table of Contents

Acknowledgements.....	5
List of symbols.....	10
List of Figures.....	11
List of Tables.....	14
Chapter 1.....	15
1. Introduction.....	15
1.1. Motivation.....	16
1.2. Problem Statement.....	16
1.4. General objective.....	17
1.5. Specific objectives.....	17
Chapter 2.....	19
2. Background.....	19
2.1. Trends in Manufacture of medical devices.....	20
2.3. Titanium alloy.....	23
2.3.1. Characteristics & Properties.....	23
2.3.2. Applications.....	24
2.3.3. Powder for additive manufacture.....	24
2.4. Micro milling.....	24
2.5. Minimum Quantity Lubrication.....	28
2.6. Additive Manufacture.....	29
2.6.1. Post processing additive manufacture of metals.....	30
2.6.2. Mold applications.....	31
2.7. Micro milling sintered materials.....	32
2.8. Selective laser melting combines with micro milling.....	33
2.9. Economic analysis.....	35
2.9.2. Cost Estimation in additive manufacture.....	37
Chapter 3.....	40
3. Methodology.....	40
3.1 Micro array of Titanium.....	41
3.1.1. CAM.....	43
3.1.2. Tools Measurement.....	46

3.1.3.	Experimental Setup	48
3.1.4.	Results	51
3.1.5.	Tool Wear	52
3.1.6.	Surface roughness	55
3.1.7.	Geometric dimensions	57
3.2.	Linear array of Titanium	58
3.2.1.	CAM	59
3.2.2.	Tools Measurement	59
3.2.3.	Experimental Set up	62
3.2.4.	Results	64
3.2.5.	Tool Wear	65
3.2.6.	Surface roughness	70
3.2.7.	Force Measurements	71
3.2.8.	Economic analysis	74
3.3	Milling + AM experiment in Stainless Steel	75
3.3.1	Geometry definition and fabrication	76
3.3.2	Characterization	77
3.4	Milling + Machining in Ti-6Al-4V	79
3.4.1	Geometry	79
3.4.2	Characterization	81
3.4.3	Experimental Set up	84
3.4.4	CAM	85
3.4.5	Results	86
3.4.6	Tool Wear	90
3.4.7	Surface Roughness	93
3.4.8	Cutting Forces	94
3.4.9	Economic analysis	96
Chapter 4	97
4.	Results & Discussion	97
4.1	Geometrical dimensions	97
4.2	Surface roughness measurements	98
4.3	Tool wear	99
4.5	Economic analysis	101

Chapter 5	103
5. Conclusions	103
5.1 Contribution	104
5.2 Future Work	105
5.3 Recommendations	106
6 References	107
7 Annexes	111

List of symbols

a_e	Axial depth of Cut (mm)
a_r	Radial depth of cut (mm)
AM	Additive manufacture
CAD	Computer aided design
CAM	Computer aided manufacture
CEL	Cutting edge length
CNC	Computer numerical control
D	Diameter of tool
f_z	Feed per tooth ($\mu\text{m}/\text{tooth}$)
HSM	High speed machining
L_c	Cutoff Length
MLSS	Milling combines laser sintering systems
MQL	Minimum quantity lubrication
MRR	Material Removal Rate
N	Spindle speed (rev/min)
R_a	Roughness average
RPM	Revolutions per minute
SEM	Scanning Electron Microscope
SLM	Selective Laser Melting
SM	Subtractive Manufacture
Ti6Al4V	Titanium Alloy
v_c	Cutting speed (m/min)
v_f	Feed speed (mm/min)
z	Number of teeth

List of Figures

Figure 1 Global value market of medical devices, information from global health care equipment & supplies, published by Daramonitor, may 2010.	20
Figure 2. Particle size dispersion of Stainless Steel with SEM [10]	24
Figure 3. Difference between conventional milling and hybrid manufacture process	33
Figure 4 Cost and Cost Structure for Piece A [42].....	38
Figure 5 Methodology for fabricating micro needles.....	40
Figure 6 Dimensions of micro array.....	41
Figure 7. Height and base dimensions of micro array.....	42
Figure 8. Dimensions of titanium blocks.....	42
Figure 9. 0.2mm and 1.0mm tools by Mitsubishi.....	43
Figure 10. Vortex toolpath simulation.....	45
Figure 11. Tool edge radius for flat end mill.....	47
Figure 12. Tool edge radius for ball end mill.....	47
Figure 13. Alicona Infinite Focus Microscope.....	47
Figure 14. 3D scan and overlap of 2 datasets.....	48
Figure 15. Kurt Clamp with Titanium block.....	49
Figure 16. Makino F3 Vertical Machining Center.....	49
Figure 17. Noga Mist Coolant System.....	50
Figure 18. Blum Laser for measuring tools height.....	50
Figure 19. Titanium after rough operation.....	52
Figure 20. Titanium after finish operation.....	52
Figure 21. Chips adhered to flat and end ball mills.....	53
Figure 22. Comparison of both edges of micro ball end mill.....	54
Figure 23. Curved dataset before and after form removal.....	56
Figure 24. Area of measurement for each needle.....	56
Figure 25. Height and Diameter for 09 needles machined.....	57
Figure 26. Linear array of 9 needles.....	58
Figure 27. Diameter measurement of flat end mill.....	59
Figure 28. Cutting plane to measure tool diameter.....	60

Figure 29. Experimental Set up with dynamometer and MQL	62
Figure 30. 4 probes machined with high and medium feed.....	63
Figure 31. Height measurement of 27 needles with 3 speeds	64
Figure 32. Lower diameter measurement of 27 needles with 3 speeds	65
Figure 33. Upper diameter measurement of 27 needles with 3 speeds	65
Figure 34. Edge wear on 800 um tool in SLM probe	66
Figure 35. Diameter reduction for 800um tool in SLM probe	66
Figure 36. Edge wear for cutting speed of 150 on tool 01 and 03	67
Figure 37. Edge wear for cutting speed of 180 on tool 02 and 04	67
Figure 38. Edge wear for cutting speed of 120 on tool 05 and 06	68
Figure 39. Ball end mill diameter wear	68
Figure 40. Tool wear for flat end mill	69
Figure 41. 3D dataset comparison of tools	70
Figure 42. Roughness measurements for different feeds on titanium block	71
Figure 43. Data for Fx Measurement of 01 needle.....	72
Figure 44. Forces applied at feed of 180mm/min.....	72
Figure 45. Forces applied at feed of 150mm/min.....	73
Figure 46. Forces applied at feed of 120mm/min.....	73
Figure 47. Experiment 14.....	74
Figure 48. 3D CAD model for needle array in SLM.....	76
Figure 49. SLM array in Stainless Steel 316L	77
Figure 50. SEM images from needles	77
Figure 51. Height measurement in Alicona.....	78
Figure 52. CAD model of 6 probes with 6mm base thickness	80
Figure 53. Part fabricated with SLM	80
Figure 54. SEM image from SLM needle	81
Figure 55. Tip of needle skewed to one side	82
Figure 56. Warping effect on SLM probe	83
Figure 57. Optical image of surface after polishing and after chemical attack	84
Figure 58. Manual alignment of cutting tool.....	85
Figure 59. Height measurements	86

Figure 60. Diameter measurements	87
Figure 61. Top diameter measurements	87
Figure 62. Cross section of needle.....	88
Figure 63. Morphology of top of the needles	89
Figure 64. Morphology of base of the needles	90
Figure 65. Cutting edge radius for .2mm ball end mill	91
Figure 66. Cutting edge radius for .2mm ball end mill	91
Figure 67. Diameter reduction for .2mm tools	91
Figure 68. Tool edge radius for .8mm tool	92
Figure 69. Tool diameter reduction for .8mm tool.....	93
Figure 70. Roughness measurement of 54 needles	94
Figure 71. Cutting forces for tool 01 of .2mm	95
Figure 72. Cutting forces for tool 02 of .2mm	95

List of Tables

Table 1. Mechanical properties of Ti-6Al-4V	23
Table 2 Parameters for 1mm flat end mill.....	51
Table 3 Parameters for 0.2mm ball end mill	51
Table 4. Tool edge radius comparison of micro ball end mill.....	54
Table 5. Parameters for roughness measurement	55
Table 6. Roughness and average Ra for 3 needles	57
Table 7. Diameter measurement of 0.8mm flat end mill.....	61
Table 8. Tool edge radius for both sides of tools used	61
Table 12. Cost estimation of micromachined array.....	75
Table 9. Geometrical measurements	78
Table 10. Results from SLM measurements	82

Chapter 1

1. Introduction

The technologies developed in the last 30 years allowing device miniaturization have increased considerably, making viable the manufacture of objects beyond the limits of the machining capabilities. Currently, it is possible to achieve closed geometric tolerances, to use new materials, tool geometries or toolpaths more adapted to machine miniature devices.

Drug delivery devices present characteristics that need to be attained for operability. Amongst others, they must be manufactured with materials biocompatible such as Titanium alloys (Ti-6Al-4V) which can be used in surgical environments and may be in contact with the human body for long periods of time. These devices also require high precision in the order of microns and finally, the economic factor to be able to satisfy the demand of the market must be taken into account.

Until a few years ago, the only way to manufacture these devices was by means of the conventional machining process. However, the development of advanced metal additive manufacturing process and micro machinability offers a new possibility to design and fabricate these micro devices without the need of large machining times and post processing work. The result is a faster and cheaper process that combines the best characteristics of both additive and subtractive technologies that could open doors in the manufacture of micro devices, as well as for the medical mold design industry.

1.1. Motivation

Design and development of new products with aid of state of the art technologies to manufacture devices with high impact in the micro fabrication for the medical industry that can be replicable and economically viable for mass production. Demonstrate the advantage of the micro needles over the conventional needles for drug delivery systems.

1.2. Problem Statement

Experimental investigation that combines Micro milling and Selective laser melting has not been investigated to validate the feasibility to produce micro geometries that can be economically viable. There should be a proper combination of parameters to apply the principles of subtractive and additive manufacture to reduce fabrication time and obtain the desire quality for micro devices.

1.3. Thesis Hypothesis

It is possible to produce and replicate micro geometries applied to medical devices with the combination of Selective laser melting for producing net shapes and using Micro machining for surface finish to reduce manufacturing costs and fabrication time without removing precision or quality in the geometry fabricated versus a single step manufacturing process.

1.4. General objective

Replication, fabrication and validation to manufacture a 9-needle shape geometry array with additive manufacture of Titanium alloy (Ti-6Al-4V) post processed with micro cutting tools with the aim of comparing this process planning versus a single step process.

1.5. Specific objectives

Specific objectives of the thesis are the following:

- Design, program and fabricate a needle shape array with aid of CAD/CAM technologies
- Evaluate the minimal excess material that can be added to the final shape before being micro machined to identify the benefits and limitations of the material added.
- Measure the surface roughness of the conical geometries generated for the micro machining process
- Obtain the desired measurement of the needles according to the CAD program evaluated through the measurement of the final finishing process
- Evaluate the tools implemented during the milling process to compare tool wear against time
- Implement a minimum quantity lubrication system to help reduce the tool wear, preventing tool breakage and reduce coolant waste to help the environment
- Analyze the forces applied on the top surface of the needles to compare the speed of the cutting tool related to the quality of the top surface

- Evaluate the economic factors that take the most impact into costs for producing this micro geometry
- Compare the results from micro milling vs AM technology in terms of surface roughness, forces applied and tool wear.

Chapter 2

2. Background

Conventional Milling has been for years a standard in the industry for fabricating molds and dies for the automotive, aerospace or medical industry with different materials such as titanium, stainless steel or other metallic alloys. At the same time, metal powder additive manufacturing technologies had been widely used for rapid prototyping for medical implants, dummies or functional parts for small batches or replacements parts in components that are very expensive to replace with a conventional machining process.

Both technologies have advantages and can create objects with high precision and quality depending on its size and shape. Combining both processes has led to an improvement in manufacturing time, decreasing costs and increasing capability for producing more variety of pieces in the same time.

Additive manufacturing (AM) for metal powders is used for creating net shapes of complex components while conventional milling is used as a post process required for improve surface finish leaved by the AM. Nevertheless, there is still a gap in the field of micro components that can be filled with these technologies. Overall, several studies are still required to demonstrate the feasibility of creating micro geometries of Titanium with AM for minimal material removal prior to be milled for finishing process with micro end mills in the range of hundreds of microns in diameter.

2.1. Trends in Manufacture of medical devices

According to data obtained by the “National Institute of Statistics and Geography (INEGI)” In Mexico, the industry of medical devices is composed by small and median enterprises that have a good performance in assembly and manufacturing process. Mexico has become a leader in the worldwide manufacture, being the country that supplies the most medical devices to United States and the 9th in the world. This represents between 2010 and 2015 an average of the 0.3% of the total gross domestic product and 1.5% of the GDP of manufacture[1].

The Trans-Pacific partnership treaty has helped to obtain 2,289.5 million dollars of investment into Mexico, directly into the medical devices industry. The outstanding production and export capability shown by Mexico has led to a consolidation for this type of industry. Devices such as suture needles, instruments, syringes and catheters are some of the products produced and exported to new markets such as Canada, Singapore and Chile. Estimated data from the “Global Health Care Equipment & Supplies” points to an ascending trend in the market value with an annual growth of 4.4%. By the year 2014 this value will ascend to 368,000 million dollars, as represented in Figure 1.[2]

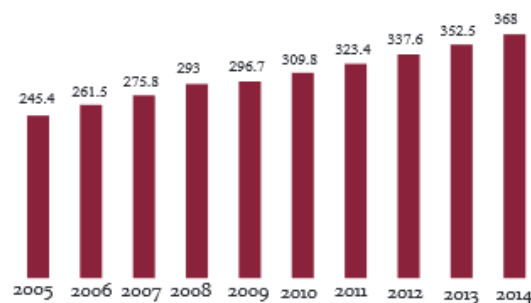


Figure 1 Global value market of medical devices, information from global health care equipment & supplies, published by Daramonitor, may 2010.

The main states that represent the primary source of manufacture for medical devices are Baja California, Chihuahua, Ciudad de Mexico, Jalisco, Sonora, Nuevo Leon,

Morelos, Tamaulipas and Estado de Mexico. Most of the main products exported by Mexico at a global scale are medical instrumentation for surgery and odontology. With a total participation of 77.9% in 2010 and strong competitively in the manufacturing process, its costs are 25% lower than United States, being Mexico the 8th best country for investment.

Over the last decade there has been an increase of 7% in the number graduated students from engineering according to data obtained from the National council for science and technology. This represents a great opportunity to continue developing research projects in the field of medical device manufacture. At the same time it is of great importance to continue the investigation into the micro devices that uses one or more different technologies that could achieve promising results[2].

Combining additive manufacture of metals & micro machining can also allow the development and fabrication of micro molds leading to the creation of other type of medical devices that need to be manufactured through plastic injection processes or ultrasound injection. According to the Secretary of Economy, 95% of the molds used in Mexico are brought from other countries. Having an important factor in costs and production time, the mold industry in Mexico has made an agreement to support the local manufacture, which has a potential of 8 billion dollars. Currently there are 106 companies registered in the “Mexican Association of Manufacture of Molds and Dies” (AMMMT) that work in the development and fabrication of dies and molds, and it is expected that by 2030 the mold manufacture can cover from 40 to 50% of the total market need in Mexico[1].

2.2. Advantages of micro needles

With annual growth for development of micro devices, new ways for drug delivery options are becoming available to be introduced in the market. These new devices can be found in different versions as patches that are placed over the skin to allow for medication to be absorbed through the skin into the bloodstream [3].

There are different types of needles such as hollow, solid, made with polymers or coated. Most of the disadvantages of conventional needles are the pain or discomfort caused in the injection site. This can be painful specially for patients that need weekly rounds of vaccines and a transdermal patch can be a pain free alternative. Another advantage of patches is the specific site dosing for placing the patch over selected areas where there can be inflammation or some injurie. Micro needles are capable of deliver macromolecules like insulin, growth hormones, immunobiologicals, proteins and peptides [4].

New materials and manufacturing processes can lead to create new patches that are biocompatible and biodegradable. Results from several groups suggest that micro needles are a promising, possibly and powerful technology for the administration of therapeutics into the skin[5]. These patches can allow the prevention of contracting diseases like HIV or hepatitis caused by injuries of sharp needles after they have been used.

There are lots of advantages that are being explored with different materials to allow a better and safer way to deliver drugs to patients, one of the materials explored in this thesis is the titanium alloy Ti-6Al-4V to manufacture them by mechanical micromachining with different technologies available.

2.3. Titanium alloy

Titanium alloy was discovered by William Gregor in 1791, it is considered as one of the more versatile metals due to its high resistance to water, salt and heat as well as its low density, making it suitable for applications where weight and resistance have dominant roles. There is a wide variety of titanium alloys that contains traces of Aluminum, Molybdenum, Vanadium, Niobium, Tantalum, Zirconium, Manganese, Iron, Chromium, Cobalt, Nickel and Copper [6]. One of these titanium alloys is the Ti-6Al-4V which is a grade 5 titanium alloy, one of the most commonly used.

2.3.1. Characteristics & Properties

Ti-6Al-4V has a high strength, low weight ratio and an excellent corrosion resistance [7], as well as good machinability and excellent mechanical properties used in a variety of applications that require lighter materials. Table 1 shows the mechanical properties of this alloy. There are several factors required for machining this type of alloy such as low cutting speeds, high feed rates, use of cutting fluid, sharp tools and a rigid setup to prevent shatter.

Mechanical Properties of (Ti-6Al-4V)	
Density	4.42g/cm ³
Hardness, HB	345
Tensile Strength	995 MPa
Modulus E	113.8 GPa
Melting Point	1670°C

Table 1. Mechanical properties of Ti-6Al-4V [8]

2.3.2. Applications

Ti-6Al-4V is generally used to manufacture parts and prototypes for aerospace industry, biomechanical application, gas turbines, chemical industry, marine application, dental, hip or head implants and prosthesis. This material is biocompatible, which means it does not harm living tissue or bone when in direct contact [9].

2.3.3. Powder for additive manufacture

This and other materials such as stainless steel or aluminum can be found in powder presentations for applications with SLM technology. Particle size distribution from stainless steel was obtained through Scanning Electron Microscope (SEM) shown in Figure 2. It can be seen that the majority of the particles presents a spherical shape. The size distribution was found to be between 7 and 55 μm , with an average diameter of 25 μm [10]

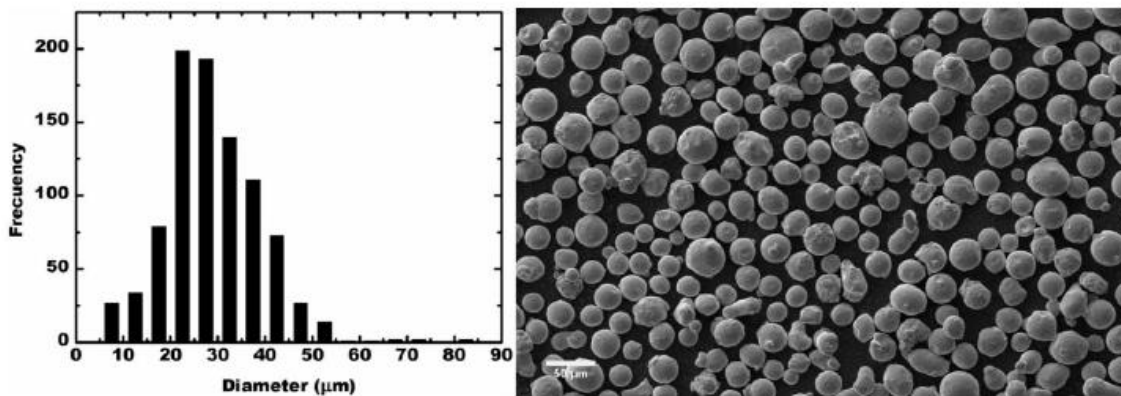


Figure 2. Particle size dispersion of Stainless Steel with SEM [10]

2.4. Micro milling

New milling and miniaturization technologies have intensively increased over the last years [11]. Everyday objects are getting smaller and possess improved characteristics or features that add functionality, saves time, money and material [12]. Large demand of these components represents an area of opportunity to develop new ways to manufacture micro

devices implementing more than one technology for reducing time while saving costs and maintaining high precision.

Milling is the process where a rotary tool removes material from a defined work piece with x,y and z dimensions by moving in a specified direction and angle to obtain a final shape. There are different processes or strategies covered by the milling technologies such as rough operations where large quantities of material are removed with large tools to get a stepped surface. Thereafter, a second process called finish is performed with another tool of smaller diameter to remove less material with a specified direction to obtain a desired surface finish. Finally, there can be another machine for a post process where aesthetics can be improved according to the specifications of each product manufactured.

Mechanical Micro machining process is the manufacturing method for miniaturized devices and components of sizes ranging from tens of microns to several millimeters [13]. Micro milling differs in many aspects from the traditional milling processes due to the increase of Revolutions Per Minute (RPM) needed for the micro tools, generally greater than 18,000 rpm and up to 110,000 rpm in some special machine tools. Cutting processes also differs from conventional milling for the chip thickness and quantity of the material removed by teeth, as well as the diameter of the tools which is smaller. Due to these factors, the cutting speed (v_c) is slower than the conventional process and more expensive due to the time involved in cutting small quantities of material and the need of several tools to perform this.

Micro milling has been widely studied performing experimentations over several materials such as aluminum, hardened steels or titanium. Cutting parameters are of big importance to obtain different geometries, shapes and analyze surface roughness, burr,

defects, tool wear, as well as measuring forces during the experiments. Micro milling presents new opportunities for a demanding market with new software for CAD/CAM simulations for improving the cutting strategies according to the shape that it will be manufactured.

Several investigations have been performed to analyze the machinability of titanium alloys, its applications and the challenge of machinability due to its properties. A particular trend show support for the environment by using cutting fluids like water vapor, air and other gases in order to improve the machinability and ensure a green cutting process [14].

Cutting parameters such as tool position, speed, feed and engagement of the tool were analyzed during milling of concave surface of Ti-6Al-4V. The position of the tool influenced the surface roughness using a ball end mill of 16mm with removable inserts coated with TiAlN, showing that values of the roughness increases according to the increase of the speed feed [8].

Other evaluations performed in milling titanium are the burr height predictions by mathematical modeling. This model predicts the burr height at high cutting speed, reducing burr height by 90% compared to lower cutting speeds when using uncoated tungsten carbide tools with helix angle of 30° and diameter of 300 and 500 microns[15]. Several studies have used finite element simulation to investigate micro milling and its effects on tool wear. This has been done by performing a process to improve performance of carbide micro end mills of $508\mu\text{m}$ with application of coating of CBN, differentiating the tools without coats and analyzing the results in terms of surface roughness, burr formation and tool wear with FEM analysis. This shows that the CBN coated tools outperformed the

uncoated carbide tool in wear and cutting temperature, concluding that the cutting forces in the micro end mills is mainly influenced by edge radius and feed per tooth [16].

Conventional micro machining differs from micro milling in the cutting parameters, speed needed and chips generated. Since micro milling requires high revolutions per minute and low movement of the feed direction, the proper parameters for the right cutting process and chip generation must be identified. This will result in a shear of material with every tooth of the tool instead of just apply deformation of the material without cutting, as this would generate a wrong surface finish on the processed material. Experiments performed over Ti-6Al-4V when machining with 1mm square end mill have shown that tool cutting edge radius increased and decreased during initial stages of machining. Variation of surface roughness decreased until cutting edge of the tool becomes equal to the feed per tooth, thereafter, surface roughness increases[17].

Since the objective of milling metals is to obtain a desired shape, it will not be useful if the surface quality of the work piece it is not within range of the application needed. Different toolpaths in the milling process can drastically affect the result in pieces or molds fabricated. Furthermore, it has been demonstrated that the roughness of free forms strategies after milling is much influenced by the tool path strategy. This shows that an adequate choice of the tool path can save up to 88% time and 40% cost for finishing molds compared to the less appropriated tool path using carbide end mill of 6mm diameter in AISI P20 steel [18].

Titanium alloy requires high speeds, while the heat generated must be dissipated with help of coolant that acts as a lubricant for obtaining better surface and at the same time maintains the tools sharp for longer production.

2.5. Minimum Quantity Lubrication

Cutting fluids are coolants used in the milling process to improve the tool's life, reduce the temperature and act as a lubricant for preventing chip adhesion. There are several types of coolant methods available for the milling process, among them are:

- Flood
- Minimum Quantity Lubrication (MQL)
- Cooled Air

Due to the nature of the micro milling process, flood coolant method is expensive and unnecessary because of the large amount of cutting fluid used. Its effectiveness is better under low speed conditions and it is not recommended for the environment. As a response to this, other methods are being studied to maintain the benefits from the use of coolant but without the large quantities of it.

In the MQL method, a nozzle is connected to the air supply while another hose is connected to the coolant container. Using this method, the amount of coolant used is drastically reduced from liters to milliliters per hour. MQL acts as a film covering the work piece and the tool to maintain it wet to prevent adhesion and heat increase during the milling operation. Other qualities of this method are the improvement of tool life, reduced burr formation, money saving and generating a cleaner environment for the operator.

Investigation on the use of MQL in micro geometries on various alloys has been done over the last 10 years. Vegetable coolant is one of the variations used with titanium alloys, showing that MQL machining can remarkably and reliably improve tool life and reduce cutting force due to the better lubrication and cooling effect of the mist applied [19].

Surface roughness obtained with the use of MQL is improved by varying the cutting speed and feed rate using vegetable fluid compared to no lubrication. The application of MQL at a fluid rate of 60ml/h increased tool life of carbide inserts coated with titanium carbon nitride and reduced the average surface roughness while maintaining the same cutting conditions [20].

Several cutting experiments are performed under different cutting conditions with variation such as dry machining, jet application and MQL. Analyzing the results in terms of accuracy, surface quality, tool wear, burr formation and tool geometry shape, MQL reduced burr formation, tool wear and presented better results than traditional cooling techniques [21].

2.6. Additive Manufacture

3D printing has become a massive industry for the prototyping and final product fabrication. The 3D printing process for creating three dimensional objects can be made from different sources of materials such as photo curable resins, polymer or metal powders. This last method has been in the eye of the researchers and enterprises for developing new applications for different fields as opposed to a few years ago, where it was not even considered as a method for functional parts.

AM has the advantage of using fewer materials than subtractive technologies by adding layer by layer to create a final form with complex shape. More specifically, AM for metal powders can create geometries that other processes cannot accomplish like casting or machining methods. AM uses a high fiber laser to fuse the fine metallic powder together to

form a fully functional 3D part for different applications as the ones described in the previous section.

AM systems can process a different range of metals from Ti6Al4V, cobalt chromium, stainless steel and aluminum alloys, saving time compared to the traditional milling [22] and using only the amount of material needed. Limitations of this technology in powder fusion include the surface quality achieved in micro geometries. Compared to pieces in the range of centimeters for mechanical purposes where tolerances are not so closed, in micro geometries it becomes important to achieve closed tolerances and high-quality surface finishes for the applications involved. Ultimately, in most cases a post process method must be carried out to improve the look of the final part for aesthetics or functionality when the piece fabricated must be in contact with another piece for rotational movement.

Experimental investigation of machinability of nano-TiC reinforced nickel based super alloy Inconel 718 fabricated by selective laser melting conducted in terms of wear, cutting forces and chip morphology points that the effect of feed rate is statistically insignificant, contradictory to the conventional machining [23].

2.6.1. Post processing additive manufacture of metals

Most of the processes carried out when using additive manufacture of metals requires a post processing. This has been proved when sintering stainless steel 316L printed in a Renishaw AM250 post processed with solid carbide of 0.5” followed by fine abrasion finishing to reduce the surface roughness. The effectiveness of the post processing strategy shows an improvement on the overall surface roughness below 40 nm and porosity over

89% when compared to the pieces fabricated from laser fusion bed process without post processing[24]. Some post process can be required to meet particular mechanical properties, but also this properties can be regulated by changing the energy density and the combination of the machining parameters[25].

2.6.2. Mold applications

AM has also been used to analyze the feasibility to produce molds & dies for producing large quantities of products in the plastic injection industry. Through FEM analysis it is possible to study the behavior of the sintered material when a milling process is applied. AM is also convenient to test molds for plastic bottles and giving a reliable solution in the case of rapid injection of tens of thousands of plastics parts and there is no time to produce a conventional mold [26]

These studies have been performed in macro geometries, showing numerous advantages of the AM process. Amongst them are: the capacity to fabricate and implement conformal cooling channels using indirect SLM with combination of high speed machining operation with Electrical discharge machine (EDM), saving up to 25% in productivity and 11% in energy saving, creating complex shapes for tooling leaving an excess material of 0.5 to 1mm for the post processing and reaching a surface roughness Ra of 2 μm [27].

Plastic injection molds can be produced via indirect SLM methods, but a post process is always required for this kind of molds. The plastic injection industry requires process and surface finish that conventional machining sometimes cannot accomplish. However, production of these molds can consume less time with different types of powders mixed

with composite elemental metal powders [28] or AISI 1055 using ball end mill for reaching the final form [29]. There are a lot of materials that can be applied for mold fabrication using AM, such as rapid steel, copper polyamide and Cibatool-Express for modular tool inserts that can offer a fast low cost alternative to aluminum mold tooling [30].

It must be considered also the effectiveness of the process of AM technology depending of the size of the piece required. For large models in aviation industry there is not an advantage due to the slowness of the process. It is however more flexible in the freedom of design when lattices or evolutive shapes are required in reduced dimensions when applied to AISI4340 alloy steel[31]. Combining additive manufacture with HSM is significantly cheaper and faster than CNC machining, it can take 42% less time and 28% less cost than producing with CNC only [22]. Time and cost savings are produced by the reduction of parameters by eliminating rough machining from the traditional process where a block of metal has to be slowly reduced to the final shape. [32].

2.7. Micro milling sintered materials

There is a limited amount of literature on the machinability of micro milling sintered materials. This area is being investigated in tungsten copper composite material with micro end mills of 0,5mm diameter for applications for electrical discharge machining [33]. It is expected that with adequate parameters, the dimensional accuracy and surface quality desired can be obtained. There is a great opportunity to investigate the feasibility to fabricate and machine micro geometries produced by AM technologies by combining both processes.

2.8. Selective laser melting combines with micro milling

The combination of the process of additive manufacture & machining can be made by two ways. In the previews section it was discussed the capabilities of the process where a machine tool fuses powder of metal into a shape, after that process, it is taken into a milling center to generate the post processing. This means that there are two machines involved in the process but no necessarily in the same area. There is a new term called Hybrid manufacturing process where both technologies are combined into one single machine. The main difference relies on the fact that one layer of material is deposited and after several layers, the milling tool rectifies or gives shape to the green part making the desired geometry since the very beginning of the fabrication of this piece.

Figure 3 shows a representation of these two manufacture methods, on the left is represented the conventional milling where complex geometries with negative walls cannot be manufactured due to the collision of the holder against the work piece. On the left it can be seen that when both processes are combined, since each layer is deposited one after the other, the tool can manufacture several parts with no risk at all.

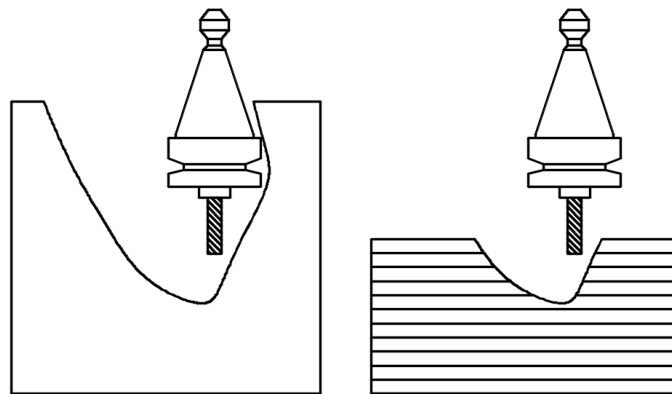


Figure 3. Difference between conventional milling and hybrid manufacture process

Milling combines laser sintering systems are used to investigate the machinability of chromium molybdenum and maraging steel. By measuring the cutting force and temperature using ball end mills to understand the influence of different hardness of the sintered materials, maraging steel showed a great prospect of producing molds by MLSS due to its high hardness and good machinability [34]. There are several strategies for adding and removing material at the same time. Other type of strategy is applied for fabricating complex structures combining direct metal deposition and a five axis CNC milling process for accessing difficult internal features with an undercutting mill, being more economic than traditional machining when dealing with expensive materials [35].

This machine tools combination naturally leads to the fabrication of molds for plastic injection industry. This was studied by fabricating a mold of SS41 steel for an injection device of 4mm with a sloping surface. Fabricating also the runner with this process with a layer thickness of .5mm to reduce fabrication time, with advantages of fabricating it with cooling channel and giving the proper finish with other tools like drills for pin ejectors. Injected parts demonstrated that the mold fabricated is feasible if the layer thickness can be reduced but the time of fabrication will significantly increase [36]. This exemplifies the fabrication of small molds in a reduced scale, but not as small as micro components fabricated by micro milling.

Applying this process to the mold industry can have several benefits: it halves the lead time required in the conventional machining processes, molds with deep ribs can be manufactured in one process, and adequate cooling channel can be composed freely improving the injection accuracy and mold cycles[37]. There are however several aspects to take into consideration when combining milling and AM process, such as the material

needed to mill in the finishing pass to get to the final dimension required according to the CAD model. By using cooling channels in this hybrid process, the cycle time is reduced by 37% and cooling time is reduced 50%, generating cost reduction directly. [37].

There is still a great window of opportunity to investigate the milling of micro geometries fabricated by AM process. Experiments were carried out with flat end mills of 2.0mm [38] and ball end mills of 0.6, 1.0, 2.0 and 6.0 mm in rectangular blocks of 120mm x 5 x 8mm made by MLSS. Different passes were created to evaluate the flank wear using micrometer with microscope and obtaining forces at a speed of 56m/min of 93 to 126 Newton's with a 6mm ball end mill. Small scratches appeared in the surface of the milled work pieces, results suggest that there is a possibility that powder interfered with the cutting process and that affects the surface finish[29] .

It can be concluded that MLSS can produce macro geometries with overall good surface roughness applied to the plastic injection industry. It is required to verify if this technology can be applied to the manufacture of micro devices with the required variation of parameters due to the limitation of size of the device fabricated which can be in millimeters or less with the use of Ti-6Al-4V.

2.9.Economic analysis

Cost estimation for conventional and micro milling differs in many ways from additive manufacturing process, both technologies are used to fabricate high quality end-useable parts[39], each part depends on the complexity of the geometry, size, precision and material involved in the development.

2.9.1. Cost estimation in micro milling

Cost estimation for micro milling is composed of four items shown in equation 1. This model presented by Kang & Ahn calculates the total machining cost for a specific designed part. Parameters considered are the estimated time of the toolpath, preparation time, tool cost and operators wage[40].

$$C_{total} = C_w + C_p + C_m + C_t \quad (1)$$

C_w is the material cost, C_p is preparation cost, C_m is machining cost, and C_t is tool cost. Material cost is estimated with equation 2.

$$C_w = V_p C_{um} \quad (2)$$

V is the raw material in m^3 , p is the material density (kg / m^3) and C_{um} is the unit price (\$/kg). Preparation cost is calculated with equation 3.

$$C_p = W T_p \quad (3)$$

T_p is the time for preparing the machine setup and W is the operator's wage per hour of labor. Machining cost is calculated with equation 4.

$$C_m = T_m (W + B_m) \quad (4)$$

T_m is the machining time and B_m is the indirect cost calculated with the depreciation of the machine (M_t) and the indirect cost of the maintenance and repair. B_m is obtained with equation 5.

$$B_m = M_t + M_t \left(\frac{\text{Machine overhead [\%]}}{100} \right) \quad (5)$$

M_t is calculated with equation 6.

$$M_t = \left(\frac{\text{initial purchase cost of machine}}{\text{working hours} \times \text{repayment period}} \right) \quad (6)$$

Finally tool cost is calculated with equation 7.

$$C_t = y \left(\frac{T_m}{T} \right) \quad (7)$$

In this equation, y is the initial cost of the tool, T_m is the machining time and T is the average tool life obtained by Taylor's equation from empirical results from regression analysis with a specified tool and material. Other models for calculating costs in conventional milling were developed and like in SLM cost estimation. It can be divided into five sections, main machine cost, manufacturing auxiliary cost, material cost, energy cost and labor cost[39].

2.9.2. Cost Estimation in additive manufacture

Cost estimation in AM should be able to capture the overall cost tendency with changes in certain parameters of the application. The priority of the method is to see when the part complexity changes and how does the overall costs of the SLM manufacturing process change [39], as the major fraction of cost is the investment on the machine [41]. There are basic build models developed that work with powder addition time, machine idle time and scan time, post processing is not considered because of the variation that can be possible due to the requirements of each company. Total cost can be calculated using Equation 8 [42].

$$C_{\text{build}} = C_{\text{indirect}} * T_{\text{build}} + W * \text{Price}_{\text{material}} + E_{\text{build}} * \text{Price}_{\text{Energy}} \quad (8)$$

This formula was implemented in a case study, showing that for 42 pieces produced by AM process, the cost per part starts to decrease compared to the other part made by

conventional mold. For small pieces, a test was performed in two scenarios for one piece alone in the base and a full base with 210 pieces. Single piece of type A costs 258 euros against 32.30 euros with a platform full of pieces with saving of 126 euros, meaning a 79.6% with a time of fabrication of 1h 42min for the full platform. Figure 4 shows the cost structure of the test build of piece A.

Piece A			
Cost components	Single piece	Full platform build (40 pieces)	Full platform build savings %
Machine cost, €	158.00	29.50	81.30
Material cost, €	2.44	2.44	-
Energy cost, €	1.94	0.37	80.90
Total cost, €	162.38	32.30	79.60
Work time, min	529	102	80.70

Figure 4 Cost and Cost Structure for Piece A [42]

Other ways to explore the cost of AM is the fabrication of tools and molds. After the fabrication of a die made by SLM, the dimensions have to be measured by a 3D scanning system to confirm that dimensions are within tolerances before milling or EDM. The molds are hardened by heat treatment, polished and reviewed again for dimensional accuracy, finally, all the components are assembled for their first trials. The potential for saving costs and time depends on the complexity, shape, dimensions, material and the chosen style of tooling and modular design. The rising demand of additive manufacture technologies will cause a reduction of the costs of metal powders and therefore, molds, devices or tools will decrease over the next years to come [43].

Estimating costs for multiple parts in a full platform can be obtained by dividing the total cost between the total pieces built in the platform. However, there is a problem when calculating costs if the pieces are not always of the same size or shape. Currently, models

are being developed to take care of this issue, including the pre and post processing steps linked to the AM process. Enabling a precise determination of the total cost per part and avoiding that any geometry is preferred are of great importance when building parts for different projects, helping optimize build jobs and manufacture SLM parts more economically [44].

In this section it was discussed the economic factors that influence the cost in the AM process for building single or multiple parts from one or several customers. In the SM process, most part of the cost remains dominant by the metal bulk purchase [39]. Cost in the SM process increases in parallel as the complexity increases while AM process shows more cost advantages in parts with higher complexity scores, which gives an advantage to the SM process under the same conditions. Customization is another driver for economic products. Using AM has economic advantages with lower production volume compared with SM cost. It also has a lot of freedom of fabrication regardless of the shape complexity, does not require tool change and gives a substantial saving compared to conventional subtractive manufacturing process[39]. Studies showed that SLM has economic advantaged over SM machining process when production volumes are relatively low and with expensive materials.

Chapter 3

3. Methodology

This chapter gathers and discusses all the information relevant to this thesis in response to the problem statement presented in Chapter 1 regarding the fabrication of micro devices of Titanium alloy with the combination of AM and Micro milling. It also presents various procedures, strategies and experiments to identify the proper parameters for the development of micro needles. Several experiments were performed before reaching the combination of both technologies. This section specifies all the instrumentation required, data obtained, tools used, materials and design as well as data processed. Figure 5 describes the methodology and steps performed to fabricate and validate the feasibility of the micro needles in Titanium Alloy.

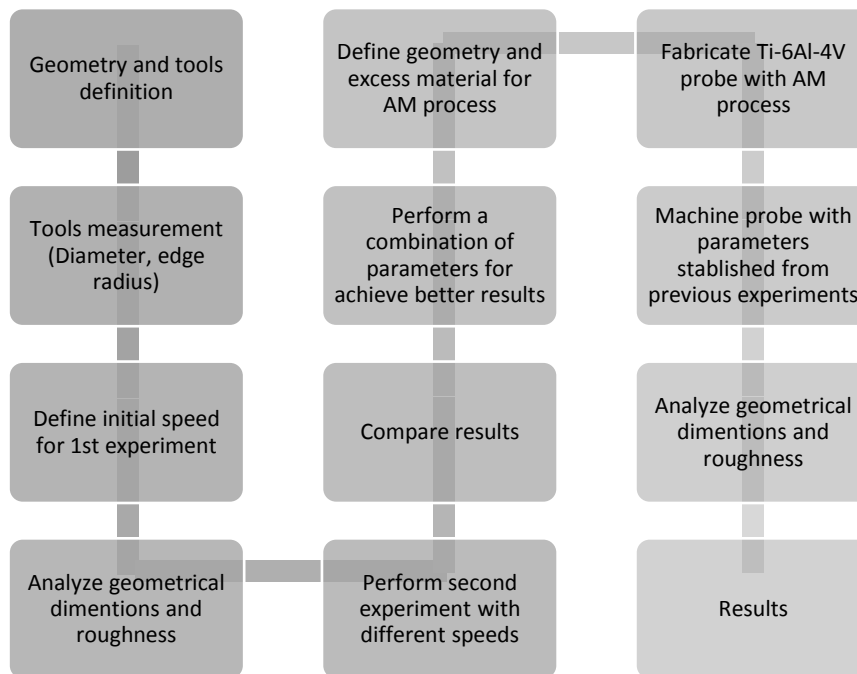


Figure 5 Methodology for fabricating micro needles

3.1 Micro array of Titanium

A micro geometry was developed with aid of computed assisted design, using Solid Works and Inventor by Autodesk, the geometry consisted of an array of 9 needles with a diameter and height of 100 μ m. Figure 6 and Figure 7 shows the initial geometry and dimensions in millimeters.

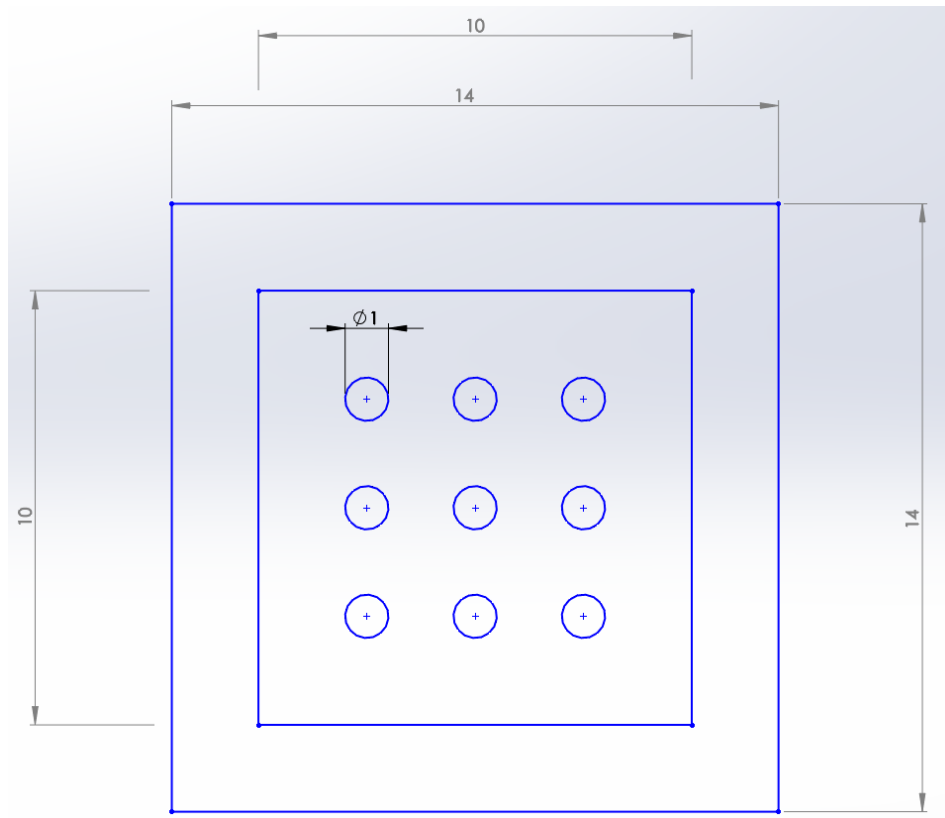


Figure 6 Dimensions of micro array

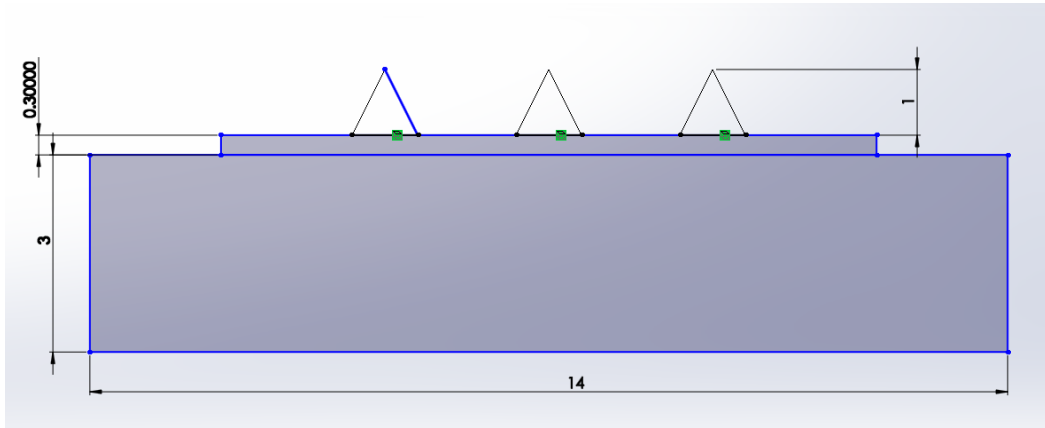


Figure 7. Height and base dimensions of micro array

The material used for all experiments involving machining operations are blocks of Titanium alloy (Ti-6Al-4V Eli) of 9.52mm height, 38.1mm width and 80.0mm length with drills for screwing the block to a fixture later explained in this chapter (Figure 8). Tools used were a 1mm Diameter Mitsubishi Flat End Mill (CRN2MSD100S04) with 2 flutes and a Cutting edge length (CEL) of 2.5mm and a 200 μ m Ball end mill (MS2BR0010S04) with 2 flutes and CEL of 0.3mm (Figure 9).

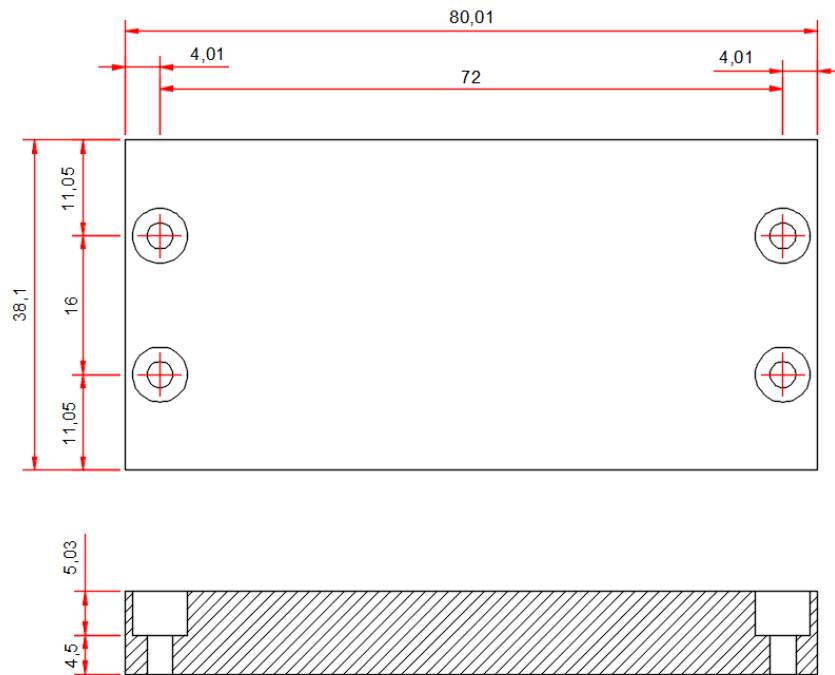


Figure 8. Dimensions of titanium blocks

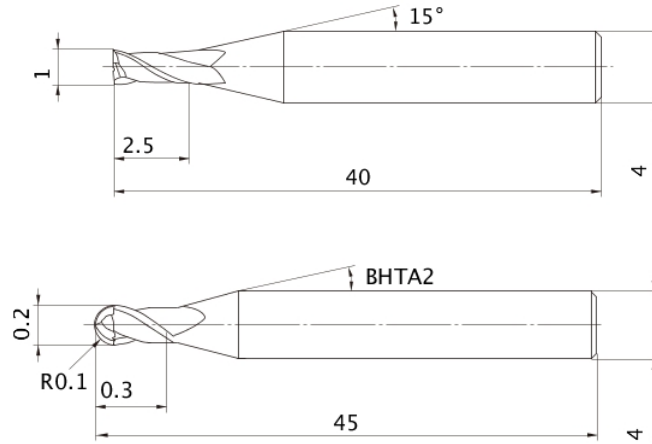


Figure 9. 0.2mm and 1.0mm tools by Mitsubishi

3.1.1. CAM

CAD design was exported to Autodesk Power mill software to perform its G code with aid of Computer Aided Manufacturing solutions (CAM). A newly developed method for fast material removal was selected to study its feasibility in the micro scale called Vortex, used in the rough operation. This strategy was developed by Delcam and it was introduced in 2014 to remove large quantities of material with aid of the full cutting edge length of the tool, achieving savings of time from 40% to 70% compared to conventional machining where the depth of cut is smaller. Vortex toolpath is calculated by following the shape of the piece by keeping raise moves at the minimum. This is especially helpful when deep areas of material must be removed, as opposed to using a depth of cut very low that is time consuming and will wear the tool's tip early in the milling process.

Vortex strategy remains the engagement angle for the complete operation, maintaining the same cutting conditions for the complete toolpath. This strategy is used primarily for the mold industry when tools used are in the range in the macro scale from 10 to 25mm of

diameter, however, this advanced improvement in material removal will be applied to the micro milling process for the same principle in a reduced scale. Strategy for milling the Titanium block is based on the following steps.

Clearance area removal (Vortex)

Vortex strategy is used in the rough operation during the experiment using only .5mm from the 1.5mm of the CEL of the tool. Since a large engagement part of the tool is exposed to cutting forces, a small amount of radial depth of cut (a_e) is selected; specifically using a 5% of the tool diameter at a constant spindle speed of 30,000 rpm and a feed rate of 480 mm/min, lower than the recommended supplier's feed which is 1500mm/min. With this parameter, a constant feed per tooth is set at 8 microns/tooth during rough operation. Time involved for this operation was of 1 hour and 40 minutes. Figure 10 shows the simulation of vortex strategy showing how this process follows the shape with small movements in 3 different steps, the first step removes 0.5mm, the second step removes another 0,5mm and the final step removes the 0.3mm of the outer area of the probe. To prevent a lot of ramping moves, a section of the CAD model was modified with boundaries to indicate to the software that in this area, the tool can start cutting from the outside of the stock material, this allowed the toolpath to make this operation with no ramp movements at all.

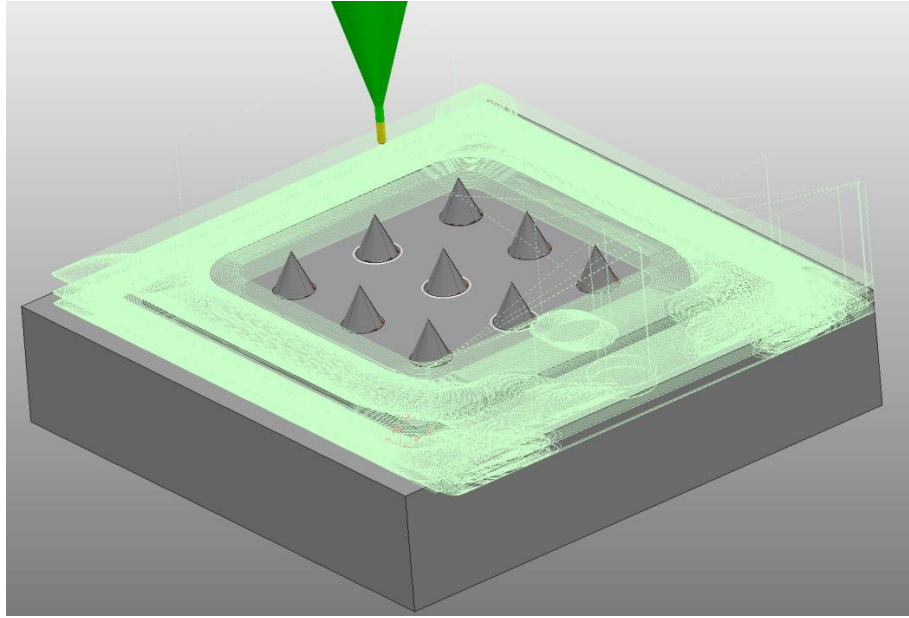


Figure 10. Vortex toolpath simulation

Needle Semi finishing

For the semi finishing process, a constant step down strategy was used with passes of .05mm, leaving the same 0.05mm of material left on the stock model to be removed by the micro ball end mill. Toolpath generated starts at the top of the needle and continues until reaching the next flat area which is the base of the needles; this process took an estimated time of 5 minutes to be completed with the 1mm flat end mill.

Constant step-down and spiral finishing

Two different strategies were used to finish the needles, fist strategy used with the micro ball end mill of 200 μm is a constant step down toolpath. This strategy creates a constant step following the shape of the needle from the top to the bottom, every time a level is finished, the tool goes down .003 mm and continues to mill the next level until reaching to

the flat area of the model. Feed was interpolated due to the high speed required according to the supplier from 40,000 RPM to 30,000 RPM according to the limit of the machine used for this process. Second strategy is the same principle as the first one with the different in the approaching of the tool for every level. In this strategy the tool is always changing in the Z direction, this means that the Z axis is all the time going down causing a spiral towards the floor of the needle. The speed was kept the same and each toolpath was implemented in 3 needles, estimated time for each needle was 5 minutes.

3.1.2. Tools Measurement

Tools used were measured using a system specially designed to measure tools called Alicona Infinite Focus. A coordinate measurement machine and surface roughness measurement device in one system showed in Figure 13. This machine combines high resolution, high repeatability and high accuracy with resolution down to 10 nanometers, minimal measurable roughness Ra of 7 to 0.03 μm with objective magnifications of 2.5x, 5x, 10x, 20x, 50x and 100x. Edge Master Module is an optical 3D measurement device for automatic cutting-edge measurement included as part of the software included in the microscope. This module was used to measure the cutting edge for both flat and ball micro tools. Figure 11 shows the measured profile for flat end mill and Figure 12 shows the measured profile for ball end mill.

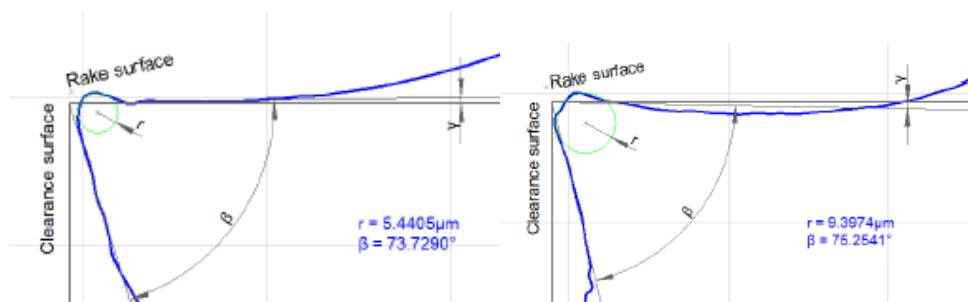


Figure 11. Tool edge radius for flat end mill

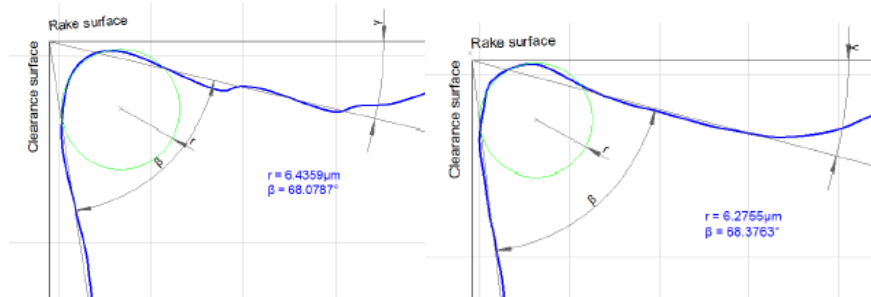


Figure 12. Tool edge radius for ball end mill



Figure 13. Alicona Infinite Focus Microscope

A specific angle of measurement was established for measuring each type of tool. For the flat end mill 30° was set, while 45° was chosen for the ball end mill due to the visualization of the edge of the tool. Real 3D module is a combination of different surface measurements merged to create a fully 360 scan dataset by overlapping measurements. This is allowed by using the 5th axis of the machine by rotating the unit with single measurements joined together.

Tool wear is analyzed on the entire tool by combining the 3D information obtained before and after the milling process (Figure 14). This provides useful information about the deviation presented and how the machining process is affecting the shape and edges of both micro tools. To perform the overlapping of the datasets, a manual alignment must be performed by the user by selecting points shared by both 3D, which generates an initial comparison. Right after the overlap, the software automatically aligns both scans to obtain a better result to initiate the comparison and see the deviation in microns in the whole new dataset generated.

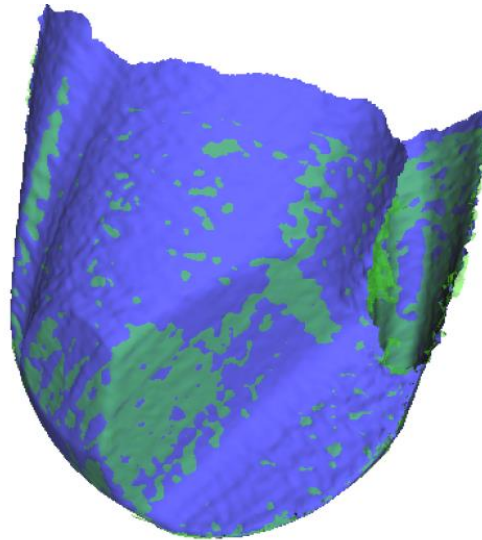


Figure 14. 3D scan and overlap of 2 datasets

3.1.3. Experimental Setup

First experiment was performed in a Makino F3 Milling machine with 3 Axis with a Maximum spindle speed of 30,000 RPM. Magazine up to 30 tools with a working table of 1,000mm x 500mm, positional accuracy of ± 0.0015 mm, repeatability of ± 0.001 mm and a

rapid traverse of 20,000 mm/min (Figure 16). The tool holders are Mega micro chuck by Big Kaiser and a Kurt Clamp for holding the titanium block showed in Figure 15.



Figure 15. Kurt Clamp with Titanium block

The lubricant applied for this experiment is a vegetable oil TRI-Cool MD1 by TRICO with a viscosity of 34cSt[21]. The MQL system used for this experiment is a Tankless Mist Coolant Unit Hose by NOGA with magnetic base and Loc-Line flexible hose with an On/Off air & fluid control (Figure 17). The amount of coolant used was based on experiments performed in other studies with greater tool diameters [21][19][20] giving a flow rate of approximately 10ml/h.



Figure 16. Makino F3 Vertical Machining Center



Figure 17. Noga Mist Coolant System

Tool height measurement was performed with a Blum tool laser measuring system for non-contact tool, using high quality laser optic, intelligent NT electronics and unique Blum protection system with a repeatability of $0.1 \mu\text{m}$ and minimum tool diameter of $5\mu\text{m}$ (Figure 18).



Figure 18. Blum Laser for measuring tools height

After the titanium was machined, it was cleaned in an ultrasonic machine to remove fine particles adhered to the surface for 5 minutes and air pressure was used to dry the work piece and remove other fine particles adhered. Surface roughness measurements were performed on the Alicona infinite focus microscope. Cutting parameters for ball end mill and Flat end mill were taken from the supplier, adapted to the size and geometry of the work piece. All the parameters are listed in Table 2 and Table 3.

Cutting parameters for rough operation		
Process parameters	Units	Value
Tool Diameter, (D)	mm	1
Spindle speed, (N)	min^{-1}	30,000
Feed (vf)	mm/min	480
Radial depth of cut (a_e)	μm	30
Axial depth of cut (a_p)	μm	550
Feed per tooth (f_z)	$\mu\text{m}/\text{tooth}$	8

Table 2 Parameters for 1mm flat end mill

Cutting parameters for finish operation		
Process parameters	Units	Value
Tool Diameter, (D)	mm	.2
Spindle speed, (N)	min^{-1}	30,000
Feed (vf)	mm/min	120,150,180
Axial depth of cut (a_p)	μm	3
Feed per tooth (f_z)	$\mu\text{m}/\text{tooth}$.002-.003

Table 3 Parameters for 0.2mm ball end mill

3.1.4. Results

Micro milling of titanium alloy was performed using micro end mills of 1mm for fast removal of material and .2mm for finishing the inclined wall of the needles. Both toolpaths were implemented using vegetable oil for preventing material adhesion to the

tools, reduce heat and decrease tool wear. Time involved during this experiment was at 1.4 hours with a total coolant use of 10.49ml. No tool breakage was presented, and the cutting speed of both tools was remained at about 70% to 100% of the initial parameters given in previous section. Figure 19 and Figure 20 show the process for rough operation and finishing process after the program was finished.

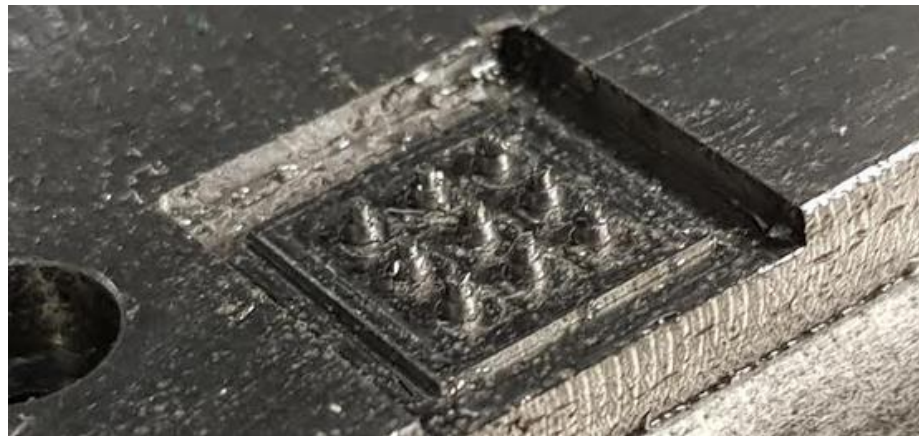


Figure 19. Titanium after rough operation



Figure 20. Titanium after finish operation

3.1.5. Tool Wear

Tools were measured before and after the milling process. Both tools were taken to inspection under the Alicona Microscope to see if there are chips adhered, possible tool breakage, tool wear and cutting edge diameter variation. At first sight, chips were adhered to both tools mainly due to the lubricant still attached to the tools causing the chips to stick

to the body as seen in Figure 21. Chips adhered to the micro ball end mill are significant larger than the ones presented in the flat end mill, this is caused by the remaining chips left on the work piece after the rough operation causing to drag large chips towards the body of the micro tool.

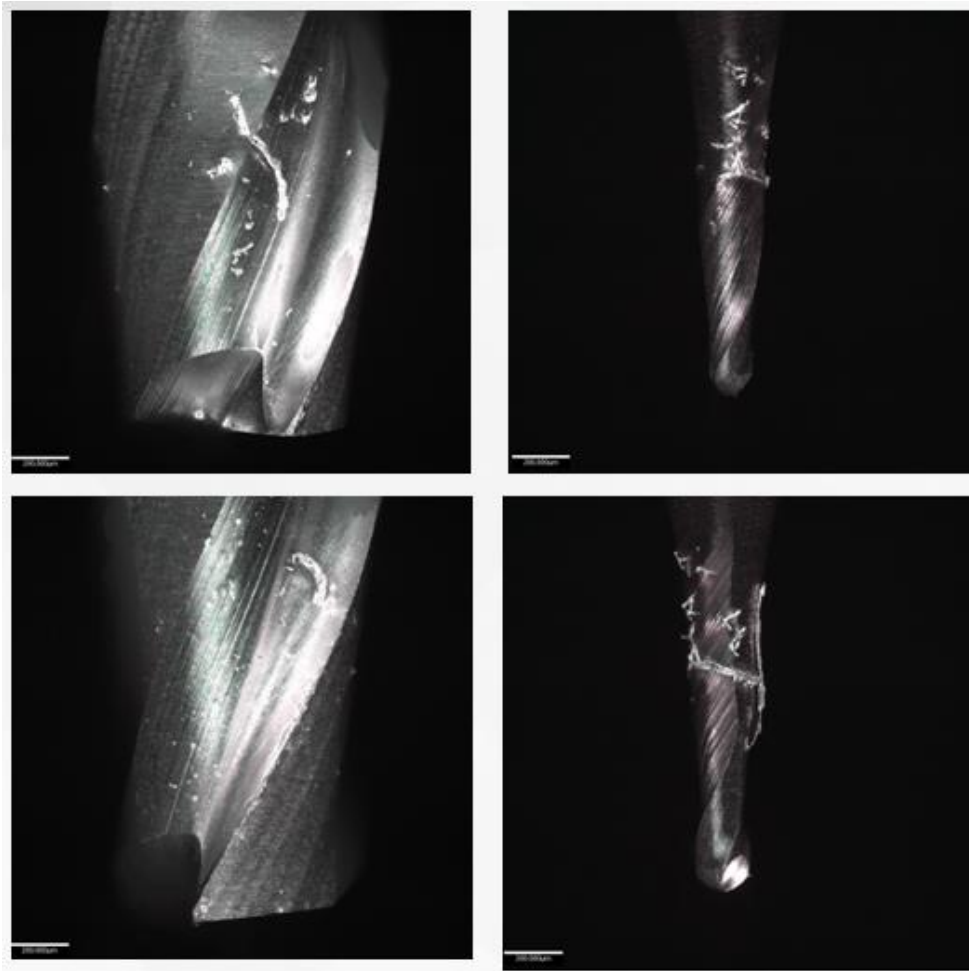


Figure 21. Chips adhered to flat and end ball mills

After cleaning the chips of the tool with Patafix and pressured air, tools were again measured to perform a 3D scan of the geometry and overlap the initial 3D scan against the newer one. Both datasets are aligned manually as described in the previous section. Figure 22 shows the result for both tools and their difference after the milling process with results

of deviation less than 3 or 4 microns for both edges of the tool, showing the performance of the tool with the use of MQL system.

Table 4 shows the difference in edge radius before and after the milling of titanium with micro ball end mill. Edge 1 of the tool increased to $.845\mu\text{m}$, while other edge increased $0.745\mu\text{m}$, showing that one of the tool edges received more impact and wear compared to the other one. Compared to the 1mm diameter tool, micro ball end mill decreased its radius size of $0.59\mu\text{m}$ of 1 edge and $0.47\mu\text{m}$ in the other edge by machining only 9 needles.

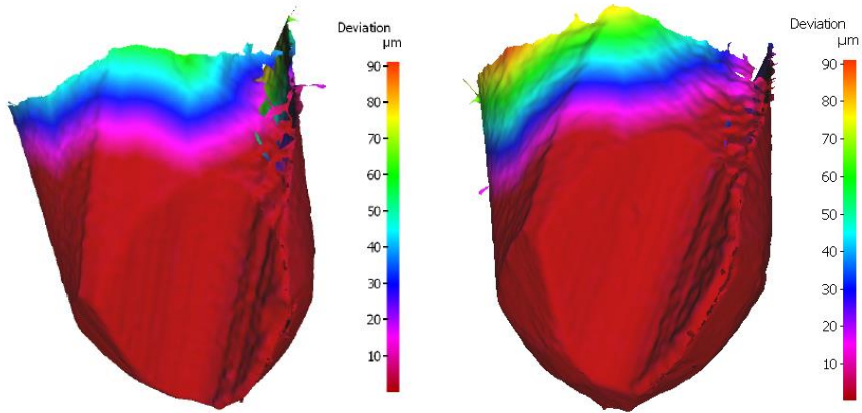


Figure 22. Comparison of both edges of micro ball end mill

Parameter	Edge 1	Edge 12
1mm Flat end mill		
Initial Radius	4.695 μm	5.465 μm
Final Radius	5.44 μm	6.31 μm
200 μm ball end mill		
Initial Radius	6.43 μm	5.84 μm
Final Radius	6.27 μm	5.74 μm

Table 4. Tool edge radius comparison of micro ball end mill

3.1.6. Surface roughness

Needles were placed in the microscope at a 90° to inspect the surface roughness and analyze if the toolpath can make a difference in the roughness obtained. Due to the array of the 9 micro needles, only 1 of each row was able to be inspected for surface roughness, but all 9 were measured for height and geometrical dimensions. Table 5 shows the parameters selected for the measurement according to the ISO 4288 for roughness between 0.1 and 2 μm .

Parameter	Value
LC (Cutoff length)	800 μm
Path length	150 μm
Lens	100x

Table 5. Parameters for roughness measurement

The surface roughness was evaluated along the x axis in the larger area of the needle (Figure 24). The form of the curved area was modified with the Software implemented in the Alicona called Form removal. This option takes into consideration the surface and makes it as flat as possible without losing the information of the roughness by selecting a desired initial geometry. The procedure can be seen in Figure 23 and how the software converts the conical surface into a flat surface without losing the information of the roughness of the dataset.

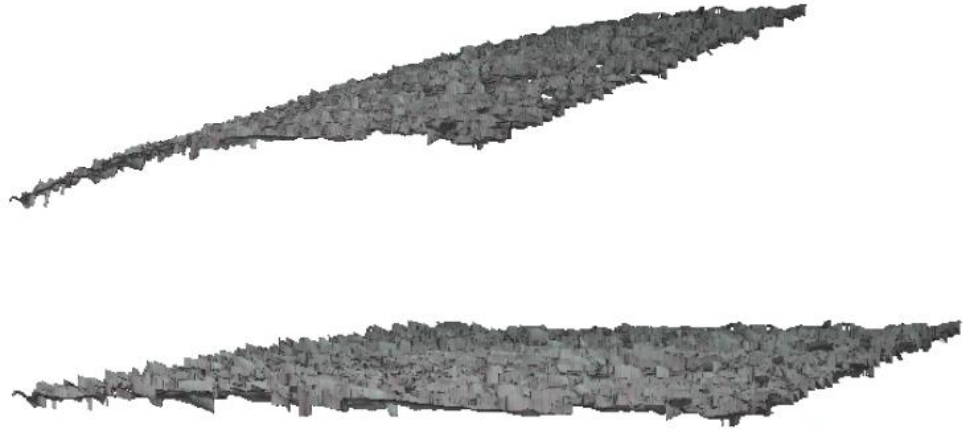


Figure 23. Curved dataset before and after form removal

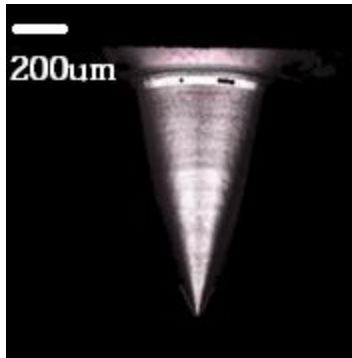


Figure 24. Area of measurement for each needle

For each of the 3 needles measured, 3 sample roughnesses were taken into consideration. Table 6 shows the data for the results of the Ra measure. Needles 01 to 03 and 04 to 07 were machined with the constant step down strategy, while the needles 04 to 07 were machined with spiral Z constant strategy. As seen from the results, when machining with a constant spiral z movement, the surface roughness decreases to an average of $0.165\mu\text{m}$. This result is validated through the experimentation performed by Souza et al. [18] by machining with different strategies and evaluating the roughness with 3D offset they got values of $0.81\mu\text{m}$ while machining with spiral offset the value was reduced to $0.77\mu\text{m}$.

Parameters	Sample 1	Sample 2	Sample 3	Average Ra
Needle 01	0.278 μm	0.339 μm	0.167 μm	0.260 μm
Needle 04	0.178 μm	0.183 μm	0.136 μm	0.165 μm
Needle 07	0.317 μm	0.252 μm	0.290 μm	0.286 μm

Table 6. Roughness and average Ra for 3 needles

3.1.7. Geometric dimensions

Machined needles were compared against the CAD model to verify the precision of the machining process according to parameters of diameter, height and top diameter of the needles. Most of the specimens were at about 70 to 80 microns below the expected result (1000 μm) for height. Diameter were from 30 to 54 microns above the expected result(1000 μm). Figure 25 shows the graph with the data of height and diameter showing that the values for height are tend to be always lower than the expected values and in diameter, values tend to be larger than the expected. Values for height can be interpreted as the result of rapid movements in the most fragile area of the needles, and for diameter can be deduced that these values are higher due to the rapid tool wear of the tip of the tool in the first 20 μm .

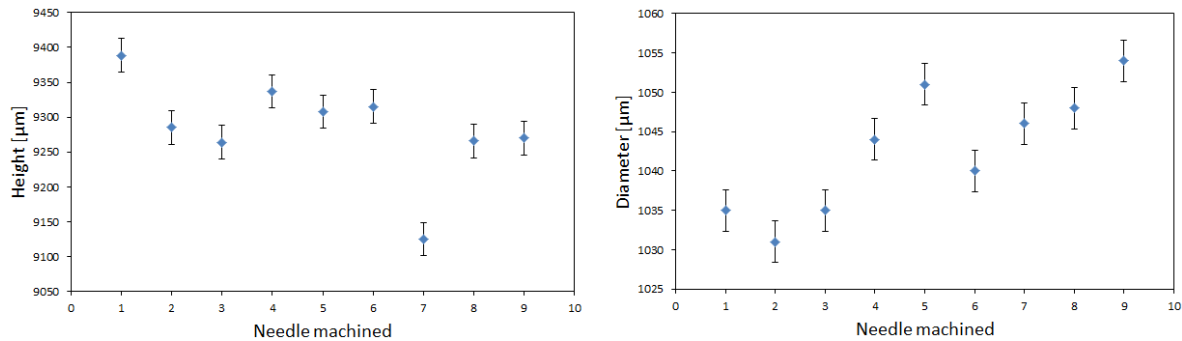


Figure 25. Height and Diameter for 09 needles machined

These measurements could be improved by varying the speed of the needle to reduce the impact over the tip of the needle. This can reduce the difference in the expected value of the height by performing other experiments with lower speeds and modifying the array for analyzing all surface roughness for the 9 needles. It is also noticeable that the measurements have an up and down tendency, for height the values are getting smaller and for diameter, values are getting larger due to the wear of the tool involved in this operations.

3.2. Linear array of Titanium

Based on the experimental results from the array of 3 by 3 needles performed in previous section, a new experimental design was performed by changing the array to a linear of 9 by 1 needles as shown in Figure 26. This modification can allow inspecting all the needles in the microscope to analyze the roughness of each one and how the tool wear is affecting the geometrical dimension according to the cutting feed performed.



Figure 26. Linear array of 9 needles

3.2.1. CAM

The experiment is design according to the result of roughness taken from previous experiment where the constant Z spiral toolpath resulted in a better surface roughness for the body of the needle. The tools used for the new experiment are provided by Mitsubishi tools, 1 square tool of diameter of .8mm with 2 flutes and 6 micro ball end mills of .200mm diameter were used. For the CAM the same procedure for rough operation is being performed by using Vortex strategy and a constant Z spiral finish for surface finish with the same cutting parameters as previous experiment.

3.2.2. Tools Measurement

Flat tools used were measured with aid of the Real 3D module. A visual inspection of the tool diameter could be performed as seen in Figure 27. However, due to the lack of information (perpendicularity of the tool against the lens in reference to the edges of the tool), there was no warranty that the analysis is correct. In addition, human errors were involved in the interpretation of the image.

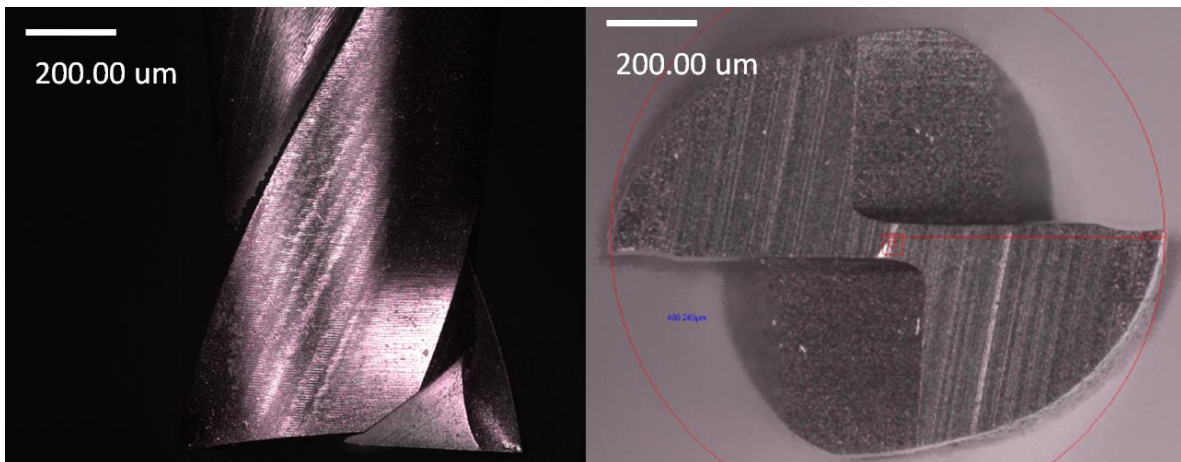


Figure 27. Diameter measurement of flat end mill

Since that method was not reliable, another method was implemented by using the 3D Scan of the tool and establishing planes from the top and lowering that plane at a certain level to measure 2 contact points in the dataset. 2 different measures were performed: the first intersection plane was located at 20 microns below the top of the tool and second intersection plane was located at 100 microns of the top of the tool for flat end mill and for ball end mill the plane was located 100 microns below the top of the tool. This can provide information about the diameter and wear of the edge in the large portion of the tool that cuts the most part of the material, and the tip of the edges that is in contact with the flat surface of the base of the needles. This method can be appreciated in Figure 28 where a cutting plane intersects the 3D Dataset and how the diameter is being measured by aligning 2 cross lines in the last portion of the cutting edge and measuring the distance between them. Table 7 shows the measurements of the initial diameter of flat and ball end mills.

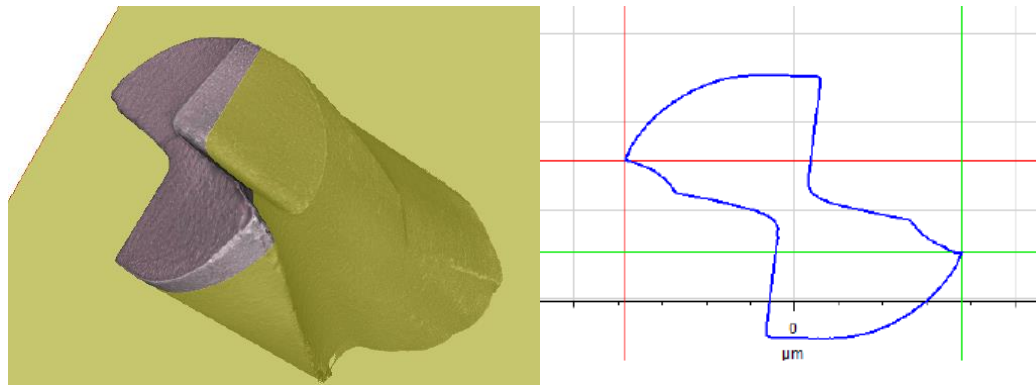


Figure 28. Cutting plane to measure tool diameter

1mm Flat end Mill	
Tool	Diameter (μm)
01	799.339
.2mm Micro ball end mill	
01	199.249
02	198.512
03	198.537
04	199.546
05	198.766
06	197.84

Table 7. Diameter measurement of 0.8mm flat end mill

For the tool edge measurement, the same process was performed in the Alicona microscope with the Edge Master module. Results from measurements are listed in Table 8 for .2mm micro ball end mill and .8mm flat end mill. To identify each of the side of the tool, the number printed on the tool was aligned with the microscope to establish an order for measuring the tool edges; this gives the advantage to analyze both edges of the tool separately for wear after the machining process.

Tool	Edge radius 1 (μm)	Edge radius 2 (μm)
Flat end mill		
02	3.7703	3.5716
Ball end mill		
01	5.6397	5.4966
02	6.0890	5.5229
03	5.8624	5.7713
04	5.9410	5.1341
05	6.2810	5.6195
06	4.8079	4.8549

Table 8. Tool edge radius for both sides of tools used

3.2.3. Experimental Set up

Same setup is maintained to perform this experimentation with the implementation of a Kistler dynamometer, used to measure forces experienced in the top of the needle to see the difference and effect that causes the speed in the top surface of the needle. The dynamometer used is a Multicomponent Dynamometer up to 250Newtons type 9256C with sensitivity of F_x , F_z of 26 and F_y of 13 pC/N. This device is clamped at the working table and the titanium block is screwed to the base of the dynamometer (Figure 29).

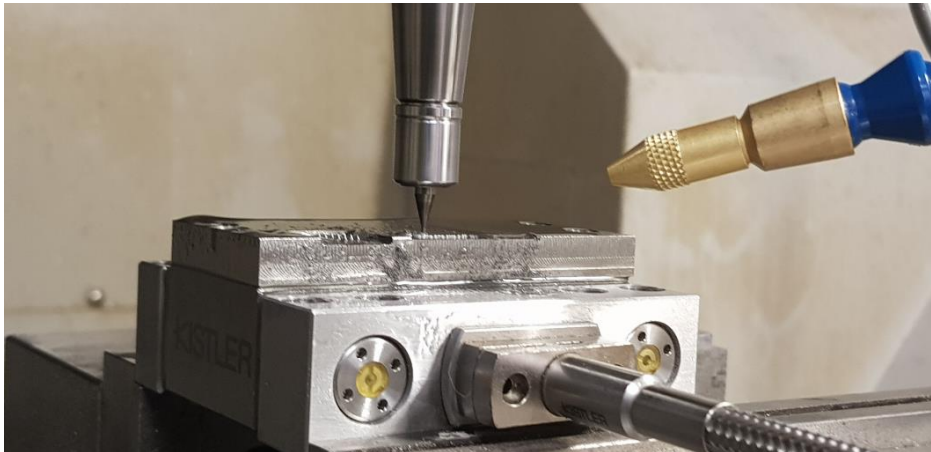


Figure 29. Experimental Set up with dynamometer and MQL

Three speeds were tested for the initial experiment: high (180mm/min), medium (150mm/min) and slow (120mm/min). 27 needles were machined with each feed two times. The time involved in rough operation was about 2h45min in removing the most part of the material. The 0,05mm of the remaining stock left for the finishing operation took an estimated time of 5 minutes per needle with an overall time of 3:35 hours for each set of 09 needles. For each process for machining the needles, a warm up cycle was carried out to run the spindle for 13 minutes in order to reach an equilibrium from experiments performed in micro ball milling by Garcia et al [45]. After the 13 minutes warm up process,

height showed a variation from 6 to 20 μm , 3 needles were machined and after that, the tool edge radius was measured for both sides. This was followed by another warm up process to machine another 3 needles and so on until completing 9 needles to finish 1 probe. Finally, after that probe was machined, a 3D scan was performed get a complete image of the tool.

Due to the nature of the machine, the cutting speed was not always constant at the top of each needle, while the parameter for high feed was set at 180mm/min. When milling each of the 9 needles, it was seen that the cutting feed was starting at 150mm/min and it increased until 180mm/min. The same occurred at medium, with cutting feed starting at 130mm/min and slow feed starting at 95mm/min. This is caused by the machine to prevent rapid movements in reduced areas, if the machine moves to that feed, the needle geometry would be probably affected by deformation or fracture and shatter presented in the machining process. Figure 30 shows the needles after the milling process with high and medium speed before cleaning in ultrasound and air pressure to measure roughness and geometrical dimensions.



Figure 30. 4 probes machined with high and medium feed

3.2.4. Results

All 27 needles were measured for compare the difference in geometrical dimensions and surface roughness. The titanium block was divided into 4 pieces to allow the measurement in the optical microscope. Results for the measurements are divided into 3 areas: height of the needles, lower diameter in the base and upper diameter on top of the needles. The results are presented in Figure 31 for height measurement, Figure 32 shows the lower diameter measurement and Figure 33 presents the data for the upper diameter on top of each needle.

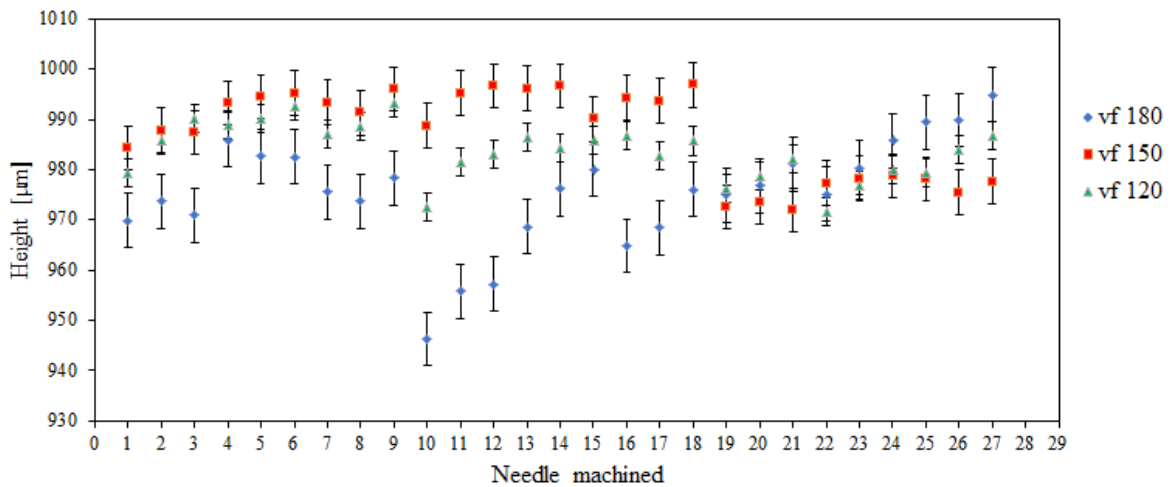


Figure 31. Height measurement of 27 needles with 3 speeds

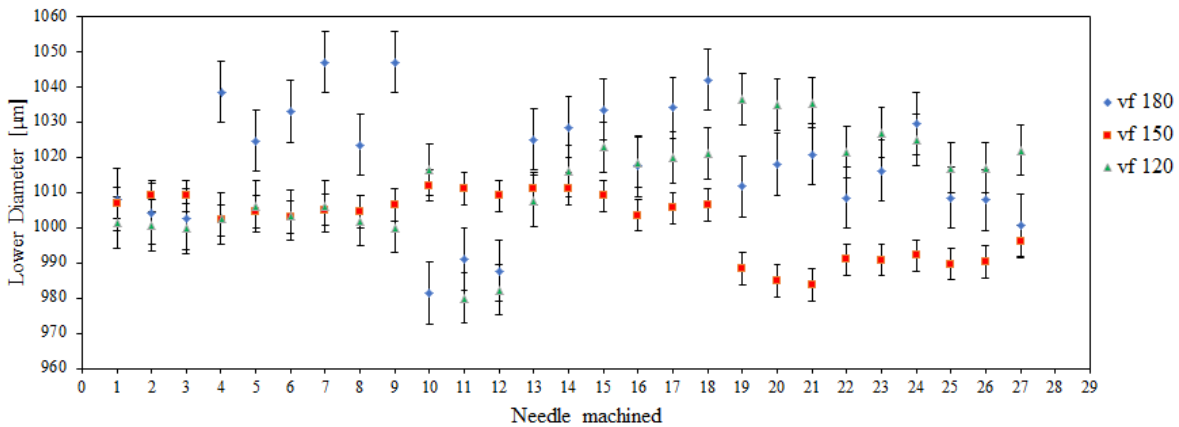


Figure 32. Lower diameter measurement of 27 needles with 3 speeds

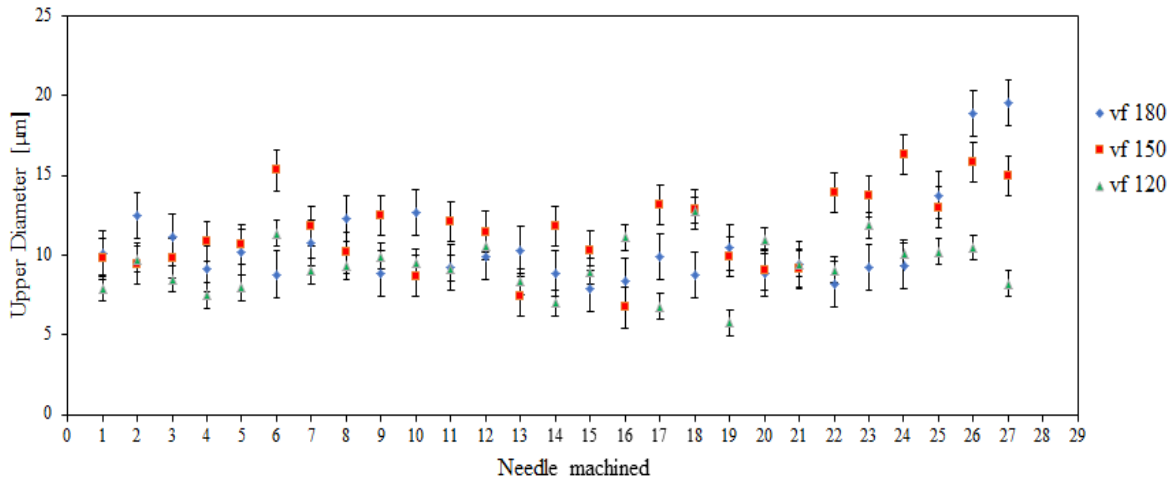


Figure 33. Upper diameter measurement of 27 needles with 3 speeds

Cutting feed with better results for height and lower diameter was 150mm/min and for upper diameter, best results was obtained with feed of 120mm/min. Effect of minimum chip thickness was not evaluated during this experiment, but it may cause an impact on the results of the measurements, since the values of CER are at about 3 to 6 µm, that values are higher than the chip thickness generated that from CAM it would be at 3µm which could be causing deformation in the work piece.

3.2.5. Tool Wear

Tool wear for 800µm and 200µm diameter end mill was analyzed in terms of wear of both edges of the tool and reduction in diameter. Both results are presented in Figure 34 and Figure 35 for flat end mill. Tool diameter was measured at 20 and 100 microns below the tip of the tool to analyze the difference wear presented along the cutting edge during the machining process. Figure 36 to Figure 38 shows the results of wear presented in both edges of the micro ball end mill during the finishing operations for the 3 feeds tested. Figure 39 presents the tool wear vs the material removal rate which shows how the tools presented a reduction in diameter of approximately 3µm for each feed rate. This reduction

in diameter can affect the height and upper diameter of the needles, lower diameter is not affected since the radius of the tool cannot reach the corner of the work piece generated by the 800 μm tool. Effect on diameter reduction can generate a flat tip of the needle, since this material is no longer removed, the tip of the needles can no longer be sharp enough, but the height it's not affected. Height is based on the toolpath generated by the flat end mill after the rough operation.

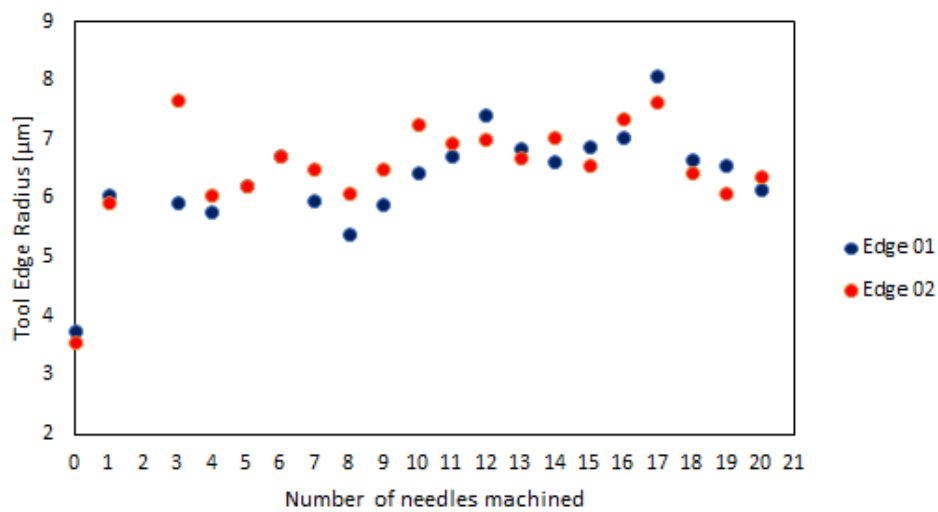


Figure 34. Edge wear on 800 um tool in SLM probe

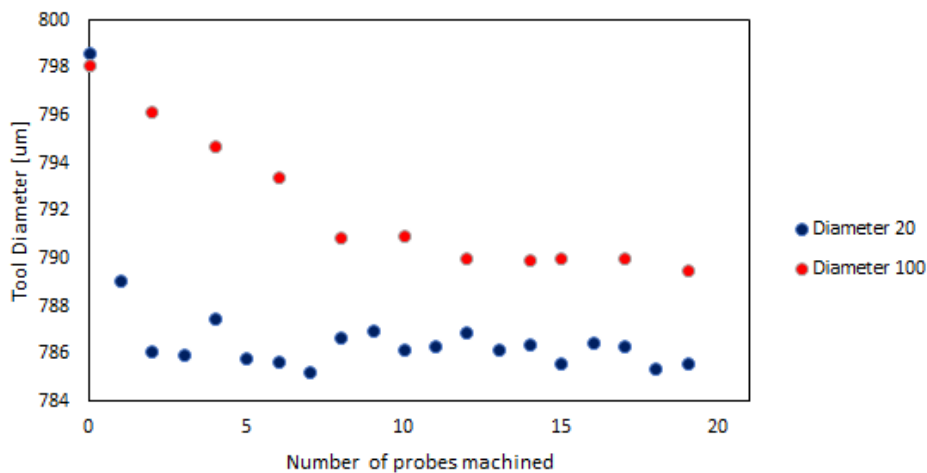


Figure 35. Diameter reduction for 800um tool in SLM probe

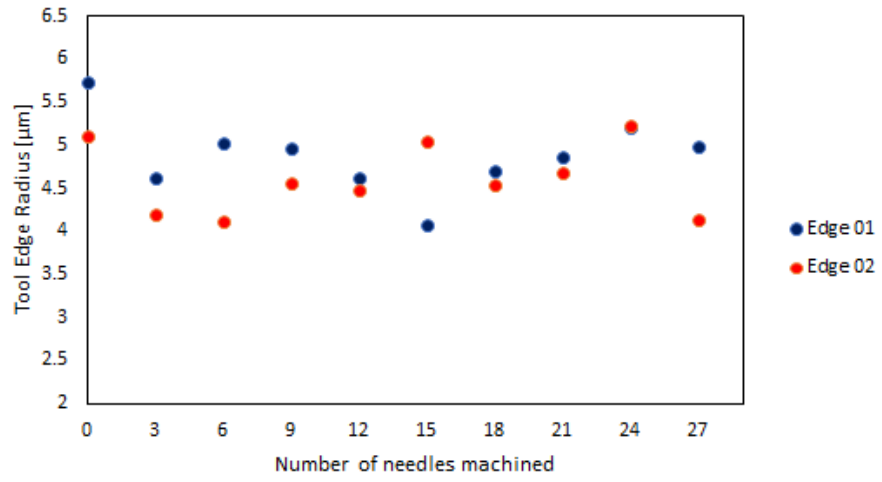


Figure 36. Edge wear for cutting speed of 150 on tool 01 and 03

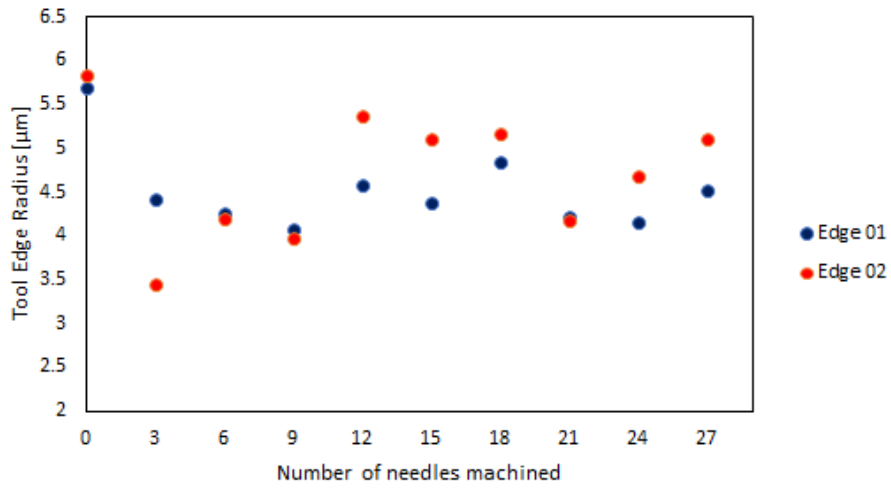


Figure 37. Edge wear for cutting speed of 180 on tool 02 and 04

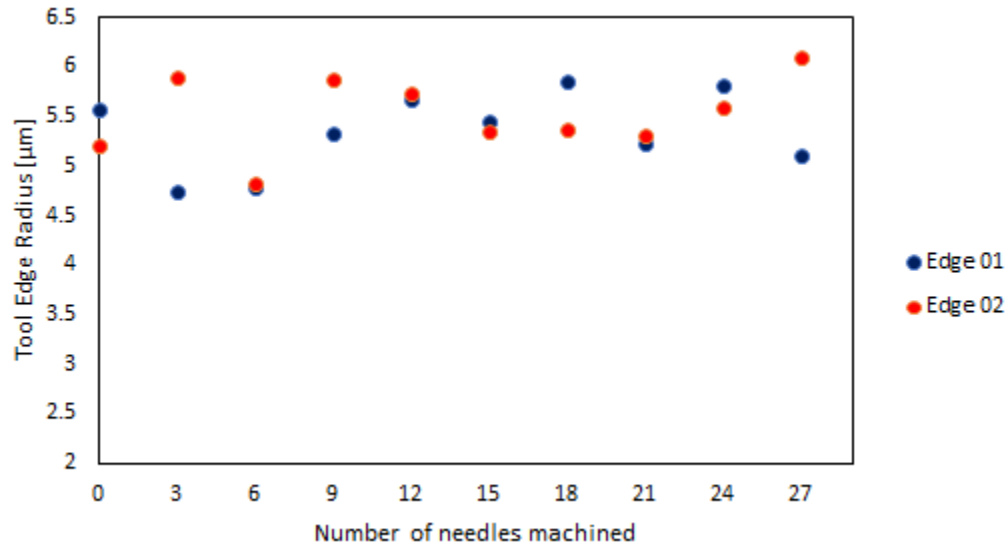


Figure 38. Edge wear for cutting speed of 120 on tool 05 and 06

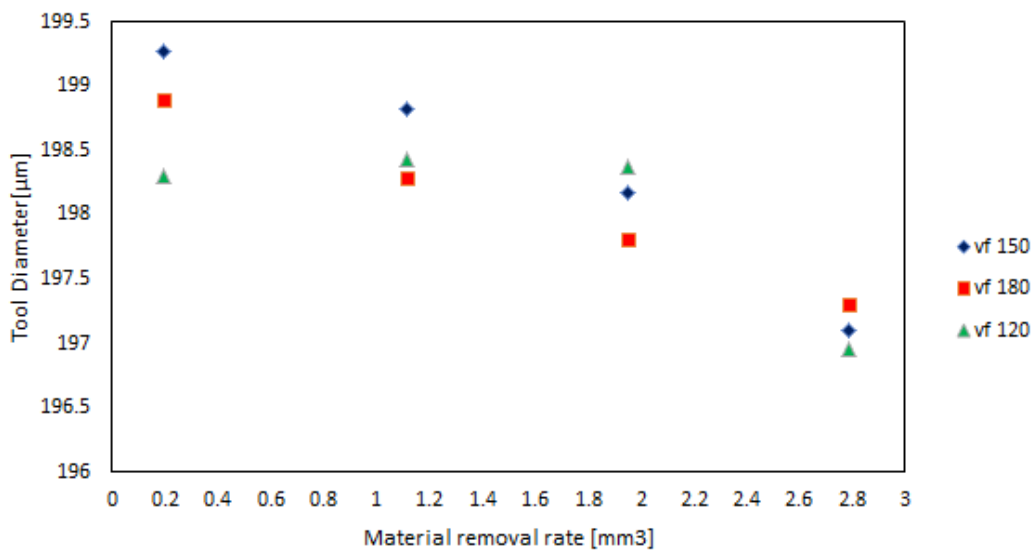


Figure 39. Ball end mill diameter wear

Results showed variation in tool edge radius for three cutting feeds in the range between 4 and 5.5 μm. The only feed that increased considerably the CED was at 120mm/min with values that surpassed the initial CED of the tool with values of 5.8 μm. All tools at different speeds showed reduction in diameter after being machined 2.8mm³ of material- Cutting feed of 120mm/min was the one that decreased more at that value,

however all tools were still in the initial wear zone and variations in diameter were not so noticeable in some cases.

All probes were machined with the 800 μ m tool for rough operation and images were obtained at a 90° to appreciate the progression of the tool wear in the shape of the tool. This is presented in Figure 40, showing a rapid tool wear in the sharp end of the tool from probe 01 to probe 04 and a slow wear progression from probe 4 to 18. a) represents the tool before any milling process, b) tool after probe no 9, c) tool after probe no 15, d) tool after probe no 18, and e) tool after probe no 20.

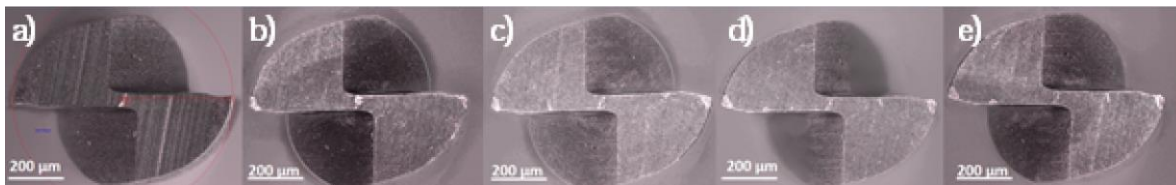


Figure 40. Tool wear for flat end mill

3D scans were used to visualize how the tool is reducing in terms of difference presented between 2 datasets. This method is helpful to identify where the tool is receiving more impact during the machining process and what part of the tool has more wear to analyze the whole cutting area, instead of analyzing a specific cutting plane at a certain level. This method was implemented for all the tools taking the last 3D scan and comparing it to the first scan where the tool was new. Figure 41 shows the difference for the 800 μ m tool after being machine 18 probes with vegetable oil applied with MQL system and the 6 micro tools applied for finishing 27 needles each one.

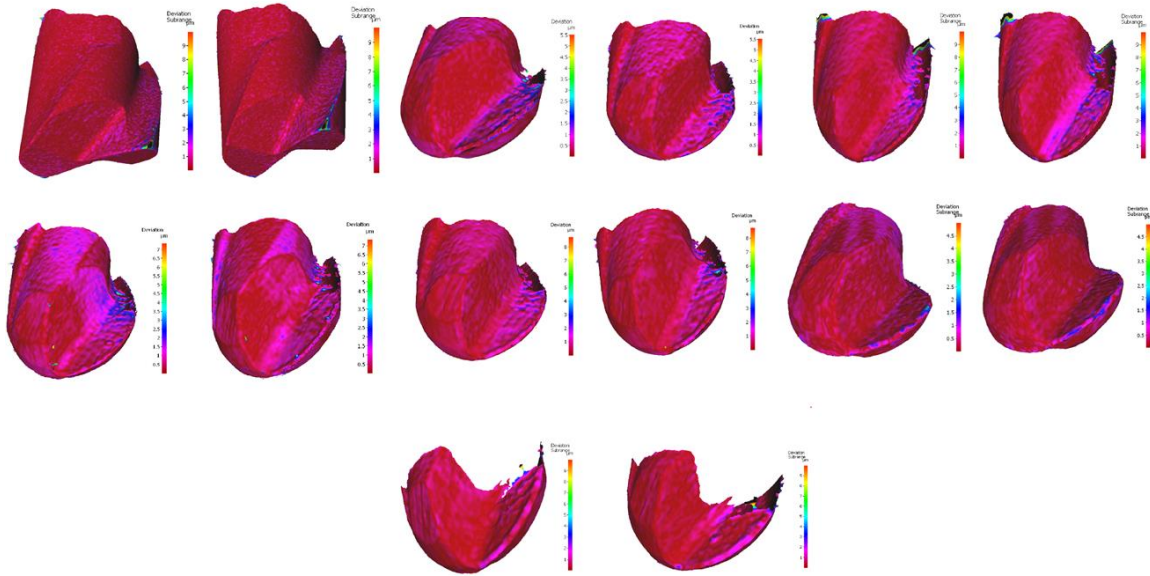


Figure 41. 3D dataset comparison of tools

3.2.6. Surface roughness

Profile roughness was evaluated by the parameters of Ra after milling with no post processing for additional finishing operations such as manual polishing or chemical baths. Figure 42 presents the average value for 3 different feeds; each feed performed in 2 experiments and the average value is reported with its standard error. Results showed that the cutting feed that gave the lower roughness was 120mm/min with an average roughness of .393 μm , followed by cutting feed of 180mm/min with .398 μm and finally the cutting feed of 150mm/min gave a value of .504 μm , being the feed that was with the largest values of roughness for the experiment.

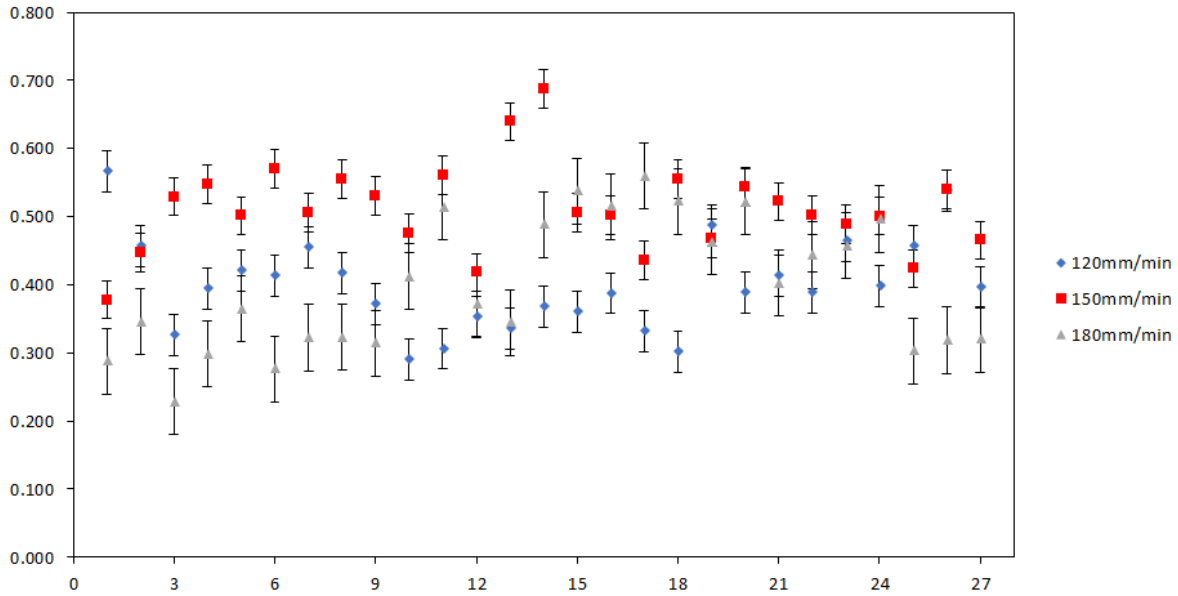


Figure 42. Roughness measurements for different feeds on titanium block

3.2.7. Force Measurements

Data acquisition was evaluated every 3 needles for all the experiments. 10 second of measurements was recorded and data was post processed with MATLAB R2018a with a resolution of 0.0001s. Figure 43 shows the data collected in 11 seconds. The initial two seconds are considered noise because of the manual setup applied to start the data collection. All of the measurements begins with noise, as a result of that, data was filtered by removing the first data and selecting only a certain number of values where the force is at its maximum peak, this number was set at 500 data for each axis.

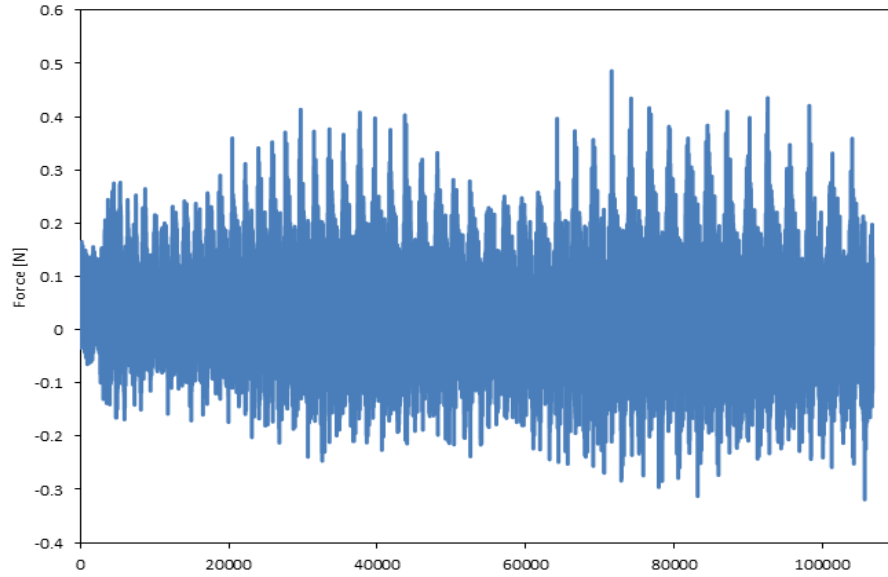


Figure 43. Data for Fx Measurement of 01 needle

Results from forces applied in needles with a vf of 180mm/min to 120mm/min are shown from Figure 44 to Figure 46.

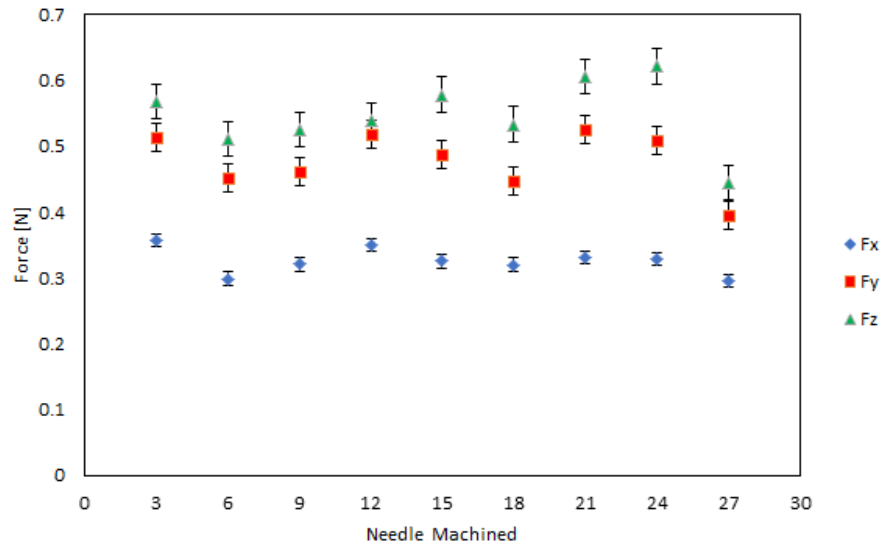


Figure 44. Forces applied at feed of 180mm/min

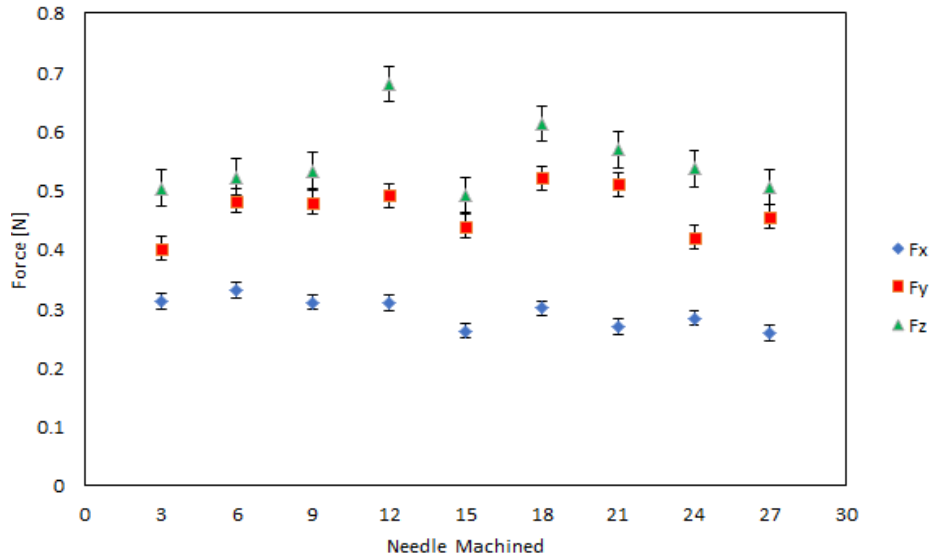


Figure 45. Forces applied at feed of 150mm/min

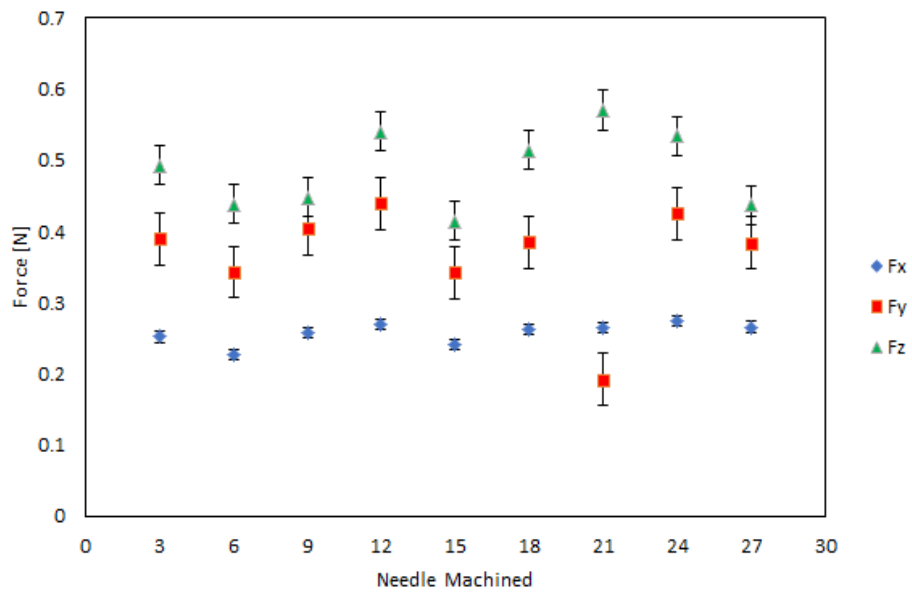


Figure 46. Forces applied at feed of 120mm/min

Axis that experienced more cutting forces was the Z axis with values over .4N for all tests. No high peaks were found, meaning that the cutting feeds were correct for that process and neither the tool or needle were affected during the milling process. When machining with lower feeds, lower forces were experienced in x and y axis with a decrease in force at about .5N for each different feed. This variation in force change was not so

noticeable in the Z axis, where the forces were kept almost the same in approximately .55N for all 3 experiments.

The experiments were planned to analyze the influence of the cutting speeds in the top surface of the needle with the selected toolpath and see if the forces applied were causing a possible tool breakage or defects in the needle. Figure 47 shows the original cut signals for 5 revolutions of the micro ball end mill for the 3 axes involved in the movement for the finishing process with a feed per tooth at 0.0025mm/tooth.

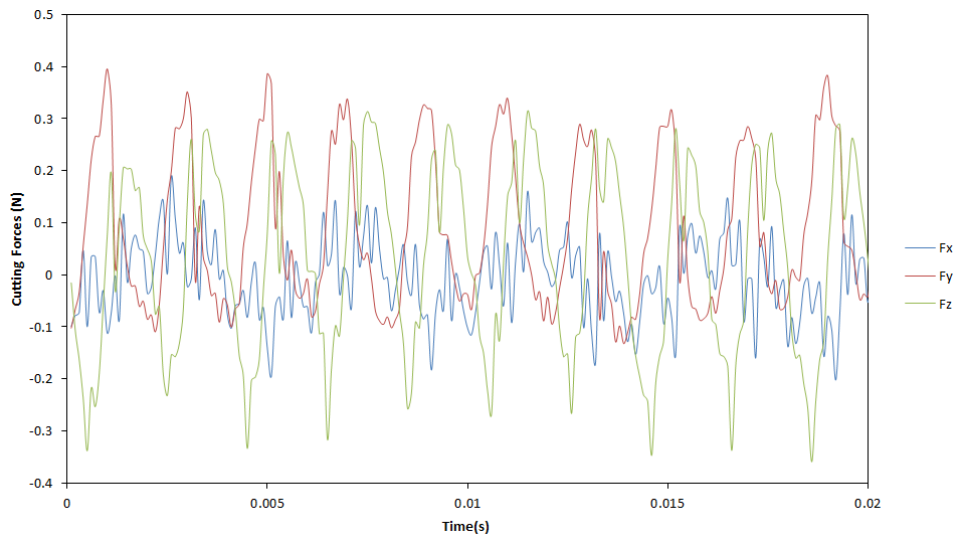


Figure 47. Experiment 14

3.2.8. Economic analysis

An economic analysis was performed in terms of material used, tools involved and time for each machining process. This will give a general review of the cost that the micro machining process only to produce a patch of 9 needles.

Item	Finishing operation	Rough operation
Raw Material	19.0\$	19.0\$
Tools	64.0\$	22.0\$
Machining cost	680.00 \$	2064.00 \$
Total	763.00\$	2105.00\$
Cost/patch		358.00 \$

Table 9. Cost estimation of micro machined array

Cost for SM was evaluated separately for both tools and divided by 8 pieces that can fit on a single block of titanium. Cost for the tools was evaluated by using 1 single tool per 8 patches, given the conditions that the tools are capable of machining with little wear. Total cost per part for SM process is estimated at 358.00\$. Considering that the major cost involved in micro machining is machining time, followed by the tools cost and third is the material cost. This evaluation gives an estimated value for mechanical micro machining for simple geometries when large quantities of material in a micro scale have to be removed. Further experimentations could be performed to reduce time with different tool diameter for apply the Vortex strategy as an improvement for reducing machining time and therefore, reduce costs.

3.3 Milling + AM experiment in Stainless Steel

Advantage of the AM with micro machining is the reduction in processing time, material use and possibility of manufacturing pieces with lower costs. To implement this manufacturing process, the initial array of 3 by 3 needles was selected to be manufactured in SLM process as described in previous section. The considerations required for milling

the needles are based on the quantity of material added to the final geometry desired to allow a good milling process that can shear these grains instead of just smear along the cutting area leaving a bad surface roughness.

3.3.1 Geometry definition and fabrication

For the initial experiment, a 50 μ m excess material was selected to see how the piece is manufactured and analyze its shape, surface finish and geometrical properties. Figure 48 shows the geometry definition with the amount of excess material selected. This file was exported to a .STL to be printed in a Renishaw SLM machine with a maximum power of P=400 W. Powder used was austenitic stainless steel 316L with a layer thickness of 50 μ m, scan speed of 2000(mm/s) and hatch spacing of 0.115mm. 2 sets of arrays were printed to compare them under a SEM microscope and Alicona microscope.

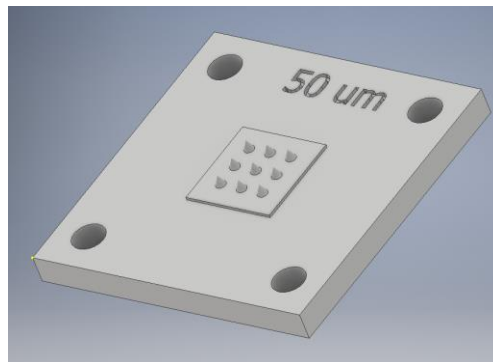


Figure 48. 3D CAD model for needle array in SLM

Figure 49 shows the result after the additive manufacture process. It is clearly visible that the quality of the AM process on the surface of the piece is not as smooth compared to macro geometries of dies and molds, this is why it is so important to select the proper parameter for the excess material in order to reduce to the minimum the machining time.



Figure 49. SLM array in Stainless Steel 316L

3.3.2 Characterization

Needle arrays were cleaned with ultrasound to remove any particles left or slightly attached to the surface of the probe. Each set of needles was cleaned for 5 minutes in a Metason 200 ultrasound machine. After being cleaned, both probes were taken to a EVO MA25 Zeiss Scanning Electron Microscope (SEM) (Figure 50) to analyze the shape, top diameter circle, height and diameter based on the CAD model. The needles were also measured in the Alicona Microscope. These results are presented in Table 10.

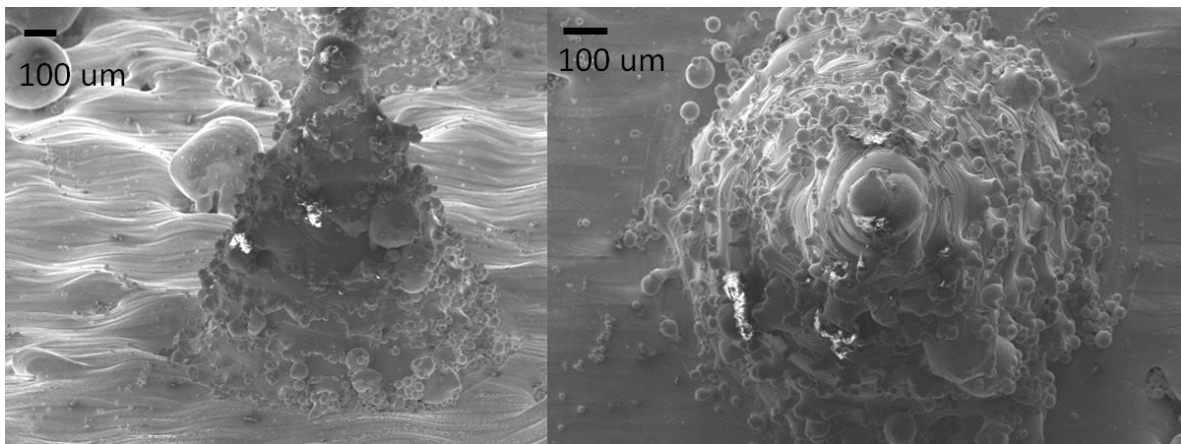


Figure 50. SEM images from needles

Needles	Height (mm)	Diameter (mm)	Top Diameter (um)
00	1.112	1.112	
01	1.168	1.341	71
02	1.194	1.115	71
03	1.176	1.338	98
01	1.182	1.254	60
02	1.139	1.105	76
03	1.131	1.218	79

Table 10. Geometrical measurements

Different methods for measuring the needles were applied taking into consideration the advantages of each equipment, the height and diameter of the needles. The Alicona measurement system gave a clear advantage in the method. Just as the microscope scans the needle, it creates a 3D model where the user can apply a line profile that trims the data, resulting in a projected 2D space for measuring the desired point, line or angle. This gives a more accurate result by taking exactly the area of interest that the user wants to measure, in this case, height and outer diameter (Figure 51). The same principle is used to take the diameter of the base by dividing in half the dataset and taking the 2 outer points of the measurement.

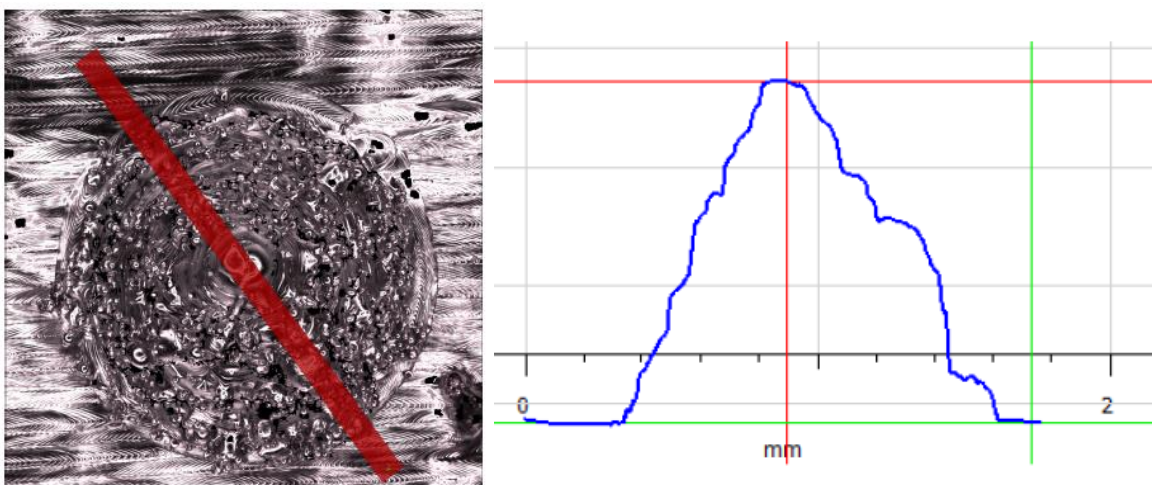


Figure 51. Height measurement in Alicona

An advantage using SEM is the clarity of the image and details presented in each capture. This gives a more detailed view of the particles joined or defects presented in the AM process. This method showed the lack of flatness in the floor while showing large particles of 100 microns fused and partially melted, also a lot of 10 to 50 micron particles were clearly seen in the whole needle by distorting the conical shape. As a result for the measurement with both equipment it was concluded that it is needed more material to perform the milling process. It is needed to increase this excess material to perform a semi finishing process with a flat end mill to first remove the irregularities and finally implement the finishing process to obtain the final geometry.

3.4 Milling + Machining in Ti-6Al-4V

As a result from experiments performed with Stainless Steel, another experiment was performed by modifying the CAD model. New parameters were taken from linear experiment of titanium from the previous section using the feed and toolpaths that gave the best results in geometrical dimension and roughness.

3.4.1 Geometry

The design criteria for using AM with titanium is very important for obtaining good results that can be useful to combine with the machining process. There are some phenomena involved when using AM technologies known as warping and shrinking than can be presented if the design is very thin or very large and this can be cause errors in the final piece. As a result of that, the probe for this experiment was design with a base of 6mm thickness to prevent warping due to the length of the piece. Figure 52 shows the new CAD model with the modifications required to be economically affordable with dimensions

required to prevent defects in fabrication and holes for fixing the probe to the dynamometer.

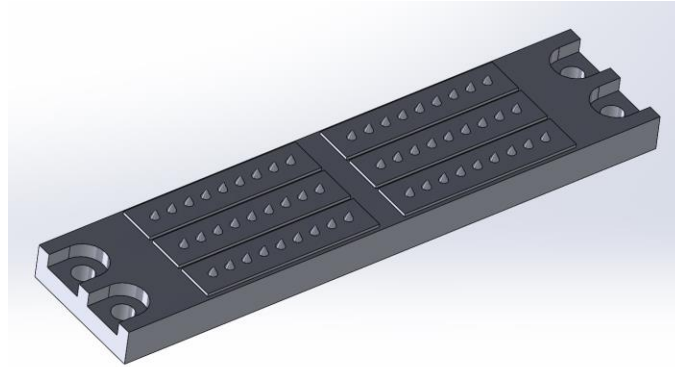


Figure 52. CAD model of 6 probes with 6mm base thickness

After the new design was performed, STL file was sent to a SLM supplier to perform its fabrication with Ti-6Al-4V Powder with a M2 machine for direct metal laser sintering with a high resolution of 0.153mm and tolerances of $\pm 0.076\text{mm}$ and a layer thickness of $20\mu\text{m}$. Figure 53 shows the new piece fabricated for generating a new experiment with 1 cutting feed. New tools were used to compare the performance, quality, and cost efficiency of this method compared to subtractive process only.

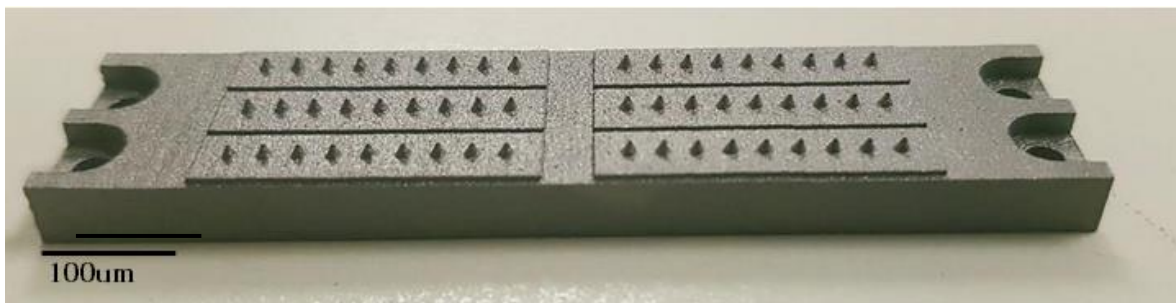


Figure 53. Part fabricated with SLM

3.4.2 Characterization

SEM images were obtained to visualize the quality of the AM process of the probe made in titanium; results can be seen in Figure 54 where the images were captured at a 90° and 45° to appreciate its shape after the manufacture process. It can be seen that the quality presented was improved due to new parameters applied in the manufacturing process. There were no signs of visible particles of powder attached to the body or floor of the needles compared to the first experiment shown in Figure 50.

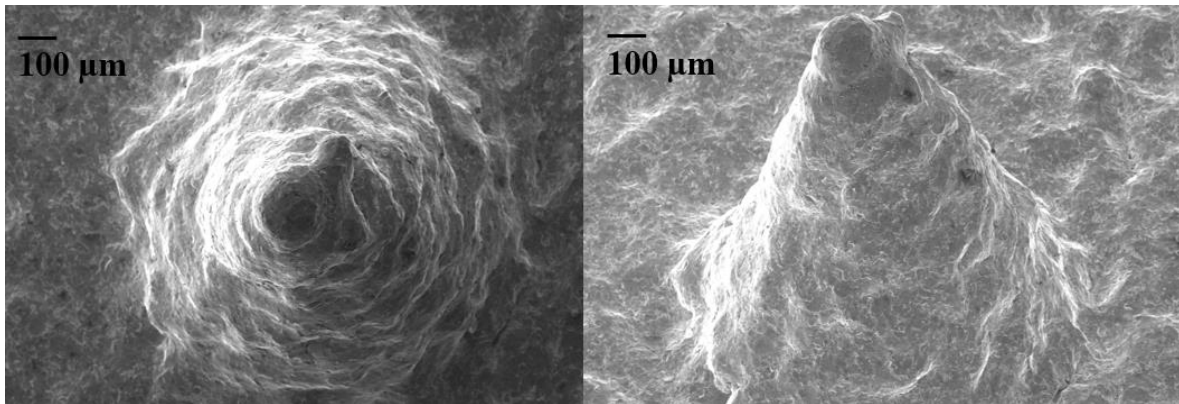


Figure 54. SEM image from SLM needle

Titanium probe was test with Energy Dispersive X rays spectroscopy (EDX) for elemental analysis and chemical characterization to corroborate the elements in the SLM piece. Results from several measurements in different points showed that the concentration mass % of vanadium was below the materials specification with a mas% of 1.515. Vanadium composition according to AMS4967 should be within a minimum of 3.5 and a maximum of 4.5.

Titanium probe was taken to Alicona microscope for geometrical inspection to verify if the manufactured piece was within specifications from the CAD model. This is useful to identify if it should be considered a modification in the CAM before taking the

probe to the machining center. Results from measurements showed that the average of height and lower diameter were below the expected value from the CAD model. Table 11 presents the results from geometrical measurements. Because of lower values, there was no need for modification of the CAM simulation.

Parameters	Height	Diameter
Average value	1113.79	1159.18
Expected value	1190	1190

Table 11. Results from SLM measurements

Visualization from the geometrical inspection showed that all the needles manufactured via SLM have the tip skewed to one side, this defect in the manufacturing process can be appreciated in Figure 55. A circle was drawn into the top view of the needle at 90° and it can be appreciated that the center of the circle does not fit within the tip of the needle. However, this defect may be despised due to the excess material that can take some errors within the shape of each needle.

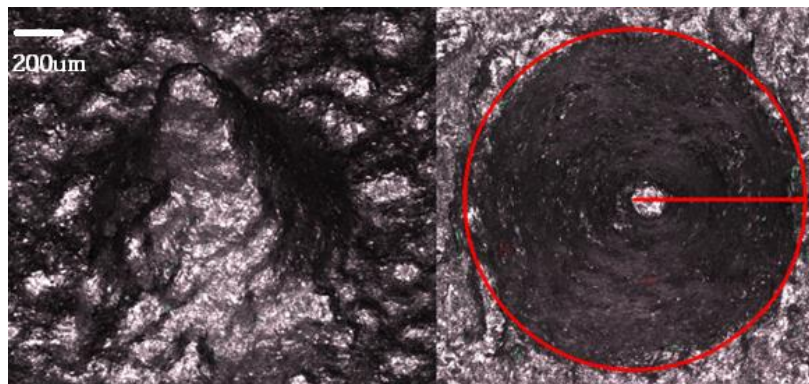


Figure 55. Tip of needle skewed to one side

Another process defect detected in the SLM was the effect of warping presented in the piece. As seen in Figure 56, probe was located in the Alicona microscope for inspection of

flatness of the piece. An image field inspection was realized to analyze a large image that the single lens cannot cover itself. This data shows that the probe has a difference of $60\mu\text{m}$ from the left corner to the middle section of the piece. As a result of that, the setup of the piece should be carefully set to avoid the sum of errors and calibrate the work piece to allow a full machining of all the needles.

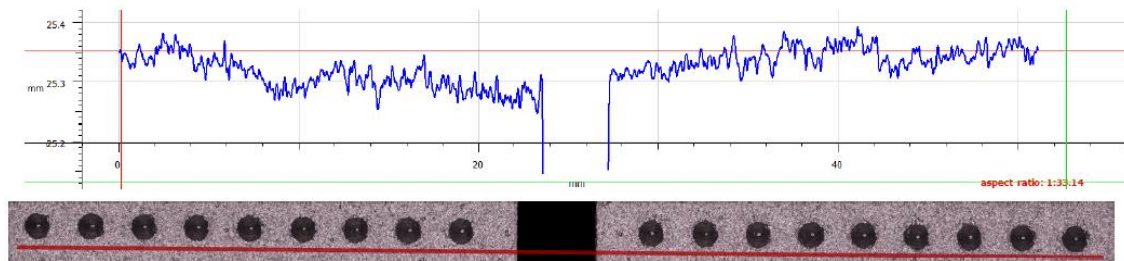


Figure 56. Warping effect on SLM probe

Metallography was performed on a piece of the titanium alloy to analyze the structure and obtain useful information about the material for composition, properties, grain size, phases or chemical homogeneity. Specimen is prepared by sanding the piece with waterproof papers of grain 120 up to 1000 grit, producing a flat surface finish with fine scratches that are no longer visible at naked eye. Once the specimen was grinded, polished process is now carried out with particles of alumina of $1\mu\text{m}$ in another machine with rotating wheels covered with a cloth impregnated with the abrasive. Final step was another polishing process with alumina of $.3\mu\text{m}$ for removing the tiniest scratches still visible in the optical microscope. Figure 57 shows the optical image taken from an optical microscope comparing powder titanium in the left vs solid titanium in the right.

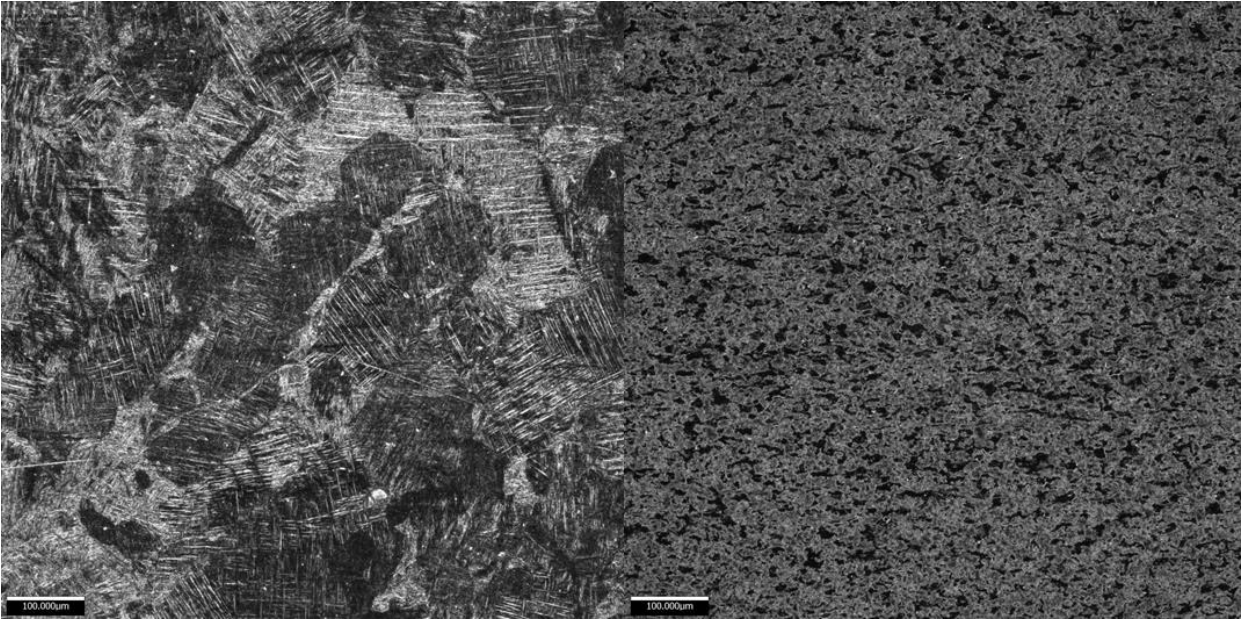


Figure 57. Optical image of surface after polishing and after chemical attack

Grain size in sample of titanium block suggests an extrusion of the material according to the alignment of the grains. Size of grains are in the range of 10 to 20 μm , showing that this material could be harder to machined according to the grain size in the sample of SLM with grains in range size of 100 μm which would require less force in the milling process.

3.4.3 Experimental Set up

Titanium probe was mounted on the Kistler dynamometer screwed to the base and new tools were used for machining the new needles. Cutting feed selected for machining was set at 120mm/min according to the results from minimal surface roughness obtained from previous experiments. Cutting parameters were kept the same for semi finishing at 480mm/min. For locating the origin of the work piece into the machine tool, 2 methods were used for minimal error. First method implemented was locating the edge with a 06mm

mechanical edge finder to locate both X and Y edges. After that process, an optical USB microscope was used to visualize the position of the first needle referenced to the origin set from the edge finder. After the approaching of the micro cutting tool to the top of the needle, a manual movement was implemented to relocate the origin to a more precise position as seen in Figure 58.

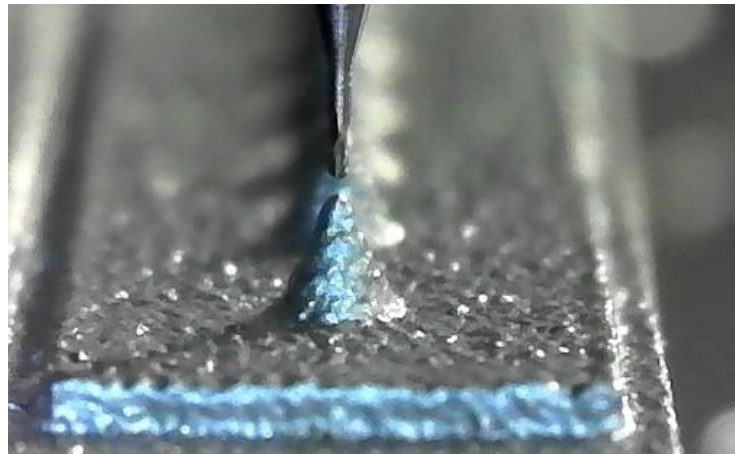


Figure 58. Manual alignment of cutting tool

3.4.4 CAM

Results obtained from toolpaths used in linear experiment in titanium block were applied to realize the programming of the probe made by AM technology in Titanium alloy. The vortex strategy is no longer needed, since the probe has a shape with only 150 microns of stock material left on the model. Also, there is no need for large quantities of material to be removed, and instead, only a semi finishing operation is performed to remove the excess material with the 0.800mm flat end mill to leave only 0.05mm left to be milled by the micro ball end mill. First semi finishing pass with the .8mm flat end mill took an estimated time of 45 minutes and second pass with .2mm ball end mill took 50 minutes.

3.4.5 Results

A total of 54 needles were machined from a manufactured piece of SLM made with Ti-6Al-4V. A total of two micro ball end mills were used to perform both experiments with the same feed. Results from measurements of height, diameter and top diameter are presented in Figure 59, Figure 60, and Figure 61.

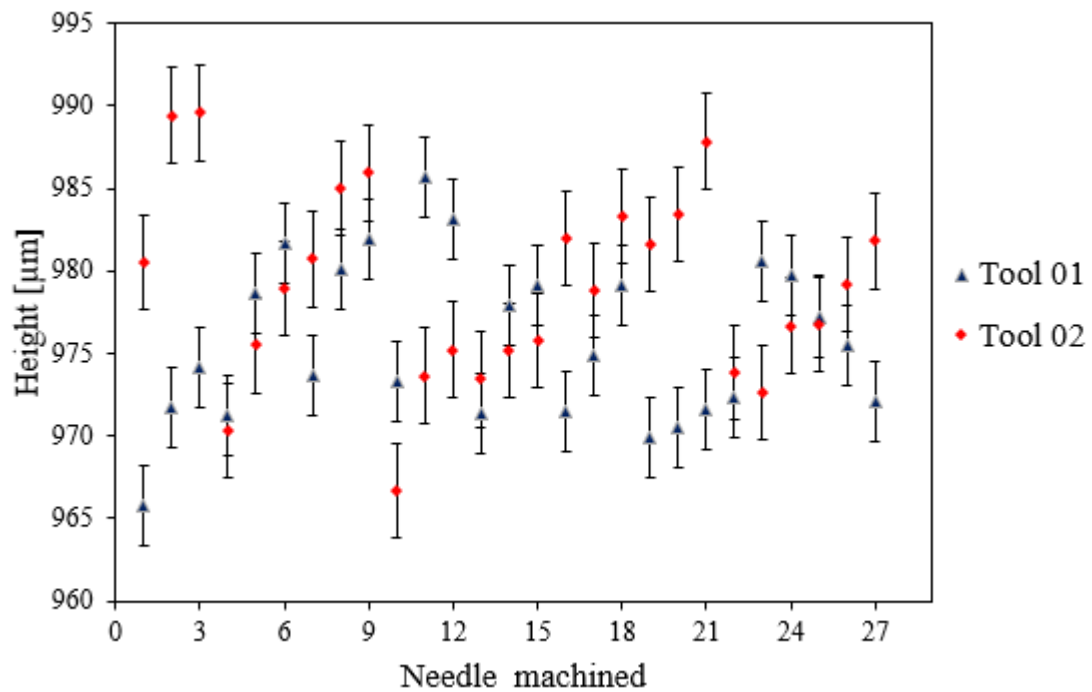


Figure 59. Height measurements

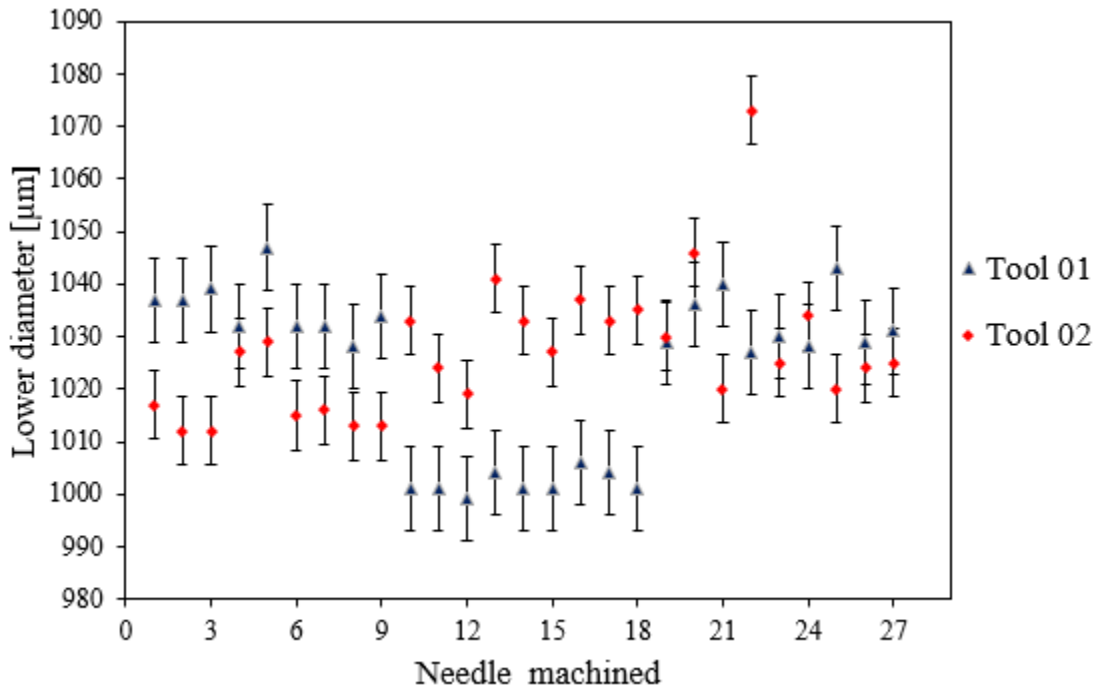


Figure 60. Diameter measurements

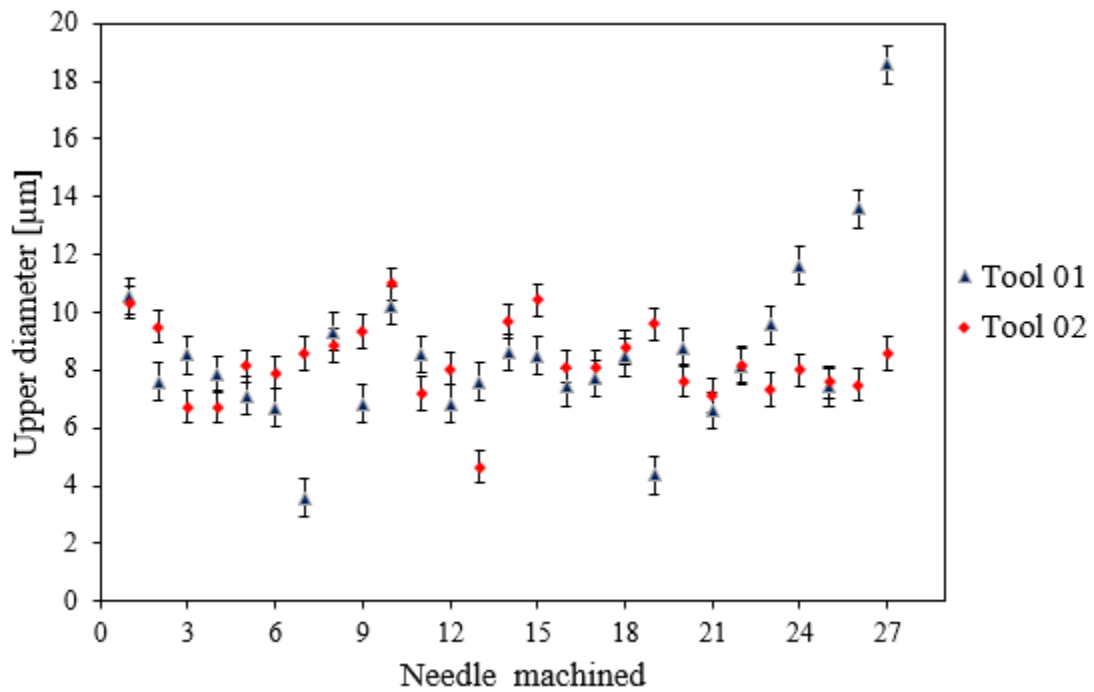


Figure 61. Top diameter measurements

Results were compared to the same dimensions obtained with the machined titanium that was manufactured with the same cutting feed. Height parameter obtained by SM gave

betters results in terms of accuracy of the measures obtained by the machining process with an average height of $983.75\mu\text{m}$ compared to SLM with an average height of $977.37\mu\text{m}$. Base diameter also gave more accurate results with an average diameter of $1012.70\mu\text{m}$ for SM against $1025.22\mu\text{m}$ for SLM. Top diameter measurements obtained by SLM were betters with average value of $8.35\mu\text{m}$ against $9.32\mu\text{m}$ for SM. Due to the variability of the micro machining process, it can be seen that groups of measurements are clearly distinguished within the graphs, this could be reduced by machining all 27 probes in one single process reducing variation in movements of tools, human error or recalibrating tool in the same process.

Different types of shapes were found on the manufacturing process of the needles, for the lower diameter. Figure 62 Shows the cross section of the needle and how the geometry should be after being machined.

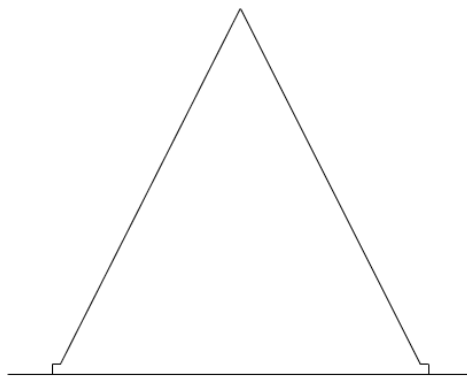


Figure 62. Cross section of needle

For both AM and SM process, three different types of shapes were detected, Figure 63 represents the cross section of the three shapes detected. (a) shows the standard shape with no defects in symmetry. (b) Represents a geometry with no tip of the needles with possible causes of lack of material due to the height measurement of the tool. (c) Shows the

most critical shape obtained that represent the tip of the needle with no symmetry at all, possibly caused by rapid movement of the machine in a very small area. This effect causes movements so quickly that the machine has no time to respond for such a high speed. Rapid movements prevents a smooth circumference around the tip of the needle and creates an irregular circular shape that does not corresponds to the desired results and creates this type of shape in the needles.

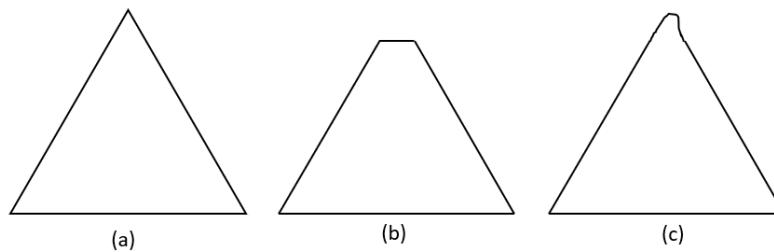


Figure 63. Morphology of top of the needles

Another type of shape was detected in the base of the needle as showed in Figure 64, these shapes are affected by the calibration of the micro ball end mill. (a) represents a calibration that exceeds the limits of the needle height and removes material from the bottom of the base. (b) stands for a less defective part where the micro ball end mill slightly touches the base of the titanium block, causing a fillet in the edge of the needle, again caused by error in calibration of the tool. (c) shows the best result obtained with the best result in calibration where the micro tool does not overpass the base and leaves a 90° corner shape in the final shape of the needle. This last is the best possible result obtained that reflects the actual shape of the needles in the CAD file, however, tool wear was affecting this result by causing to increase this angle according to the reduction in diameter for the .8mm flat end mill.

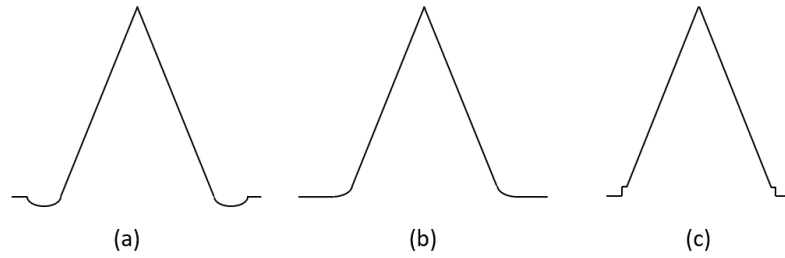
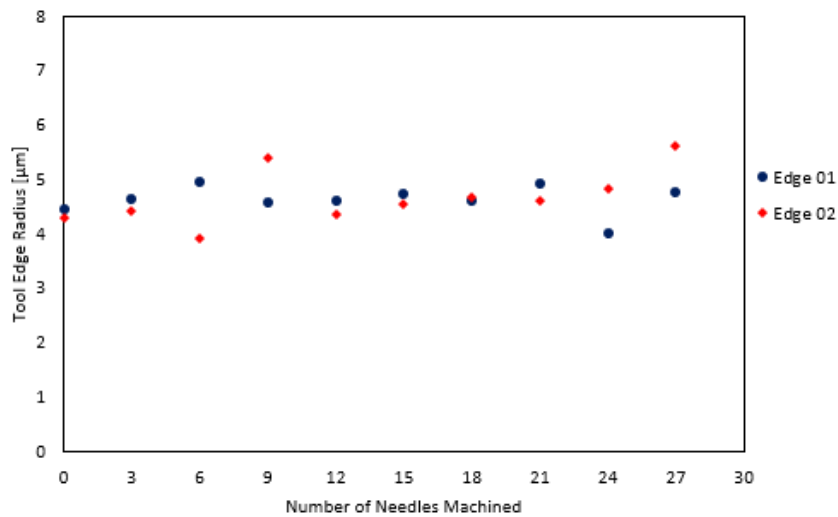


Figure 64. Morphology of base of the needles

3.4.6 Tool Wear

Both ball and flat end mills were measured in edge radius and diameter to analyze if there is a significant difference when cutting titanium manufactured with SLM technology. Measurements were made with the same parameters as the tools analyzed before in terms of light, contrast, tilt angle and measured area. Results of cutting edge radius for feed rate of 120mm/min with .2mm ball end mills are presented in Figure 65 for tool 01 and Figure 66 for tool 02, while diameter for both tools is shown in Figure 67.



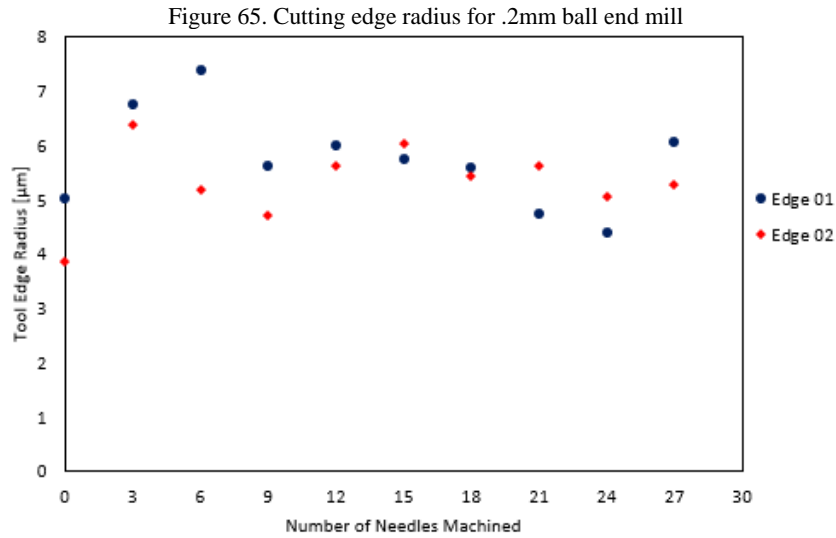


Figure 66. Cutting edge radius for .2mm ball end mill

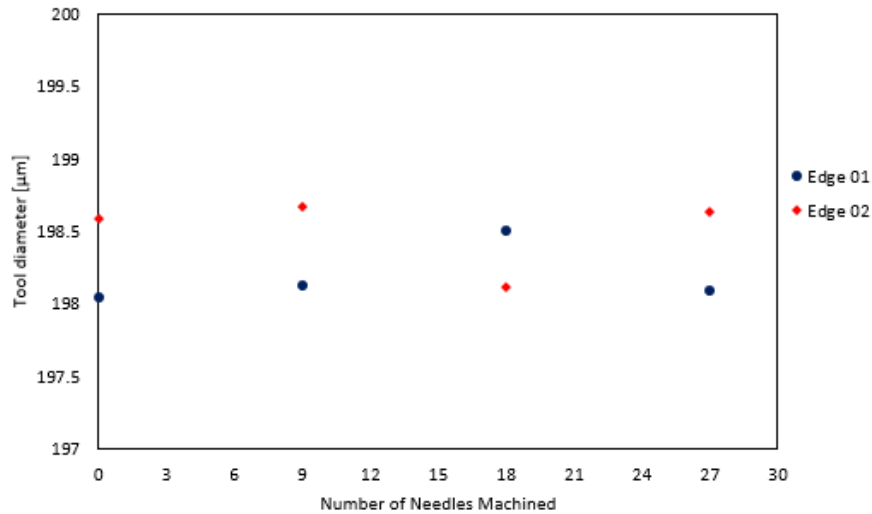


Figure 67. Diameter reduction for .2mm tools

Data shows that tool 02 received more impact in tool edge radius with a maximum radius presented in edge 01 of 7.4μm and 6.4μm in edge 02, while tool 01 presented a radius in edge 01 of 4.94μm and 5.59μm in edge 02. Tools diameters were around the same values with some variation in the measurements due to the resolution established in the microscope and the resultant 3d model that is used to measure the diameter. Measurements for .8mm Flat end mill were also performed only for 6 needle arrays instead of 20 as the experiment made with the titanium block. However, this will give enough data for compare

the wear in the tip of the tool and diameter reduction. Results for tool edge radius presented in Figure 68 can show how the radius is increasing for both sides at a similar rate, reaching equilibrium after the 3th needle with no further increment in the radius for both edges.

Diameter reduction is presented in Figure 69 for a measurement of the diameter 20 μm below the lowest part of the tool, this is due to the cutting parameters where the depth of cut is set at 30 μm per pass. Data presented can suggest that a rapid tool wear is presented in the transition to the 1st probe machined with a dramatic reduction from 798 μm to 786 μm . This represents a change in 1.62% caused by the rapid initial wear in the first minutes of the machining process. After probe 01, tool reaches the uniform wear rate, however, no enough data was acquired to establish the failure region of the tool.

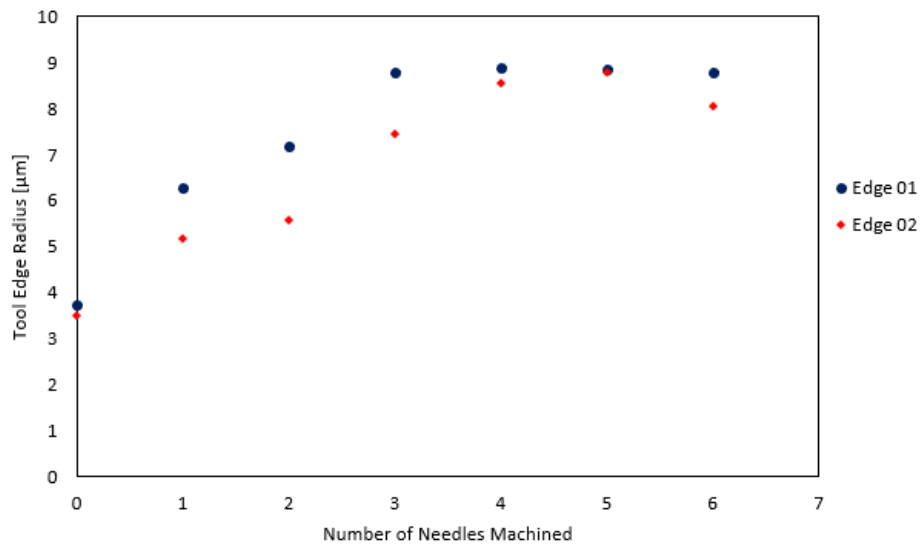


Figure 68. Tool edge radius for .8mm tool

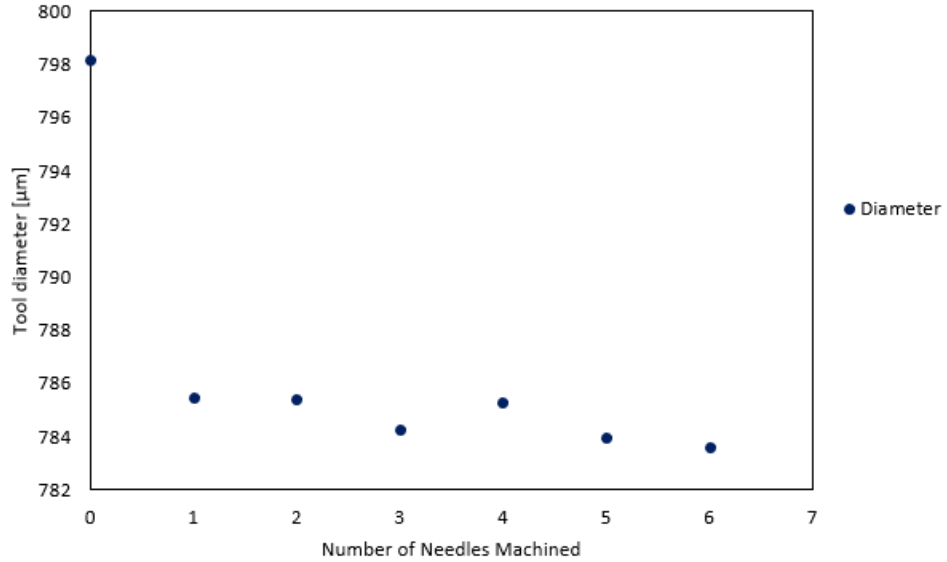


Figure 69. Tool diameter reduction for .8mm tool

3.4.7 Surface Roughness

Measurements for surface roughness on both experiments were performed and results are presented in Figure 70. Contrary to experiments presented by several authors where surface roughness increases with tool wear [46] [47], surface roughness with tool 02 decreased with the initial wear of the tool edge radius. This results are compared with experiments performed by Zhao et al (2017), where at cutting speed of 120(m/min), roughness values decreased with an incremental size of the tool edge radius, possibly caused by the stability of the cutting process [48]. Cutting edge radius with lower roughness value was at 5.6197µm with a Ra of 0.227µm. Further experiments should be perform to validate how the cutting edge radius affects the roughness in 2D and 3D for a complete analysis of the data available performed in milling sintered titanium alloy.

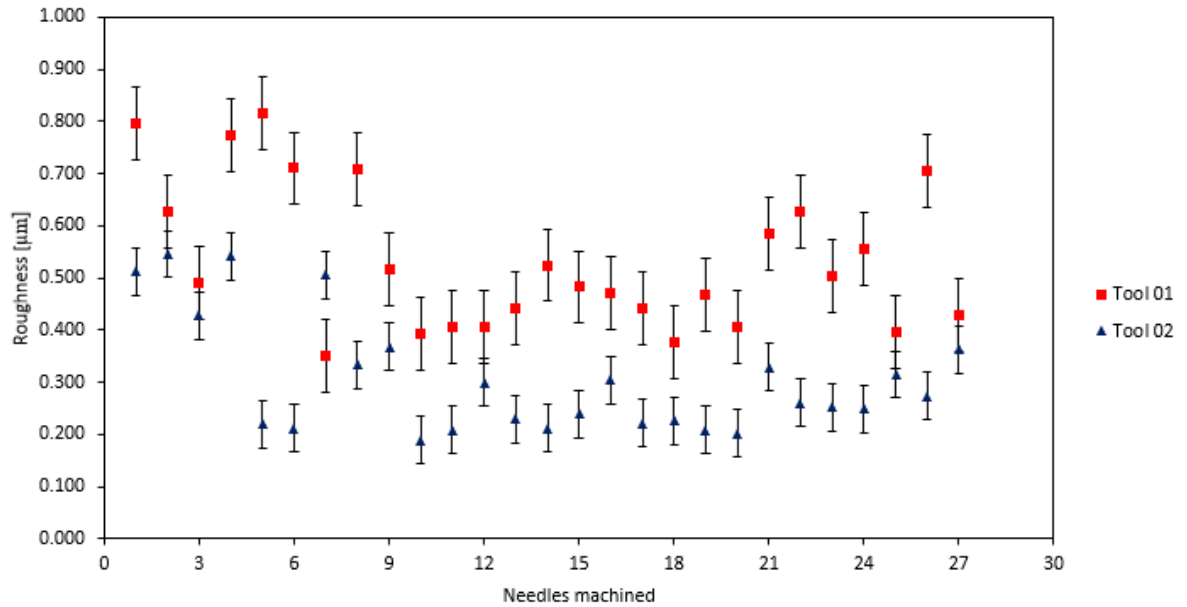


Figure 70. Roughness measurement of 54 needles

3.4.8 Cutting Forces

Cutting forces measurements results are showed in Figure 71 for tool 01 and Figure 72 for tool 02. It is clearly seen that cutting forces were significantly larger in needles of the second experiment in all three axes with data reaching almost 1 newton. This data can be explained by comparing the results obtained with the cutting-edge radius of that tool. It can be seen that cutting edge radius of tool 01 resulted in average values of 4.55 to 4.60µm caused an average force in X axis of 0.245N, Y axis of 0.36N and Z axis of 0.43N. Tool 02 showed an increment in cutting edge radius with values from 5.33 to 6.03µm, causing an increment in cutting forces in X axis of 0.383N, Y axis of 0.5217 and Z axis of 0.736N. This force variability between tools may be presented by a defect on the tool fabrication or impact with larger voids in that area of the probe, more experiments in this material should be applied to discard defects on the tool. All three force components showed an increment

when the cutting edge radius increase. Cutting forces remain the same order as previous experiments where the major force is carried out by the Z axis, followed by Y and X.

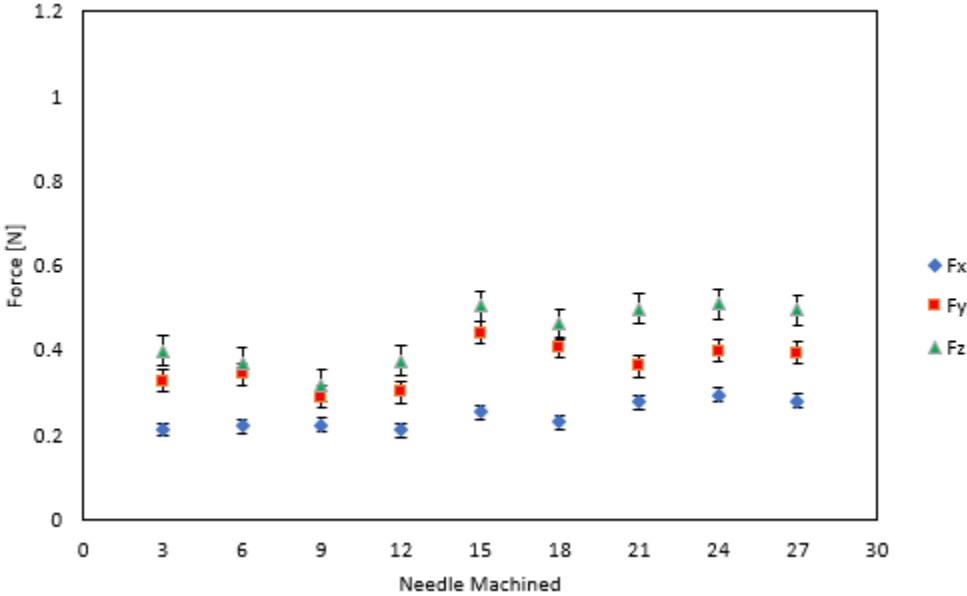


Figure 71. Cutting forces for tool 01 of .2mm

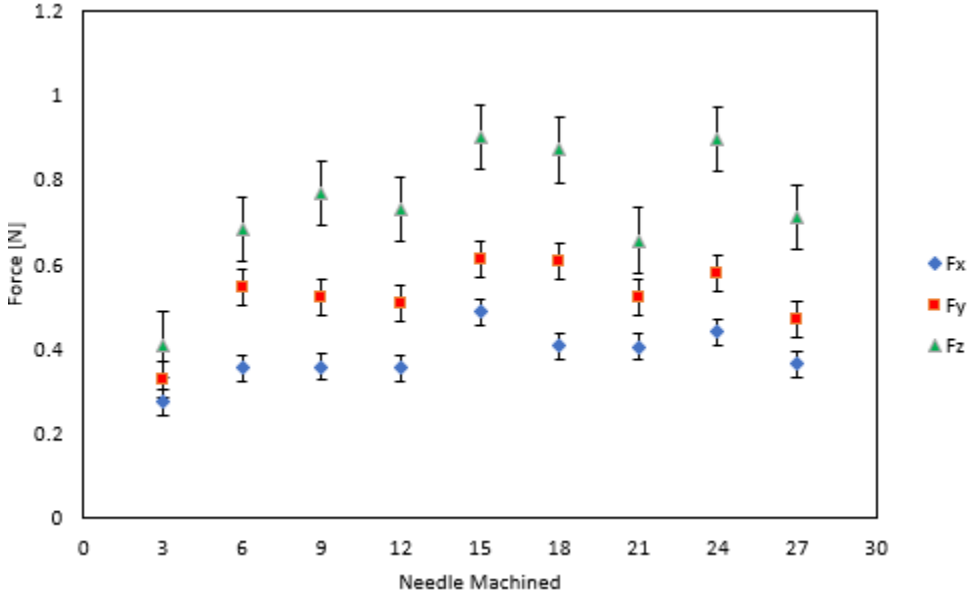


Figure 72. Cutting forces for tool 02 of .2mm

3.4.9 Economic analysis

Costs for SLM piece was calculated using software estimation costs by introducing the .STL file, as well as tool costs and machining costs. This gives an estimates total cost per part for AM process of 243.66\$ per part of 09 needles as seen in Table 12. As reviewed in the SM cost, the machining time, even though it is drastically reduced by 64%, it is still the main factor that affects the total price per part. Machining time for flat operation on the floor of needles could be reduced by half, since the 150 μ m in excess material it was seen that with 2 passes it is enough to complete the operation with no defects. This could reduce even more the total price per part, other ways to reduce costs is to analyze another arrays or forms to maintain the same or better physical conditions with less time consumption in the SLM process.

Item	SLM + Micro machining
Material	386
Tools	86
Machining cost	990
Total	1462
Cost/patch	243.66

Table 12. Cost estimation for SLM and milling process

Chapter 4

4.Results & Discussion

An experimental work was performed on Titanium alloy with MQL system applying vegetable oil with cutting tools of 800 μm and 200 μm diameter by machining 27 needles 2 times with 3 different feed set at 180, 150 and 120 mm/min. Geometrical dimension and roughness were evaluated to analyze if there are any differences in the results according to the cutting conditions established during the machining process. Forces were measured every 3 needles as well as tool wear in edges and diameter. 1 Probe with 54 needles was manufactured with SLM technology to replicate experimentation made with titanium block. This is done with the AM to skip the time involved in the rough operation to reduce drastically time consumption and start directly to semi finishing and finishing operation with the same type of tools. Feed selected for the SLM probe was set at 120mm/min according to the best roughness obtained in the previous experiment. Finally, results are compared for both manufacturing process, which are presented in this section.

4.1 Geometrical dimensions

Parameters considered for evaluating the geometrical dimension were taken from the CAD model as the reference in height and diameter of the needles set at 1000 μm and the top diameter was measured to appreciate the quality of the tip of the needle according to the feed involved. Results showed that cutting feed of 150m/min gave the most accurate results in height and diameter with an average measure of 987.24 μm for height and 1001.32 μm of diameter over values of 975.39 and 1018.15 from cutting speed of 180mm/min which

gave the most inaccurate results. Feed rate of 120m/min gave the most accurate results for top diameter with an average value of 9.3252 over 11.5084 from experiments with cutting speed of 150mm/min, only 1 outlier was found in the dataset but the addition of subtraction of this data does not impact considerably the results. Dimensions for needles manufactured by SLM were not as competitive in the results presented for height and diameter, this caused possibly by an increase in the tool wear, causing larger diameters in the base of the needles. Porosity also played an important role due to the voids that can be presented anywhere in the probe or the weak bonding of the material, causing to drag the top surface of the needle while the semi finishing or finishing process is carried out. However, top diameter in both probes made with SLM gave slightly better results with an average of 8.35 μ m. Different manufacture of the same material can impact the outcome for geometrical dimensions in the micro machining. This can lead to a model to analyze the different results to predict the behavior of the tools to estimate the desired final dimensions when one process or another has to be applied.

4.2 Surface roughness measurements

Different cutting feed parameters were selected to machine 27 titanium needles with 3 feed variations (120,150,180mm/min) over two different manufacturing processes. Surface roughness was evaluated in specific points in the lower area of each needle. Results for roughness are evaluated directly with the tool wear; experiments showed that when the cutting edge radius decreases below the initial measurement, roughness values are around .53 to .54 μ m for cutting feed of 150 and 180mm/min. Those values are higher, compared to the roughness when the cutting edge radius did not change and remained at the same or

even at a higher value, obtaining a roughness of $.491\mu\text{m}$ for SM process with a cutting feed of $120\text{mm}/\text{min}$. Taking this values into account, SLM process was performed and roughness values were evaluated. However, values were different for each experiment with average values of $.533$ and $.286\mu\text{m}$ for cutting feed of $120\text{mm}/\text{min}$. Value with lower roughness experienced a tool wear higher than the other 7 tools, meaning that the best roughness obtained is achieved when the edge radius is at $5.2\mu\text{m}$.

4.3 Tool wear

Experiments conducted with Mitsubishi tools on titanium block showed that $800\mu\text{m}$ can be used with Vortex Strategy to remove large quantities of material with advantage of using a large part of the cutting edge with no considerable wear on the tool. Diameter of the tool reduced from $800\mu\text{m}$ to $789\mu\text{m}$, reduction of 1.375% of tool diameter with a material removal rate of $119.8856\text{ mm}^3/\text{hr}$. with a coolant rate of $12.09\text{ ml}/\text{hour}$. For the tool radius the initial measurements were at 3.77 and $3.57\mu\text{m}$ each edge and after 18 probes machined the radius increased up to 6.1585 and $6.3711\mu\text{m}$ respectively, this demonstrates the effectiveness of the toolpath strategy combined with cutting fluid to machine Titanium alloy with no rapid tool wear or tool breakage presented. Rapid wear was presented at the initial process for $.8\text{mm}$ square tool on the first probe, followed by a normalization in the reduction rate for the entire experiment until probe 19.

For the micro ball end mill tools, stock material left on the model was $50\mu\text{m}$, with a Material removal rate of $1.1136\text{ mm}^3/\text{hr}$. Results showed that 3 speeds can be able to machine the desired surface with little wear presented in all the tools used. The diameter of the tools was reduced from $200\mu\text{m}$ to 196.84 , meaning a reduction in only 1.58% , while the

tool edge radius remained in constant variation between 4 to 6 μm in radius while still reaching surface roughness below 1 μm .

In contrast with the results obtained when machining a titanium block, when machining the SLM probe with the .8mm, a higher tool wear was detected in the first probe with a decrease from 798 to 785 μm . This result shows the difference in the way the material can affect the tool wear. For the micro ball end mill, .2mm tools for SLM experienced less tool wear than the tools that machined a block of titanium with a difference of 1 μm less than the SM.

4.4 Cutting Forces

Data collected by the Kistler dynamometer in a titanium block showed that the axis that experience a higher force is the Z axis, followed by the Y axis and next the X axis. Feed that gave the higher force in Z axis was 150mm/min with an average value of 0.5508 N, higher force in the Y axis was the feed of 180mm/min with a an average force of .4785N and higher force in the X axis was the feed of 180mm/min with an average force of .3255N. Higher feed does not necessarily means a higher force, since the first part of the needle is very thin, a feed of 180mm/min can cause a fracture of the top of the needle, causing to register less force in the first part of the milling process. The experiment did not showed a strong difference between the two flutes involved in the cutting operation. Feed per tooth affects the force involved in the X and Y axis by increasing the force applied by the rotating tool when the feed is increased.

Cutting forces measured while machining the SLM probe with a feed of 120mm/min showed a higher force applied in one of the two experiments. This increment in the force required to cut the material is due to the increment in the tool edge radius causing to have more contact area which increases the force required to cut the stock left in the work piece. Experiment two showed a rapid increment in the tool edge radius up to 6 μ m for both edges at the 6th needle, while in the first experiment for the same needle; values of edge radius were of 4.5 μ m. Same as the titanium block, Z axis received higher force followed by Y axis and next the X axis, maintaining this order for both experiments.

4.5 Economic analysis

Two different micro manufacturing processes were analyzed by fabricating needle arrays made with titanium. Total cost per part for AM process gave a value of 243.66\$ compared to cost per part of 358.00 in SM process. This estimated comparison shows that SLM combined with micro machining has a clear advantage due to the machining time involved. Most part of the cost over SM goes directly on the rough operation where time involved is larger than the SLM because in this last one, there is no rough operation involved. Cost reduction could be presented with modification of parameters in SLM to reduce time consumption by designing a hollow structure to only support the needles. This could provide a cheaper cost while maintaining the design features required. A comparison was made based on cost models for SLM and SM with aid of empirical experience and it is focused directly on micro machining applications for parts with no complex structures or cooling channels. This estimation can work on cost estimation for a comparison when machining cavities for application of dies and molds for the plastic injection industry.

Chapter 5

5. Conclusions

In this paper, micro machining of titanium alloy for needle fabrication was discussed by making a comparison with selective laser melting (SLM). The manufacturing process and characteristics of each process were studied and compared. A literature revision was performed to identify the parameters that can affect the results for surface finish, tool wear, or costs. Benefits from micro needles were reviewed compared to the conventional needles and several advantages were highlighted. Finally, a comparison was performed to analyze the results obtained with both manufacturing processes and a cost calculation made using several cost calculations.

Results showed that it is possible to fabricate micro needle arrays in Ti-6Al-4V alloy with two different processes. Each one with its own unique features and capabilities with considerations for every manufacturing process from design to fabrication. Results showed that it is of critical importance the stock material left when creating a piece with SLM in micro scale with a value established in this work of $150\mu\text{m}$ to allow a correct material removal. Surface roughness was evaluated and evaluated in specific points of each needle. Roughness was very similar on both technologies and showed that it is possible to obtain values below $1\mu\text{m}$ with the proper cutting parameters. Physical measurements obtained with SLM showed that the process cannot reach the required precision for creating micro components. Tool length also showed that the calibration method it is very important due to the external parameters that affects the length and therefore, the physical dimension is affected directly.

Tools were evaluated during and after the milling process and results gave enough data to conclude that the use of vegetable oil as a lubricant can improve the tools life. Experiments showed that the fabrication method also affects the initial wear of the tool and after that initial wear, reduction reaches an equilibrium. No further experiments were performed to reach the failure stage of the tools. Force measurements were also analyzed, and it was concluded that the main axis involved in the cutting force is the Z axis. Both materials behaved in the same way and the only parameter that increased the resultant Z force was the increase in the cutting edge radius.

Economic comparison show that SLM has economic advantage over SM process when large parts need to be removed by rough operations. Further analysis is required to improve the way the pieces are manufactured to reduce costs while maintaining the desired geometrical dimensions and functionality.

5.1 Contribution

This dissertation contributes to the area of manufacturing process to allow the fabrication of medical devices. It involves the use of different state of the art technologies available to measure, fabricate and analyze the different aspects of the devices fabricated. The main objective of this thesis is to fabricate a patch of titanium needles made by Selective laser melting to post process with mechanical micro machining. Major contribution from this study are the following:

1. Vortex strategy for removing large quantities of material can be used in the micro scale to reduce time consumption and improve cutting life with the use of MQL with vegetable oil.

2. Cutting edge radius has a high impact over surface roughness of the needles, and lower parameters for cutting feed can improve the surface finish for conical shapes with spiral toolpath strategies.
3. Micro machining combined with additive manufacture has a clear advantage over SM process.
4. Quality obtained with SLM must be improved due to the voids and bonding of particles during the fabrication, these defects have a high impact over the final device for aesthetics and functionality.
5. 150 μ m of excess material is a good starting point to create different geometries to compensate possible errors from calibration and manufacture.

5.2 Future Work

For a complete validation of experiments, a higher number of needles could be manufactured with the same cutting feeds to obtain detailed information about the tool wear until failure. Different design modifications could be implemented in the SLM array to allow a reduction in time and cost. Lower excess material could be set in the base of the needles, since this part of the device does not require to be strongly machined to obtain a good surface finish. An accurate cost estimation could be performed considering the capacity of needles machined while maintaining acceptable geometrical dimensions and discover the new design considerations to lower costs.

Prediction models could be developed for an estimation of the physical measurements according to the available precision of the actual SLM technology. Finally, another cost

estimation could be made for a high production rate with an array of the patch that could be used when the design parameters had been optimized for mass production.

5.3 Recommendations

This study has shown the capabilities of and limitations of the available technologies for actual fabrication and future fabrication of micro devices. To reduce the risk of failure in the micro tools or affect the precision in the tip of the needle, cutting feed in the highest part of the needles should be reduced to avoid the rapid movements of the machine tool. Calibration of the tools could be performed every 9 needles instead of 03, as reported, calibration plays an important role and it certainly modifies the result when taking out the machine tool to measure the cutting edge radius. Since wear values for micro tools were not changing so drastically, spacing the measurements could give fast results with fewer errors due to the human interaction with the cutting tools and set up in the machine. Tool diameter for rough operation could be increased to reduce time consumption to the minimum; this will allow removing larger quantities of material with less tool wear for high productivity and lower overall costs.

6 References

- [1] E. Tovar, “Produccion de moldes en Mexico: Un futuro promisorio,” *Modern Machine Shop*, 2016. [Online]. Available: <https://www.mms-mexico.com/artículos/produccion-de-moldes-en-mxico-un-futuro-promisorio>. [Accessed: 05-Jan-2018].
- [2] D. Federal and E. Unidos, “Sector Dispositivos Médicos Cámaras y asociaciones,” pp. 5–6, 2010.
- [3] R. Evans, “Microneedle technology and transdermal drug delivery,” *Medical design & outsourcing*, 2016. .
- [4] S. H. Bariya, M. C. Gohel, T. A. Mehta, and O. P. Sharma, “Microneedles: An emerging transdermal drug delivery system,” *J. Pharm. Pharmacol.*, vol. 64, no. 1, pp. 11–29, 2012.
- [5] J. D. Yadav, K. A. Vaidya, P. R. Kulkarni, and R. A. Raut, “Microneedles: Promising technique for transdermal drug delivery,” *Int. J. Pharma Bio Sci.*, vol. 2, no. 1, pp. 684–708, 2011.
- [6] “Types of Titanium alloys,” 2016. [Online]. Available: <https://titaniumprocessingcenter.com/the-element-titanium/>. [Accessed: 01-Feb-2018].
- [7] “Alloy, Ti6Al4V Titanium.” [Online]. Available: <http://www.arcam.com/wp-content/uploads/Arcam-Ti6Al4V-Titanium-Alloy.pdf>. [Accessed: 07-Feb-2018].
- [8] M.-B. Mhamdi, M. Boujelbene, E. Bayraktar, and A. Zghal, “Surface Integrity of Titanium Alloy Ti-6Al-4V in Ball end Milling,” *Phys. Procedia*, vol. 25, no. 0, pp. 355–362, 2012.
- [9] and E. W. C. R. Boyer, G. Welsch, “Materials properties Handbook: Titanium alloys,” *ASM International*, 1994. [Online]. Available: <http://asm.matweb.com/search/GetReference.asp?bassnum=mtp641>. [Accessed: 07-Feb-2018].
- [10] E. Segura-Cardenas, E. Ramirez-Cedillo, J. Sandoval-Robles, L. Ruiz-Huerta, A. Caballero-Ruiz, and H. Siller, “Permeability Study of Austenitic Stainless Steel Surfaces Produced by Selective Laser Melting,” *Metals (Basel)*, vol. 7, no. 12, p. 521, 2017.
- [11] J. Shanahan, “Trends in Micro Machining Technologies,” 2004. [Online]. Available: <https://www.makino.com/about/news/Trends-in-Micro-Machining-Technologies/315/>. [Accessed: 07-Feb-2018].
- [12] D. Hunt, “The Evolution of Miniaturization Within Medical Instrumentation,” 2013. [Online]. Available: <https://www.medicaldesignbriefs.com/component/content/article/mdb/features/17280>. [Accessed: 07-Feb-2018].
- [13] M. Ziberov, M. B. da Silva, M. Jackson, and W. N. P. Hung, “Effect of Cutting Fluid on Micromilling of Ti-6Al-4V Titanium Alloy,” *Procedia Manuf.*, vol. 5, no. 2003, pp. 332–347, 2016.
- [14] C. Veiga, J. P. Davim, and A. J. R. Loureiro, “Review on machinability of titanium alloys: The process perspective,” *Rev. Adv. Mater. Sci.*, vol. 34, no. 2, pp. 148–164, 2013.
- [15] P. Kumar, V. Bajpai, and R. Singh, “Burr height prediction of Ti6Al4V in high speed micro-milling by mathematical modeling,” *Manuf. Lett.*, vol. 11, pp. 12–16, 2017.

- [16] T. Thepsonthi and T. ??zel, "Experimental and finite element simulation based investigations on micro-milling Ti-6Al-4V titanium alloy: Effects of cBN coating on tool wear," *J. Mater. Process. Technol.*, vol. 213, no. 4, pp. 532–542, 2013.
- [17] K. Vipindas, G. Bhanupratap, and J. Mathew, "Investigation on Tool Wear During Micro End Milling Of Ti-6Al-4V," pp. 4–7.
- [18] A. F. De Souza, A. Machado, S. F. Beckert, and A. E. Diniz, "Evaluating the roughness according to the tool path strategy when milling free form surfaces for mold application," *Procedia CIRP*, vol. 14, pp. 188–193, 2014.
- [19] J. Sun *et al.*, "Effects of coolant supply methods and cutting conditions on tool life in end milling titanium alloy," *Mach. Sci. Technol.*, vol. 10, no. 3, pp. 355–370, 2006.
- [20] U. Garcia and M. V. Ribeiro, "Ti6Al4V Titanium Alloy End Milling with Minimum Quantity of Fluid Technique Use," *Mater. Manuf. Process.*, vol. 31, no. 7, pp. 905–918, 2016.
- [21] E. Vazquez, J. Gomar, J. Ciurana, and C. A. Rodríguez, "Analyzing effects of cooling and lubrication conditions in micromilling of Ti6Al4V," *J. Clean. Prod.*, vol. 87, no. C, pp. 906–913, 2015.
- [22] S. B. Akula and S. Suryakumar, "Techno-economic analysis of hybrid layered manufacturing K . P . Karunakaran ,* Vishal Pushpa ," vol. 4, pp. 382–394, 2008.
- [23] X. Liu and D. Rutman, "IMECE2015-51218," 2017.
- [24] A. S. Iquebal, S. El Amri, S. Shrestha, Z. Wang, G. P. Manogharan, and S. Bukkapatnam, "Longitudinal Milling and Fine Abrasive Finishing Operations to Improve Surface Integrity of Metal AM Components," *Procedia Manuf.*, vol. 10, pp. 990–996, 2017.
- [25] S. Pal, H. R. Tiyyagura, I. Drstven??ek, and C. S. Kumar, "The effect of post-processing and machining process parameters on properties of stainless steel PH1 product produced by direct metal laser sintering," *Procedia Eng.*, vol. 149, no. June, pp. 359–365, 2016.
- [26] R. Pacurar and P. Berce, "Research on the Durability of Injection Molding Tools Made By Selective Laser Sintering Technology," *Proc. Rom. Acad. Ser. a-Mathematics Phys. Tech. Sci. Inf. Sci.*, vol. 14, no. 3, pp. 234–241, 2013.
- [27] I. Ilyas, C. Taylor, K. Dalgarno, and J. Gosden, "Rapid Prototyping Journal Design and manufacture of injection mould tool inserts produced using indirect SLS and machining processes," *Rapid Prototyp. J. Prototyp. J. Rapid Prototyp. J. Iss Rapid Prototyp. J.*, vol. 16, no. 5, pp. 429–440, 1996.
- [28] J. Liu, Z. Lu, Y. Shi, W. Xu, and J. Zhang, "Investigation into manufacturing injection mold via indirect selective laser sintering," *Int. J. Adv. Manuf. Technol.*, vol. 48, no. 1–4, pp. 155–163, 2010.
- [29] A. Yassin, T. Ueda, T. Furumoto, A. Hosokawa, R. Tanaka, and S. Abe, "Experimental investigation on cutting mechanism of laser sintered material using small ball end mill," *J. Mater. Process. Technol.*, vol. 209, no. 15–16, pp. 5680–5689, 2009.
- [30] D. King and T. Tansey, "Alternative materials for rapid tooling," *J. Mater. Process. Technol.*, vol. 121, no. 2–3, pp. 313–317, 2002.
- [31] C. G. Ferro, A. Mazza, D. Belmonte, C. Secli, and P. Maggiore, "A Comparison between 3D

- Printing and Milling Process for a Spar Cap Fitting (Wing-fuselage) of UAV Aircraft,” *Procedia CIRP*, vol. 62, no. 3, pp. 487–493, 2017.
- [32] K. P. Karunakaran, S. Suryakumar, V. Pushpa, and S. Akula, “Retrofitment of a CNC machine for hybrid layered manufacturing,” *Int. J. Adv. Manuf. Technol.*, vol. 45, no. 7–8, pp. 690–703, 2009.
- [33] E. Uhlmann, S. Piltz, and K. Schauer, “Micro milling of sintered tungsten-copper composite materials,” *J. Mater. Process. Technol.*, vol. 167, no. 2–3, pp. 402–407, 2005.
- [34] M. S. A. Aziz, T. Ueda, T. Furumoto, S. Abe, A. Hosokawa, and A. Yassin, “Study on machinability of laser sintered materials fabricated by layered manufacturing system: Influence of different hardness of sintered materials,” *Procedia CIRP*, vol. 4, pp. 79–83, 2012.
- [35] T. A. Amine, T. E. Sparks, and F. Liou, “A strategy for fabricating complex structures via a hybrid manufacturing process,” *22nd Annu. Int. Solid Free. Fabr. Symp. - An Addit. Manuf. Conf. SFF 2011*, pp. 175–184, 2011.
- [36] J. Jeng and M. Lin, “Mold fabrication and modification using hybrid processes of selective laser cladding and milling,” *J. Mater. Process. Technol.*, vol. 110, no. 0, pp. 98–103, 2001.
- [37] S. Abe, Y. Higashi, I. Fuwa, N. Yoshida, and T. Yoneyama, “Milling-combined laser metal sintering system and production of injection molds with sophisticated function,” *Proceeding 11th Int. Conf. Precis. Eng.*, vol. 53, no. 2, pp. 285–299, 2006.
- [38] A. Yassin, T. Ueda, S. Tarmizi, and S. Shazali, “Experimental Study on Machinability of Laser- Sintered Material in Ball End Milling,” vol. 6, no. 11, pp. 1816–1819, 2012.
- [39] Z. Liu, “Conventional Subtractive Manufacturing Processes,” no. May, 2017.
- [40] H.-J. Kang and S.-H. Ahn, “Fabrication and Characterization of Microparts by Mechanical Micromachining: Precision and Cost Estimation,” *Proc. Inst. Mech. Eng. Part B J. Eng. Manuf.*, vol. 221, no. 2, pp. 231–240, 2007.
- [41] M. Ruffo, R. J. M. Hague, C. Tuck, and R. J. M. Hague, “Cost estimation for rapid manufacturing – simultaneous production of mixed components using laser sintering,” *Proc. Inst. Mech. Eng. Part B J. Eng. Manuf.*, vol. 221, no. 11, pp. 1585–1592, 2007.
- [42] M. Baumers, C. Tuck, R. Wildman, I. Ashcroft, E. Rosamond, and R. Hague, “Combined Build-Time, Energy Consumption and Cost Estimation for Direct Metal Laser Sintering,” *Proc. Twenty Third Annu. Int. Solid Free. Fabr. Symp. Addit. Manuf. Conf.*, vol. 53, no. 9, pp. 1689–1699, 2012.
- [43] M. Fette, P. Sander, J. Wulfsberg, H. Zierk, A. Herrmann, and N. Stoess, “Optimized and Cost-Efficient Compression Molds Manufactured by Selective Laser Melting for the Production of Thermoset Fiber Reinforced Plastic Aircraft Components,” *Procedia CIRP*, vol. 35, pp. 25–30, 2015.
- [44] L. Rickenbacher, A. Spierings, and K. Wegener, “An integrated cost- model for selective laser melting (SLM),” *Rapid Prototyp. J.*, vol. 19, no. 3, pp. 208–214, 2013.
- [45] G. Garcia-garcia *et al.*, “Calibration of ball nose micro end milling operations for sculptured surfaces machining Leopoldo Ruiz-Huerta and,” vol. 19, no. 6, pp. 587–605, 2017.
- [46] A. M. Abdelrahman Elkaseer, S. S. Dimov, K. B. Popov, and R. M. Minev, “Tool Wear in

Micro-Endmilling: Material Microstructure Effects, Modeling and Experimental Validation,” *J. Micro Nano-Manufacturing*, vol. 2, no. 4, p. 44502, 2014.

- [47] M. N. Durakba, A. Akdogan, A. S. Vanl, and A. Günay, “Surface Roughness Modeling with Edge Radius and End Milling Parameters on Al 7075 Alloy Using Taguchi and Regression Methods,” *Acta Imeko*, vol. 3, no. 4, pp. 46–51, 2014.
- [48] T. Zhao, J. M. Zhou, V. Bushlya, and J. E. Ståhl, “Effect of cutting edge radius on surface roughness and tool wear in hard turning of AISI 52100 steel,” *Int. J. Adv. Manuf. Technol.*, vol. 91, no. 9–12, pp. 3611–3618, 2017.

7 Annexes

Specification

KISTLER
measure. analyze. innovate.

Type 9256C...



Type 9256C2

Technical Data

Measuring range	F_x, F_y, F_z	N	-250 ... 250
Type 9256C1	M_x, M_z	N·m	-8 ... 8
Type 9256C2	M_x, M_z	N·m	-11 ... 11
Calibrated measuring range			
100 %	F_x, F_y, F_z	N	0 ... 250
10 %	F_x, F_y, F_z	N	0 ... 25
Overload	F_x, F_y, F_z	N	-300/300
Threshold		N	<0,002
Sensitivity	F_x, F_z	pC/N	≈-26
	F_y	pC/N	≈-13
Linearity, all ranges		%FSO	≤±0,4
Hysteresis, all ranges		%FSO	≤0,5
Crosstalk		%	≤±2
Rigidity	c_x, c_z	N/μm	>250
	c_y	N/μm	>300
Natural frequency (mounted on rigid base)			
Type 9256C1	$f_n (x)$	kHz	≈5,1
	$f_n (y)$	kHz	≈5,5
	$f_n (z)$	kHz	≈5,6
Type 9256C2	$f_n (x)$	kHz	≈4,0
	$f_n (y)$	kHz	≈4,8
	$f_n (z)$	kHz	≈4,6
Operating temperature range		°C	0 ... 70
Insulation resistance		Ω	>10 ¹³
Ground isolation		Ω	>10 ⁸
Degree of protection EN60529 (with connecting cable Type 1696A5/1697A5)			IP67
Weight			
Dynamometer	Type 9256C1/C2	kg	0,75/0,87
Top plate	Type 9256C1/C2	kg	0,24/0,36
Clamping area			
Type 9256C1		mm	39x80
Type 9256C2		mm	55x80

Dimensions MiniDyn Type 9256C...

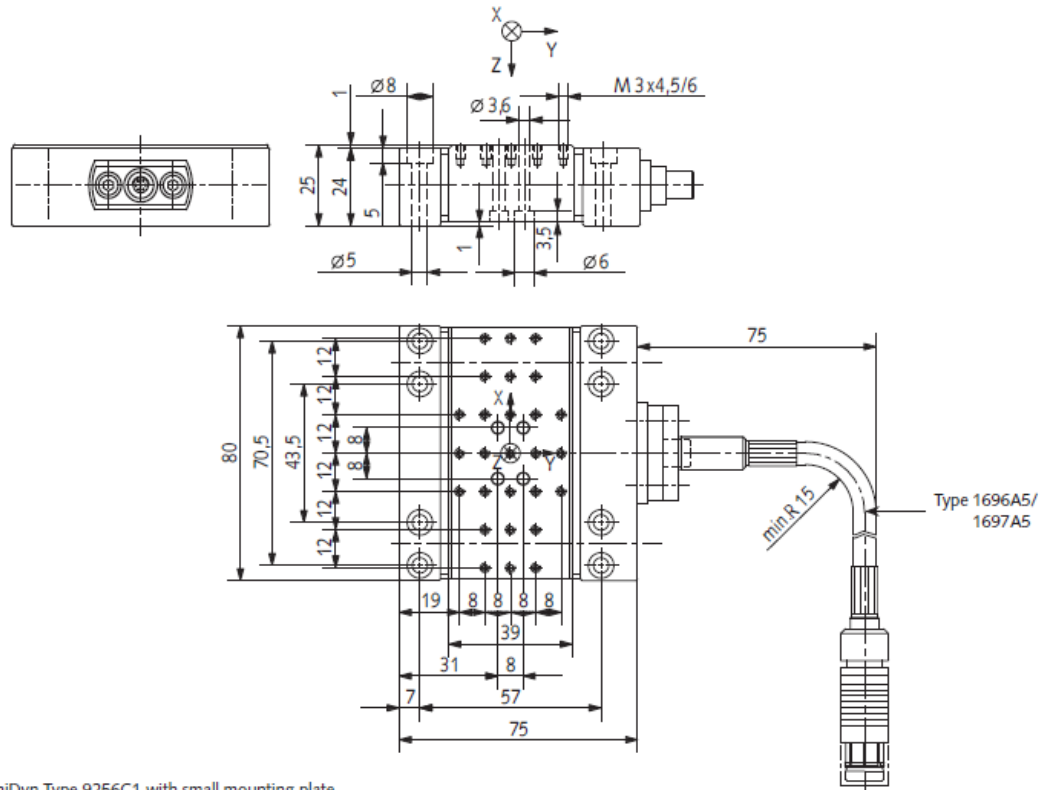


Fig. 1: MiniDyn Type 9256C1 with small mounting plate

Kistler Amplifier Specs

Technical Data

Type	Units	5010B
Measurement Range	pC	±10 ... 999 000
Scale Settings 1,2,3,4,5 sequence	MU/V ⁽¹⁾	0.0002 ... 10000000
Sensor Sensitivity	pC/MU mV/MU	0.01 ... 9990 0.01 ... 9990
Input:		
Connector Charge, voltage		BNC neg., gnd. isolated
Impedance Charge mode	Ω	70
Impedance Voltage mode	Ω	100k parallel with 1 nF
Voltage max.	V	50
Insulation Resistance at input	Ω	10 ¹⁴
Sensor power Voltage Mode	mA	4 (2 ... 18 optional)

Technical Data

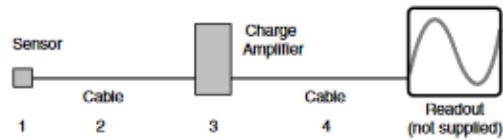
Type	Units	5010B
Frequency Response: Standard filter, Type 5311 (...3dB)	Hz	180,000
Accuracy	%	±0.50
Time Constant (range dependant):		
Long	s	0 ... 100000
Medium	s	1 ... 10000
Short	s	0.01 ... 100
Time Constant Resistor:		
Long	s	>1 ¹⁴
Medium	s	1 ¹¹
Short	s	1 ⁹
Noise:		
referred to with input shield	pC _{rms}	0.0036
1 pC/V max. (2)	µV _{rms}	500
100 pC/V typical (2)	µV _{rms}	300
100000 pC/V typical (2)	µV _{rms}	200
Drift MOSFET leakage current	pC/s	<+0.03
Zero Offset in Reset typical	mV	0.50
Output:		
Connector		BNC neg., gnd. isolated
Impedance	Ω	100
Voltage Range	V	±10
Current Limit	mA	5
Display	type	LCD 16 characters
Serial Interface (RS-232C)		
Connector		9 pin D-Sub.
Baud Rates		150 ... 9600
Maximum Cable Length	m/ft	20/65 (2500pF)
Remote Control Connector		DIN 45322 6-pol neg.
Temperature Range Operating	°F	32 ... 122
Temperature Range Storage	°F	-4 ... 158
Humidity Non-condensing	%	10 ... 90
Power Line:		
Voltage	VAC	89 ... 135
Frequency	Hz	48 ... 62
Power Consumption max.	VA	14
Weight without case	lb/kg	2.8/1.27
Dimensions without case	in	2.8 x 5.1 x 7.25

(1) MU = mechanical unit (e.g., psi, lb, g, etc)

(2) Referred to output with input shielded

1 g = 9.80665 m/s², 1 inch = 25.4 mm, 1 gram = 0.03527 oz, 1 lbf-in = 0.1129 Nm

Ordering Information



sp = specify cable length in meters

- 1 - sensor charge mode or voltage mode type
- 2 - 1631Asp charge mode cable, 10-32 pos. to BNC pos.
- 1631Csp premium charge mode cable, 10-32 pos. to BNC pos. or
- 1761B... general purpose voltage mode cable, 10-32 pos. to BNC pos.,
- 3 - 5010B1 1 channel with case and RS-232C interface
- 5010B0 same as above without case
- 5814B1 three channel with case (operates only in charge mode)
- 4 - 1511sp output cable, BNC pos. to BNC pos.

Supplied Accessories

- 1508 power cord
- 5311 plug-in filter
- 1564 remote reset connector

Optional Accessories

- 5730 rack adaptor for 6 each 5010B
- 5663 Remote control box
- 1455A5 5 m remote control cable

Plug-In low pass filters; see chart at below

Plug-In Filter Options-Bandwidth Limiting Filters

Model	Frequency
5311	180 kHz
5311A(x)kHz	1, 1.5, 2.2, 3.3, 4.7, 6.8, 10, 15, 22, 33, 47, 68, 100, 150, 220, 330
5313A(x)Hz	10, 15, 22, 33, 47, 68, 100, 150, 220, 330, 470, 680

Low pass, 12 dB/Octave Roll-off

x = cut-off frequency (-3db)

Makino F3 Specs

Table Size	850 x 500 mm
X	650 mm
Y	500 mm
Z	450 mm
Spindle RPM	20000
Rapid Traverse	19,990 mm/min
Cutting Feedrate	787 ipm
Maximum Workpiece	650 x 500 x 450 mm
Maximum Payload	800 kg
ATC Capacity	30
Tool to Tool	
Chip to Chip	
Maximum Tool Length	299.7 mm
Maximum Tool Diameter	119.9 mm
Maximum Tool Weight	8 kgs

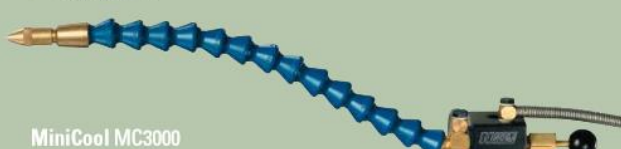
Alicona Infinite Focus specifications

TECHNICAL SPECIFICATIONS									
Measurement principle	non-contact, optical, three-dimensional, based on Focus-Variation								
Positioning volume (X x Y x Z)	100 mm x 100 mm x 100 mm = 1000000 mm ³ (optional: 200 mm x 200 mm x 100 mm = 4000000 mm ³)								
Objective magnification	2.5x	5x	10x HX	10x	20x HX	20x	50x	100x	
Working distance	mm	8.8	23.5	37	17.5	30	19	11	4.5
Lateral measurement range (X,Y)	mm	5.63	2.82	1.62	1.62	0.7	0.81	0.32	0.16
(X x Y)	mm ²	31.7	7.85	2.62	2.62	0.49	0.66	0.10	0.03
Vertical resolution	nm	2300	410	250	100	80	50	20	10
Height step accuracy (1 mm)	%	n.a.	0.05	0.05	0.05	0.05	0.05	0.05	0.05
Max. measurable area	mm ²	10000	10000	10000	10000	10000	10000	3965	990
Optional	mm ²	40000	40000	40000	40000	24780	24780	3965	990
Min. measurable roughness (Ra)	µm	7	1.2	0.75	0.3	0.24	0.15	0.06	0.03
Min. measurable roughness (Sa)	µm	3.5	0.6	0.375	0.15	0.12	0.075	0.03	0.015
Min. measurable radius	µm	20	10	5	5	3	3	2	1

MiniCool


MiniCool MC1700
For Maximum heat dissipation and extended tool life

- Strong magnetic base
- Separate on/off air and fluid controls
- Stainless steel armoured syphon hose and air hose
- Nozzle connected via Loc-Line® flexible hose
- Simple, inexpensive, rugged
- Single spray unit



MiniCool MC3000














- Same as MC1700 but with 2 spray units



order no.

One spray unit of length (mm)			Two spray units of length (mm)			Air hose	Syphon hose
264	334	479	264	334	479		
MC1700	MC1800	MC2000	MC3000	MC3100	MC3200	1 M	1 M
MC1730	MC1830	MC2030	MC3030	MC3130	MC3230	2 M	2 M

SPARE PARTS
order no.

MC0130		control valve with popeye magnet
MC0101		spray unit 270 mm
MC0102		spray unit 340 mm
MC0103		spray unit 485 mm
MC0380		air line 1 m
MC0302		air line 2 m
MC0360		suction line 1 m
MC0311		suction line 2 m
MC0204		valve stem
MC3637		filter
MC0001		nuzzle nut
MC0232		banjo screw & washer
MC0031		banjo fitting

Data of needles measurements

Needles	Height (µm)	Diameter (mm)	Top diameter (µm)
Tool 02 High Cutting speed (180mm/min)			
01	982.406	1030	10.5
02	984.163	1003	13.934
03	982.15	1002	11.8
04	991.072	1001	7.708
05	992.559	0.99942	11.01
06	982.044	1002	12.002
07	970.688	1034	10.654
08	969.057	1031	9.134
09	972.748	1043	8.692
Average	980.76522	1013	10.60377
10	933.404	958.674	11.77
11	944.445	968.012	
12	944.673	966.255	8.946
13	968.546	1033	9.712
14	978.125	1022	8.872
15	982.241	1033	7.388
16	967.624	1028	8.59
17	974.125	1066	9.496
18	981.888	1057	9.004
Average	963.9	1013.43	
19	965.152	1030	9.854

20	966.205	1044	9.2
21	968.998	1048	9.834
22	962.066	1012	8.42
23	969.599	1040	8.98
24	975.294	1049	9.966
25	979.4	1024	8.226
26	980.29	1024	9.596
27	985.904	1010	8.322
Average	972.545	1031	9.122
Needles	Height (µm)	Diameter (mm)	Top diameter (µm)
Tool 04 High Cutting speed (180mm/min)			
01	957.494	101	9.672
02	963.234	1005	11.017
03	959.717	1003	10.508
04	980.926	1079	10.586
05	972.713	105	9.408
06	982.979	1065	5.613
07	980.493	1056	10.882
08	978.353	1016	15.514
09	9383.98	1051	9.03
Average	973.3202	1036	10.2512
10	959.239	1004	13.582
11	967.203	1014	9.366
12	969.858	1009	10.866
13	968.615	1017	10.956
14	974.386	1035	8.854
15	977.86	1034	8.336
16	962.063	1007	8.174
17	962.79	1013	10.364
18	970.104	1027	8.531
Average	968.011	1017.77	9.89244
19	984.876	993.4	11.02
20	987.455	991.8	8.5
21	993.384	993.6	9.066
22	988.118	1005	8.038
23	991.054	992.3	9.412
24	996.374	1010	9.062
25	999.681	992.9	19.316
26	999.503	991.6	28.128
27	1004	991.2	30.83
Average	993.827222	995.8	14.8191

Needles	Height (µm)	Diameter (mm)	Top diameter (µm)
Tool 02 High Cutting speed (180mm/min)			
01	982.406	1030	10.5
02	984.163	1003	13.934
03	982.15	1002	11.8
04	991.072	1001	7.708
05	992.559	0.99942	11.01
06	982.044	1002	12.002
07	970.688	1034	10.654
08	969.057	1031	9.134
09	972.748	1043	8.692
Average	980.76522	1013	10.60377
10	933.404	958.674	11.77
11	944.445	968.012	
12	944.673	966.255	8.946
13	968.546	1033	9.712
14	978.125	1022	8.872
15	982.241	1033	7.388
16	967.624	1028	8.59
17	974.125	1066	9.496
18	981.888	1057	9.004
Average	963.9	1013.43	
19	965.152	1030	9.854
20	966.205	1044	9.2
21	968.998	1048	9.834
22	962.066	1012	8.42
23	969.599	1040	8.98
24	975.294	1049	9.966
25	979.4	1024	8.226
26	980.29	1024	9.596
27	985.904	1010	8.322
Average	972.545	1031	9.122
Needles	Height (µm)	Diameter (mm)	Top diameter (µm)
Tool 04 High Cutting speed (180mm/min)			
01	957.494	101	9.672
02	963.234	1005	11.017
03	959.717	1003	10.508
04	980.926	1079	10.586
05	972.713	105	9.408
06	982.979	1065	5.613
07	980.493	1056	10.882
08	978.353	1016	15.514
09	9383.98	1051	9.03
Average	973.3202	1036	10.2512
10	959.239	1004	13.582
11	967.203	1014	9.366
12	969.858	1009	10.866
13	968.615	1017	10.956

14	974.386	1035	8.854
15	977.86	1034	8.336
16	962.063	1007	8.174
17	962.79	1013	10.364
18	970.104	1027	8.531
Average	968.011	1017.77	9.89244
19	984.876	993.4	11.02
20	987.455	991.8	8.5
21	993.384	993.6	9.066
22	988.118	1005	8.038
23	991.054	992.3	9.412
24	996.374	1010	9.062
25	999.681	992.9	19.316
26	999.503	991.6	28.128
27	1004	991.2	30.83
Average	993.827222	995.8	14.8191